SOFT PNEUMATIC ACTUATOR FOR LOWER LIMB REHABILITATION: DEVELOPMENT AND ITS EFFICACY IN REDUCING MUSCLE STIFFNESS AND PAIN

HANISAH BINTI BAKERI

FACULTY OF ENGINEERING
UNIVERSITI MALAYA
KUALA LUMPUR

2024

SOFT PNEUMATIC ACTUATOR FOR LOWER LIMB REHABILITATION: DEVELOPMENT AND ITS EFFICACY IN REDUCING MUSCLE STIFFNESS AND PAIN

HANISAH BINTI BAKERI

DISSERTATION SUBMITTED IN FULFILMENT OF THE REQUIREMENTS FOR THE DEGREE OF MASTER OF ENGINEERING SCIENCE

FACULTY OF ENGINEERING
UNIVERSITI MALAYA
KUALA LUMPUR

2024

UNIVERSITI MALAYA
ORIGINAL LITERARY WORK DECLARATION

Name of Candidate: Hanisah Binti Bakeri

Matric No: S2159865/1

Name of Degree: Master of Engineering Science

Title of Thesis ("this Work"): Soft Pneumatic Actuator for Lower Limb Rehabilitation:

Development and its Efficacy in Reducing Muscle Stiffness and Pain.

Field of Study: Biomedical Engineering (Engineering & Engineering Trades)

I do solemnly and sincerely declare that:

(1) I am the sole author/writer of this Work;
(2) This Work is original;
(3) Any use of any work in which copyright exists was done by way of fair dealing and for permitted purposes and any excerpt or extract from, or reference to or reproduction of any copyright work has been disclosed expressly and sufficiently and the title of the Work and its authorship have been acknowledged in this Work;
(4) I do not have any actual knowledge nor do I ought reasonably to know that the making of this work constitutes an infringement of any copyright work;
(5) I hereby assign all and every rights in the copyright to this Work to the Universiti Malaya ("UM"), who henceforth shall be owner of the copyright in this Work and that any reproduction or use in any form or by any means whatsoever is prohibited without the written consent of UM having been first had and obtained;
(6) I am fully aware that if in the course of making this Work I have infringed any copyright whether intentionally or otherwise, I may be subject to legal action or any other action as may be determined by UM.

Candidate's Signature   Date: 19/03/24

Subscribed and solemnly declared before,

Witness's Signature   Date: 19/03/24

Name:

Designation:

SOFT PNEUMATIC ACTUATOR FOR LOWER LIMB REHABILITATION: DEVELOPMENT AND ITS EFFICACY IN REDUCING MUSCLE STIFFNESS AND PAIN

ABSTRACT

Lower limb injuries have been identified as a significant contributor to the occurrence of time lost during both physical training and daily activities. In recent years, pneumatic compression therapy has emerged as a viable alternative for managing patients who exhibit resistance to conventional compression methods. The conventional compression method exhibits limitations in consistent pressure distribution and adaptability. Recognizing these challenges, this study explores the integration of soft pneumatic actuators (SPAs) in compression therapy to enhance precision and dynamic adaptability, offering a promising alternative for improved treatment outcomes. The objective of this study is to investigate the potential application of soft pneumatic actuators (SPA) in the context of rehabilitation therapy for musculoskeletal ailments. The primary objective of this study is to analyze various aspects related to SPA including their design, material selection, fabrication, and design testing. Additionally, the research aims to experimentally validate the efficacy of lower limb rehabilitation compression therapy in reducing muscle stiffness among healthy individuals. Furthermore, ongoing investigations in the field of compression therapy predominantly focus on the advancement of soft pneumatic actuators tailored to various applications. However, there remains a dearth of definitive findings pertaining to the advantages of compression therapy in alleviating muscle fatigue. Therefore, a SPA chamber with two elastomeric layers was developed for this study, with single-side inflation using food-grade silicone. The 3D deformation profiles of the SPA chamber using three different elastomeric rubbers were analyzed using the finite element method (FEM). The best SPA-compliant behavior was displayed by food-grade silicone A10 Shore with a maximum deformation

value of 25.34 mm. Next, the SPA chamber was fabricated using A10 Shore food-grade silicone and experimentally validated. A total of 30 healthy male subjects were recruited and underwent a fatigue induction exercise. Muscle stiffness was assessed at four distinct time points in both the intervention group, which received SPA, and the control group, which did not receive SPA. The compression pressure in respect to calf circumference was measured, and both the maximum and average values were recorded. The findings suggest that the SPA system demonstrates effective pressure transmission on the skin within the pressure range of 20-160 mmHg for healthy male subjects. A positive linear trend between pressure variation and calf circumference was found. The mean muscle stiffness for the intervention group exhibited a reduction from an initial value of 496.26 ± 24.70 Nm^{-2} to a subsequent value of 382.30 ± 19.72 Nm^{-2} immediately following the application of pneumatic compression. This decrement corresponds to a percentage reduction of 22.96%, with p-value of 0.0001. There was no statistically significant difference seen between the pre-treatment and post-treatment measurements in the control group, with a p-value of 0.3500. The results of the study showed that the short form McGill pain questionnaire (SF-MPG) of the intervention group had a statistically significant impact on the pain index following a 30-minute treatment with SPA. The study demonstrates that the proposed SPA system is capable of reducing muscle stiffness and delivering the desirable pressure for treating musculoskeletal injuries, thereby aiding in the acceleration of recovery.

Keywords: Compression therapy, lower limb injuries, muscle stiffness, rehabilitation, soft pneumatic actuator (SPA).

PENGGERAK PNEUMATIK LEMBUT UNTUK PEMULIHAN ANGGOTA BAWAH BADAN: PEMBUATAN DAN KEBERKESANANNYA DALAM MENGURANGKAN KETEGANGAN OTOT DAN SAKIT

ABSTRAK

Kecederaan anggota bawah badan telah diiktiraf sebagai penyumbang penting kepada berlakunya kehilangan masa dalam latihan fizikal dan aktiviti harian. Pada masa kini, terapi mampatan pnuematik telah muncul sebagai alternatif yang berdaya maju untuk merawat pesakit yang mempunyai rintangan terhadap kaedah mampatan konvensional. Kaedah terapi mampatan konvensional menunjukkan had dalam pengagihan tekanan yang konsisten dan kebolehsuaian. Menyedari cabaran ini, kajian ini meneroka integrasi penggerak pneumatik lembut (SPA) dalam terapi mampatan untuk meningkatkan ketepatan dan kebolehsuaian dinamik, menawarkan alternatif yang menjanjikan untuk hasil rawatan yang lebih baik. Objektif kajian ini adalah untuk mengkaji potensi penggunaan penggerak pneumatik lembut (SPA) dalam konteks terapi pemulihan untuk penyakit muskuloskeletal. Objektif utama kajian ini adalah untuk menganalisis pelbagai aspek yang berkaitan dengan SPA termasuk reka bentuk, pemilihan bahan, fabrikasi, dan ujian reka bentuk. Tambahan pula, penyelidikan ini bertujuan untuk mengesahkan keberkesanan terapi mampatan pemulihan anggota bawah badan secara eksperimen dalam mengurangkan kekakuan otot di kalangan individu yang sihat. Selain itu, penyelidikan yang sedang dijalankan dalam bidang terapi mampatan lebih tertumpu kepada kemajuan penggerak pnuematik lembut yang disesuaikan kepada pelbagai aplikasi. Walau bagaimanapun, masih terdapat kekurangan penemuan yang definitif berkaitan dengan kelebihan terapi mampatan dalam mengurangkan keletihan otot. Oleh itu, ruang SPA dengan dua lapisan elastomer telah dibangunkan untuk kajian ini, dengan inflasi satu sisi menggunakan silikon gred makanan. Profil ubah bentuk 3D ruang SPA menggunakan tiga getah elastomerik berbeza dianalisis menggunakan kaedah unsur

terhingga (FEM). Tingkah laku pematuhan SPA terbaik ditunjukkan oleh silikon gred makanan A10 Shore dengan nilai ubah bentuk maksimum 25.34 mm. Seterusnya, ruang SPA dibuat menggunakan silikon gred makanan A10 Shore dan diuji secara eksperimen. Sebanyak 30 subjek lelaki yang sihat direkrut untuk menjalani latihan induksi keletihan. Kekakuan otot dinilai pada empat titik masa yang berbeza dalam kedua-dua kumpulan intervensi, yang menggunakan SPA, dan kumpulan kawalan, yang tidak menggunakan SPA. Tekanan mampatan berkenaan dengan ukur lilit betis diukur, dan kedua-dua nilai maksimum dan purata direkodkan. Hasilnya menyatakan bahawa sistem SPA menunjukkan penghantaran tekanan yang berkesan pada kulit dalam julat tekanan 20-160 mmHg untuk subjek lelaki yang sihat. Trend linear positif antara variasi tekanan dan ukurlilit betis diperolehi. Purata kekakuan otot untuk kumpulan intervensi menunjukkan pengurangan dari nilai awal 496.26 ± 24.70 Nm^{-2} kepada nilai berikutnya 382.30 ± 19.72 Nm^{-2} selepas penggunaan mampatan pneumatik. Penurunan ini sepadan dengan pengurangan peratusan sebanyak 22.96%, dengan nilai $p=0.0001$. Tidak ada perbezaan yang signifikan secara statistic dilihat antara ukuran pra-rawatan dan pasca rawatan dalam kumpulan kawalan, dengan nilai $p=0.3500$. Hasil kajian menunjukkan bahawa borang soal sedilik pendek kesakitan McGill (SF-MPG) kumpulan intervensi mempunyai kesan yang signifikan secara statistik terhadap indeks kesakitan berikutan rawatan selama 30 minit dengan SPA. Kajian ini menunjukkan bahawa sistem SPA yang dicadangkan mampu mengurangkan kekakuan otot dan memberikan tekanan yang diinginkan untuk merawat kecederaan muskuloskeletal, seterusnya membantu dalam mempercepatkan pemulihan.

Kata kunci: Terapi mampatan, kecederaan anggota bawah, kekakuan otot, pemulihan, penggerak pneumatik lembut (SPA).

ACKNOWLEDGMENTS

TABLE OF CONTENTS

LIST OF FIGURES

LIST OF TABLES

LIST OF ABBREVIATIONS

AT   :   Achilles tendinopathy

AVT   :   Arterial vascular trauma

BMI   :   Body mass index

CVD   :   Cardiovascular disease

CGs   :   Compression garments

DE   :   Electro-active

DM   :   Diabetes mellitus

DOMS   :   Delay on set muscle soreness

DoF   :   Degree of freedom

DVT   :   Deep vein thrombosis

EIMI   :   Evolutionary Inverse Material Identification

EIMD   :   Exercise induced muscle damage

EMG   :   Electromyography

FEM   :   Finite element method

FL   :   Fascicle length

GIT   :   Gastrointestinal

GCS   :   Graduate compression stocking

ICC   :   Intraclass correlation coefficient

IPC   :   Intermittent pneumatic compression

IPAQ   :   International physical activity questionnaire

ITBS   :   Iliotibial band syndrome

LDE   :   Lymphatic drainage exercise

LoA   :   Limit of agreement

MLD	:	Manual lymphatic drainage
MT	:	Muscle thickness
MTSS	:	Medial tibial stress syndrome
PAMs	:	Pneumatic artificial muscle
PCT	:	Pneumatic compression therapy
PFP	:	Patella femoral pain
PSQ	:	Pain sensitivity questionnaire
SBF	:	Skin black flow
RO	:	Research Objective
RQ	:	Research Question
RP	:	Research Problem
sEMG	:	Surface electromyography:
SF-MPG	:	Short form mcgill pain questionnaire
SPAs	:	Soft pneumatic actuators
SMA	:	Shape memory alloy
SWE	:	Shear wave elastography
VTE	:	Venous thromboembolism

LIST OF APPENDICES

CHAPTER 1: INTRODUCTION

1.1   Introduction

In recent years, the field of rehabilitation therapy has witnessed significant advancements, particularly in the area of lower limb rehabilitation. In the search for novel solutions, soft pneumatic actuators have emerged as a promising tool for improving rehabilitation outcomes (Pan et al., 2022). These actuators, characterised by their malleability and ability to replicate the natural movement of human musculature, have enormous potential in the development of effective and adaptive rehabilitation devices. Section 1.2 provides a concise account of the statistical analysis pertaining to lower limb injuries. Specifically, it examines the many elements that influence the occurrence of these injuries, the frequency at which they recur, the specific activities that lead to their manifestation, and the corresponding economic implications. The research problems are explained in Section 1.3, followed by the research questions and general aim and specific objectives of this study in Sections 1.4 and 1.5 respectively. The research scope is addressed in Section 1.6. Lastly, Section 1.7 presents the thesis structure, providing a structured overview of the organization of the thesis.

1.2   Background

Engagement in physical exercise presents significant advantages by reducing the susceptibility to non-communicable diseases such as diabetes and cardiovascular diseases. However, involvement of the lower extremities in activities characterized by high velocity, explosive movements, or sudden changes in direction such as sprinting, running, and jumping renders the lower limb prone to injury. Lower limb injuries have been identified as contributing factors to a decrease in functional capabilities, time loss in everyday activities, sports-related activities as well as diminished self-reliance and quality of life (Simon & Docherty, 2018). According to the National Health Statistics Reports of United States, there is an annual average estimate of 8.6 million injuries

associated with recreation activities. The age-adjusted rate is reported as 34.1 per 1,000 individuals in the population (States, 2016). It is noteworthy that a considerable proportion of these injuries specifically impact the lower extremities accounting for 42.0% of the total. Moreover, the financial burden associated with the treatment of lower limb injuries is projected to reach a staggering two billion dollars within the healthcare system of the United State (Prieto-González et al., 2021).

Lower extremity injuries can lead to a cascade of issues that significantly impact daily life. Unhealed or improperly healed injuries can lead to muscle weakness and instability, affecting balance and coordination. This can increase the risk of falls (Fino et al., 2019). Furthermore, lower extremity injuries can progress into chronic pain syndromes. Incomplete healing or scar tissue formation can irritate nerves, leading to persistent discomfort and limiting daily activities. This chronic pain can disrupt sleep, affect mood, and decrease overall quality of life. Lower limb injuries, encompassing conditions affecting bones, muscles, ligaments, tendons, and nerves, is a significant global health concern. Individuals with serious lower limb injuries face a heightened risk of developing complications. These complications can include infections within the wound, delayed bone healing (known as nonunion), tissue death (necrosis), and bone infection (osteomyelitis). Many of these complications may necessitate further hospitalization or surgery (Harris et al., 2009). The World Health Organization (WHO) reports that 20-33% of the global population experiences some form of chronic musculoskeletal pain, representing a staggering 1.75 billion individuals (Cimmino et al., 2011) .

Among lower-limb injuries, the most often reported conditions include patellofemoral pain (PFP), iliotibial band syndrome (ITBS), medial tibial stress syndrome (MTSS), achilles tendinopathy (AT), plantar fasciitis, stress fractures, and muscle strains. The combination of strains and sprains accounted for 36% of the entirety of injuries

concerning the lower extremities. A significant proportion of these injuries exhibit a tendency to repeat with.

Some of these injuries tend to recur frequently, particularly muscular injuries contribute to discomfort, limited mobility, and reduced overall quality of life. While the impact on daily life varies, these conditions collectively present obstacles to accomplishing everyday tasks, engaging in physical activities, maintaining an active lifestyle as well as give rise to notable socio-economic challenges (El-Tallawy et al., 2021). Recent literature has covered a range of activity types linked to musculoskeletal injuries. These include driving or riding, yard work, school, sports, and recreational and leisure activities. As depicted in Figure 1.1 from Jaimo Ahn et al. (2015), the occurrence of musculoskeletal injuries highlights that sports or exercise (22%) is the leading activity contributing to these injuries in males compared to other activities. The intensity of muscle damage, particularly involving skeletal muscles, has the potential to contribute to chronic illnesses across various organ systems, encompassing conditions such as cardiovascular disease (CVD), neurological disorders, endocrine imbalances, kidney issues, gastrointestinal (GI) disturbances, metabolic disorders, and malignancies (Schwellnus et al., 2018). The occurrence of swelling resulting from muscle injuries might potentially lead to the constriction of popliteal or gastrocnemius veins, which can then result in the formation of deep vein thrombosis (DVT).
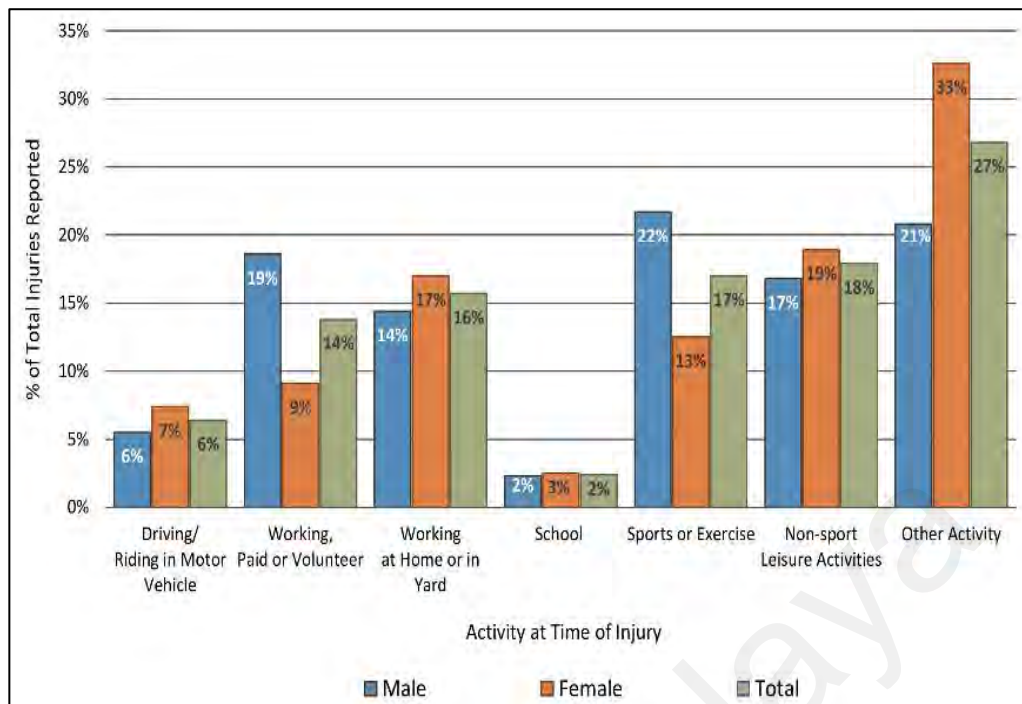
Figure 1.1: The percentage of activity at time of injury for self-reported medically consulted musculoskeletal injures adapted from (Jaimo Ahn et al., 2015).

The key to expediting the recovery process and mitigating chronic diseases in multiple organ systems caused by lower limb injury lies in rehabilitation approach. The chance of recovery for patients with lower limb injuries increases when there is a rehabilitation approach. Rehabilitation therapy is critical in regaining function and strength. Since the mechanism and clinical manifestations of lower limb injuries vary, it is necessary to make an appropriate assessment based on the patient's specific situation (Zhu & Ma, 2021). Thus, many approaches have been developed on accelerating the recovery process for various types of injuries including mirror therapy (Broderick et al., 2018) intensive exercise (Do et al., 2017), robot-assisted therapy (Gil-Castillo et al., 2022) and application of therapeutic modalities (Barassi et al., 2020).

Out of these various approaches, robot-assisted therapy has expanded its applications in recent decades to enhance the effectiveness, cost-efficiency, and convenience of physical therapy, thereby contributing to the advancement of the recovery process for different types of injuries. In conjunction with the use of therapeutic modalities technique

in rehabilitation, various advancements have been made to increase the analgesic effect of the therapy. Addition of external compression, hot and cold therapy is example of the therapeutic treatments that has improved with time. Despite the safety protocols in place for high precision robots, conventional or rigid robotics still pose risks to humans working in close proximity. The nonconformable actuators with limited degree of freedom are a major concern. This is where soft robotics comes in as a safer and more advantageous alternative. Soft robotics offers a more conformable and flexible design that reduces the risks associated with conventional robotics.

The need for specialized rehabilitation interventions to aid recovery has led to the incorporation of Soft Pneumatic Actuators (SPAs). Historically, traditional rehabilitation methods have relied on passive or manually operated devices to aid in this process. However, the emergence of Soft Pneumatic Actuators (SPAs) in conjunction with advancements in soft robotics presents a transformative approach to enhancing lower limb rehabilitation. Soft robotics, a burgeoning field focused on creating flexible and compliant robotic systems, shares fundamental principles with SPAs, including adaptability and safety. By leveraging soft robotic technologies, SPAs can closely replicate natural movement patterns of human limbs, providing a more intuitive and efficient means of rehabilitation compared to conventional methods. This innovative integration not only addresses the challenges posed by lower limb injuries but also offers tailored support throughout the rehabilitation journey, ultimately improving outcomes and enhancing individuals' independence and quality of life.

Compression therapy has become a widely used treatment for various vasculopathies and pain reduction, owing to the increasing incidence of venous disorders. This therapy is frequently deployed to prevent an0d manage conditions such as varicose veins, deep vein thrombosis, lymphatic edema, and wound management, as well as to reduce pain

(Youn & Lee, 2019). Recently, pneumatic compression therapy has gained attention as a substitute for addressing patients who show limited response to conventional methods. A recent advancement by Rosalia et al., (2021) introduced a soft robotic device designed for lower limb compression, specifically for treating lymphedema. This innovation builds upon the method initially developed by Low et al., (2019), allowing customization of actuation strength and motion based on user preferences.

Recent developments in soft robotics have shown promising capabilities in the field of assistive rehabilitation, including the use of soft pneumatic actuators (SPAs) for compression treatment of human limbs and joints. Additionally, there has been progress in crafting soft robotic exosuits tailored for individuals coping with motor disorders (C. M. Thalman & Lee, 2020), along with the innovation of soft robotic gloves aimed at aiding in the hand rehabilitation of stroke survivors (Chua et al., 2019). Their conformable nature ensures even and targeted compression along complex limb shapes, enhancing patient comfort and compliance (Baldoli et al., 2016). Furthermore, some SPAs integrate sensors to monitor pressure, blood flow, and muscle activity, facilitating real-time feedback and personalized therapy (Garcia et al., 2022) . Notably, certain SPAs even combine passive compression with active movement assistance, promoting rehabilitation exercises (Warutkar et al., 2022). Despite the potential applications of SPAs in rehabilitation, their development utilizing biocompatible components that are secure for both human use and the surrounding environment has been challenging and elusive. To solve the drawbacks of SPAs, various techniques have been used to provide better performance.

Simulation analysis is important for designing, development, and enhancement of soft robotic performance. Among these methods, finite element modeling (FEM) stands out as a technique for both modeling and simulating soft robotic components. The

performance of the SPA pressure can undergo numerical analysis through FEM, offering insights into the selection of SPA materials and optimal pressure levels for therapeutic purposes. These simulations facilitate swift and efficient cycles of refinement across diverse designs and materials, thereby elevating their overall effectiveness (Mourtzis, 2020). This impacts the efficacy of the treatment, the comfort experienced by the user, and the frequency of its application.

Therefore, this study focuses on developing a SPA to increase the recovery and performance of patients with lower limb injuries. Soft actuators have commonly employed silicone rubber elastomers due to their capacity to endure significant strains, up to 500% (Maruthavanan et al., 2021). Moreover, these materials offer flexibility, stretchability, and affordability. These silicones exhibit notable resistance to extreme temperatures, are non-toxic, and demonstrate degradability, further enhancing their utility (Miriyev et al., 2017). Briefly, soft robotics can automate repetitive and standard therapy procedures aimed at addressing musculoskeletal injuries, underscoring the significance of advancing soft robotic actuators. These actuators have the potential to significantly improve recovery outcomes by providing efficient and consistent treatments.

1.3   Problem Statement

Rehabilitation therapy of lower limb injuries using robotic devices and therapeutic therapy has been widely used in sports medicine to restore function and accelerate the recovery process. Approximately 90% of the lower limb injuries involved these three muscle groups: hamstrings, rectus femoris, and gastrocnemius. Oedema, venous thromboembolism (VTE), and inflammatory cellular infiltration are common signs of acute muscle injury. Compression therapy is a commonly used treatment method for various vasculopathies such as varicose veins, deep vein thrombosis, lymphatic edema, wound management, and pain reduction. Pneumatic compression therapy has garnered

attention as a substitute in cases where conservative methods are ineffective. This encompasses a range of soft pneumatic actuators (SPAs) composed of linear or non-linear soft materials, designed to offer specific predetermined motions or forces. However, regardless of the SPA's usage in rehabilitation, the challenge of creating these SPAs from biocompatible components that ensure safety for both humans and the environment has persisted. Several studies have explored biocompatible materials for SPAs including hydrogels (Shi et al., 2019), modified silicones and natural materials (Ostrovsky-Snider, 2017). While these materials present commendable attributes such as biocompatibility, biomimicry, and biodegradability, they often necessitate supplementary reinforcement to facilitate actuation and enhance their durability and robustness. Present research endeavors are focused on creating soft-bodies programmable motion inspired by biology characteristics, to seamlessly integrate natural compliance with manageable actuation (Coyle et al., 2018; Craddock et al., 2022; Miriyev et al., 2017). Su et al., (2022) discuss the importance of biocompatible materials in minimizing risks such as allergic reactions or toxicity, particularly for applications involving direct human contact. Silicone rubber elastomers including the Smooth-On Ecoflex series, parts of the Dragon Skin series, and Sylgard184 were predominantly used in the fabrication of soft actuators (Pagoli et al., 2021). One of the obstacles in this study domain is the absence of solid propellants with a high strain density that may effectively transmit pressure while also being nonhazardous (Huri & Mankovits, 2018). Competing priorities, material limitations, and limited research focus contribute to the scarcity of SPAs with high strain density yet non-hazardous properties. Present materials lack the optimal blend of stretchability, strength, and durability necessary for safely managing high pressure. Research efforts focused on specific aspects of SPA development, such as actuation speed or controllability, with less emphasis on achieving high strain density while maintaining safety.

Research Problem (RP) 1: Lack of SPAs with high strain density to transfer effective pressure while remaining nonhazardous.

Furthermore, persons who engage in regular physical activity are susceptible to musculoskeletal injuries in their lower extremities, necessitating the implementation of repeated and standardized rehabilitative interventions. The field of soft robotics has promised to aid in therapeutic interventions by enabling safe human interaction. Nevertheless, there is a lack of scholarly investigation about actuators in the field of soft robotics specifically designed for musculoskeletal ailments. Physicians sometimes recommend the use of compression therapy; nevertheless, the efficacy of this treatment in musculoskeletal conditions remains uncertain. Although it is widely known that the quality of compression therapy is closely connected to therapeutic outcomes, administering precise pressure and prolonged compression therapy remains a difficulty for health care workers. Since soft pneumatic actuators has excellent ability in recovery process of lower limb rehabilitation, this provides a cause to continue this research and find a way to overcome the constraint by utilizing three silicone-based elastomers composed of commercial and food-grade silicone with technical advancements that allow for simple control and programming of compression for lower limb rehabilitation as well as conducting the clinical testing to enhance the recovery process of musculoskeletal injury.

Research Problem (RP) 2: The challenge of achieving precise pressure application and prolonged compression therapy persists for healthcare workers.

Research Problem (RP) 3: Lack of comprehensive studies exploring the efficacy and optimization of these actuators in the context of musculoskeletal injury rehabilitation hinders their widespread adoption limits our understanding of their potential benefits.

1.4   Research Questions

Given the research problems presented in Section 1.3, the research questions (RQ) constituted in this thesis are:

Research Question (RQ) 1: What are the optimal design and material choices for creating safe and effective soft pneumatic actuators (SPAs) for lower limb compression therapy?

Research Question (RQ) 2: Can the proposed SPA system, comprised of commercial and food-grade silicone, provide precise pressure and protracted compression therapy for healthy males with lower limb musculoskeletal injuries?

Research Question (RQ) 3: What effect does the proposed SPA system have on reducing muscle stiffness in healthy males with lower-limb musculoskeletal injuries?

1.5   Aim and Objectives

This study aims to explore the potential of soft pneumatic actuators for assisting with rehabilitation therapies in musculoskeletal injuries. In achieving this aim, few specific research objectives (RO) are constructed as follows:

Research Objective (RO) 1: To simulate a soft pneumatic actuator (SPA) system from silicone-elastomeric materials using computer-aided design (CAD) modelling.

Research Objective (RO) 2: To design and fabricate a programmable prototype of compression for lower limb sleeve.

Research Objective (RO) 3: To investigate the effectiveness of the SPA system in reducing muscle stiffness of the calf muscles, induced by fatigue-inducing exercise on healthy participants.

The outlined objectives are mapped to the research problems and questions as provided in Table 1.1.

1.6   Research Scope

The scope of this study encompassed the simulation and analysis of a soft pneumatic actuator (SPA) chamber utilizing both food-grade silicone and commercial silicone using FEM. The primary focus was to investigate the total deformation and stress distribution of three silicone elastomers at the center of the chamber as shown in Figure 1.2. Subsequently, the developed SPA design was fabricated and subjected to testing involving 30 healthy male participants.

Figure 1.2: The point at the center of the chamber to observed total deformation and stress.

The testing focused solely on the application of a SPA for compression therapy targeting the lower limb excluding individuals with chronic pain and including those with normal to high pain tolerance as determined by the Pain Sensitivity Questionnaire (Ruscheweyh et al., 2009). Additionally, the investigation specifically examines pain reduction through the induction of muscle fatigue via eccentric exercise, specifically standing calf raises. The evaluation of pressure exerted during compression and muscle stiffness is constrained by the sensitivity and resolution of the Force Sensitive Resistor, as well as the MyotonPRO device. The MyotonPRO device was used for this investigation because of its ability to provide real-time measurements. This is because the device offers prompt feedback and evaluation throughout the process of muscle palpation or movement. This experimental testing is the initial phase, focusing on healthy participants to gain insights into the treatment's effects on individuals without underlying

conditions, evaluating factors such as treatment efficacy, user comfort, and application frequency.

1.7   Thesis Organization

The thesis is organized into five chapters, each serving a distinct purpose as outlined below:

- Chapter 1: Introduction. An overview of lower limb injury and rehabilitation approaches are presented in this section, along with the problem statements, objectives, research questions, scope of work and thesis organization. This chapter shows the rationale behind the study and reveals the scope of the study.

- Chapter 2: Literature Review. In this chapter, different compression techniques are reviewed. This chapter will go over articles related to soft pneumatic actuators, explore how they contribute to experimental design, address research gaps, and synthesize important information relevant to the research topic.

- Chapter 3: Methodology. The overall approach for this research is provided in this chapter. The main contributions are highlighted, including the techniques that develop a SPA system, data collection and analysis. The research is divided into two parts, which are design and modelling, and experimental validation on healthy participants.

- Chapter 4: Results and Discussions. The discussion on the results obtained is presented here. The efficacy of the proposed SPA is assessed through both qualitative and quantitative measurements. All results are displayed and compared accordingly, facilitating the evaluation of the performance of the proposed approach.

- Chapter 5: Conclusion and Future Work. The final chapter concludes the research and emphasizes its contributions. It discusses both the advantages and

disadvantages of employing this approach, outlines the study's limitations, and

proposes potential enhancements for future studies.

Table 1.1: Mapping between research problems, research questions and research objectives.

RESEARCH PROBLEM	RESEARCH QUESTION	RESEARCH OBJECTIVE
RP1: Lack of SPAs with high strain density to transfer effective pressure while remaining nonhazardous.	**RQ1**: What are the optimal design and material choices for creating safe and effective soft pneumatic actuators (SPAs) for lower limb compression therapy?	**RO1**: To simulate a soft pneumatic actuator (SPA) system from silicone-elastomeric materials using computer-aided design (CAD) modelling.
RP2: The challenge of achieving precise pressure application and prolonged compression therapy persists for healthcare workers.	**RQ2**: Can the proposed SPA system, comprised of commercial and food-grade silicone, provide precise pressure and protracted compression therapy for healthy males with lower limb musculoskeletal injuries?	**RO2**: To design and fabricate a programmable prototype of compression for lower limb sleeve.
RP3: Lack of comprehensive studies exploring the efficacy and optimization of these actuators in the context of musculoskeletal injury rehabilitation hinders their widespread adoption and limits our understanding of their potential benefits.	**RQ3**: What effect does the proposed SPA system have on reducing muscle stiffness in healthy males with lower-limb musculoskeletal injuries?	**RO3**: To investigate the effectiveness of the SPA system in reducing muscle stiffness of the calf muscles, induced by fatigue-inducing exercise.

CHAPTER 2: LITERATURE REVIEW

2.1   Introduction

This chapter elaborates on the overview of existing articles related to the use of soft pneumatic actuators for compression therapy in lower limb rehabilitation therapy. Section 2.2 discusses the overview of the lower limb injuries and pain associated with the injuries. Section 2.3 discusses the overview of the lower limb rehabilitation technologies, devices and modalities that have been developed to aid in recovery process. Next, Section 2.4 defines compression-based rehabilitation therapy and discusses the various types of compression therapy. Additionally, this section also explores the impacts of different compression therapies on limbs. In Section 2.5, a comprehensive explanation is provided regarding the various types of soft robotics and their distinct actuation mechanisms. The section detailed insights of the approaches employed in soft robotics to achieve movement, including the utilization of soft pneumatic actuators, shape memory alloys, and dielectric elastomers. Furthermore, a detailed review of soft pneumatic actuators for rehabilitation therapy is discussed in Section 2.6. It consists of an overview of recent developments in soft pneumatic actuators using different material focusing on designing and fabricating the soft pneumatic actuator (SPA). Lastly, this chapter is concluded with the identification of research gaps in Section 2.7.

2.2   Lower Limb Injuries

Lower limb injuries are the most common issue in primary care and sports medicine, posing significant challenges for practitioners. Active individuals or athletes often experience these injuries through diverse mechanisms, such as lacerations, strains, contusions, and indirect causes linked to factors like ischemia and neurological dysfunctions. Mechanical overload on a muscle lead to excessive elongation of muscle fibers, potentially resulting in tears near the musculotendinous junction. This phenomenon is particularly prevalent in superficial muscles that cross two joints such as

the rectus femoris, semitendinosus, and gastrocnemius (Fernandes et al., 2011). The healing process for most muscle injuries follows a common pattern with three distinct stages: an initial destructive and inflammatory phase lasting 1-3 days, followed by a repair phase spanning 3-4 weeks, and finally a remodeling phase that can take 3-6 months to complete (Baoge et al., 2012).

Individual suffering from lower-limb injuries, particularly muscular injuries, can significantly impede their ability to participate in physical activity, resulting in time loss during both training and competition. These injuries pose substantial barriers to engagement in physical activities, as they often require rest, rehabilitation, and recovery periods that interrupt regular training schedules and competitive endeavors. (Bisciotti et al., 2018). The condition of muscle injuries is characterized by microscopic tears in muscle fibers, leading to weakness, delayed onset muscle soreness (DOMS), swelling, and limited range of motion in the affected limb (Craighead et al., 2017). These injuries also trigger the release of enzymes and proteins like creatine kinase (CK) and myoglobin into the bloodstream. Following exercise-induced muscle damage, various cell types within the skeletal muscle, including satellite cells, inflammatory cells, vascular cells, and stromal cells, work together within the surrounding matrix to initiate repair and rebuilding processes. This cellular interplay significantly influence the efficiency and duration of recovery from muscle damage (Peake et al., 2017).

Muscle stiffness, also known as muscle tone or rigidity, can serve as a valuable indicator in assessing muscle injury. Injury to muscles, whether caused by trauma or overuse, often manifests as heightened stiffness owing to factors such as inflammation, micro-tears, or fiber damage (Hurtgen et al., 2016). The monitoring of alterations in muscle stiffness provides clinicians with critical insights into the severity and progression of such injuries. Clinical techniques including palpation, range of motion assessments,

and specialized tools such as myotonometers are commonly employed for quantifying muscle stiffness (Davidson et al., 2017). Numerous studies have underscored the significance of muscle stiffness measurements in assessing diverse musculoskeletal conditions. Heiss et al., (2018) employed acoustic radiation force impulse (generating shear wave velocities) to measure muscle stiffness in participants following an eccentric calf exercise intervention. The measurements were taken both immediately after the exercise and again 60 hours later to investigate the influence of compression therapy on the occurrence of delayed onset muscle soreness (DOMS). A study by Kisilewicz et al., (2020) investigated how unaccustomed eccentric muscle contractions affected the biomechanical properties of skeletal muscle at different locations. They used two techniques, shear wave elastography and myotonometry, to measure both elastic modulus and dynamic stiffness.

2.2.1 Pain Associated with Lower Limb Injuries

Pain following lower limb injuries represents a significant clinical concern due to its impact on mobility, function, and overall quality of life. Lower limb injuries, ranging from sprains and strains to fractures and ligament tears, commonly result in acute and chronic pain that can persist long after the initial injury. Understanding the nature and severity of pain is crucial for effective management and rehabilitation strategies. Research in this field has highlighted the multifactorial nature of pain perception, influenced by factors such as injury severity, tissue damage, inflammation, and psychological variables like fear-avoidance beliefs and catastrophizing tendencies (Belfer, 2013; Igolnikov et al., 2018).

Pain presents a multifaceted phenomenon influenced by various physiological and psychosocial factors. Fatigue-induced pain arises from a combination of metabolic by-products, tissue damage, altered neuromuscular control, and central sensitization

mechanisms. During strenuous exercise, such as high-intensity interval training or resistance training, the accumulation of metabolites like lactate and hydrogen ions contributes to muscle fatigue and subsequent discomfort (Wan et al., 2017). The immediate onset of pain serves as a protective mechanism, limiting further mechanical stress and promoting tissue repair processes. However, as the inflammatory response subsides, persistent or chronic pain may arise due to maladaptive neuroplastic changes, sensitization of nociceptive pathways, and altered biomechanics. Additionally, microtrauma to muscle fibers and connective tissues leads to inflammation, exacerbating pain sensations (Sonkodi et al., 2020). Moreover, central mechanisms involving the modulation of pain processing in the spinal cord and brain may amplify pain perception following eccentric exercise (Ossipov et al., 2010).

Assessment of pain associated with lower limb injuries is complex, integrating subjective reports of pain intensity and quality with objective measures to comprehensively evaluate individuals' experiences. Assessment tools such as visual analog scales (VAS), numerical rating scales (NRS), and the McGill Pain Questionnaire are frequently utilized to quantify pain intensity and characterize its qualities. Chou et al., (2018) investigated pain following surgery to repair a broken ankle in 63 patients. The Short-Form McGill Pain Questionnaire (SF-MPQ) was administered to assess pain levels before surgery (preoperatively) and again at three different time points after surgery (postoperatively). The SF-MPQ has garnered recognition for its reliability and validity in assessing various dimensions of pain, making it a preferred tool in clinical research settings (Hawker et al., 2011).

According to Lovejoy et al., (2012) the Short-Form McGill Pain Questionnaire is good at capturing the nuances of pain experience. It can distinguish between nerve pain (neuropathic pain) and pain caused by tissue damage (nociceptive pain). This makes it a

valuable tool for clinicians. Similarly, Solowiej et al., (2010) highlight the SF-MPQ's strength in clinical settings: it provides insights into sensory, emotional, and overall pain intensity. It can also detect changes in reported pain levels. However, some concerns exist. The scoring system might be cumbersome for healthcare providers, and patients might misinterpret the instructions. However, research by the developers suggests patients, including older adults, can use the SF-MPQ effectively.

In the context of rehabilitation, accurate pain assessment serves as a cornerstone for tailoring personalized treatment plans and monitoring progress over time. Regular reassessment allows clinicians to adjust interventions based on the dynamic nature of pain and individual responses to therapy.

2.3   Lower Limb Rehabilitation Therapy

Rehabilitation is the collection of therapeutic approaches that aim to maximize a person's abilities while lowering reliance and improving mechanics. To aid in the recovery process, a variety of lower limb rehabilitation technologies, devices, and modalities have been developed, including the utilization of robotic devices and system, the application of therapeutic (Yu et al., 2016), and exercise programs (Volpe et al., 2020). Nonetheless, the current research issues are mostly concerned with the development of new therapeutic and assistive modes that can help in improving the rehabilitation outcome in terms of both shortening the treatment durations and improving the activities of daily living (Bhardwaj et al., 2021). The advancement of robotics for rehabilitation treatments is growing as a solution to automate training. Various types of lower limbs rehabilitation robots have been developed to restore function and enhance the recovery process of the patient. Figure 2.1 shows a classification view of these recent lower limb robot developments.
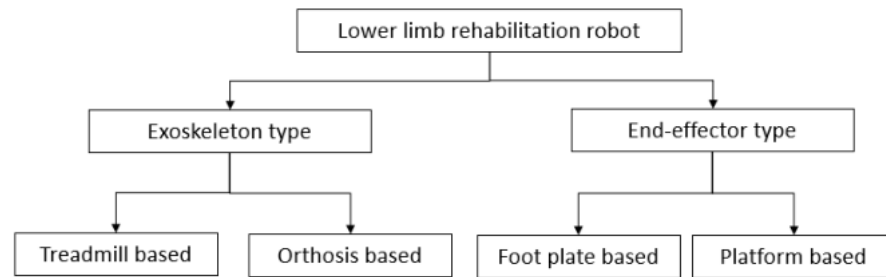
Figure 2.1:Classification of lower limb robots adapted from (Bhardwaj et al., 2021)

Exoskeleton-type robotic systems use robot axes that correspond with the wearer's anatomical axes to operate individual movement directly (Zhang et al., 2018). These robots are ingeniously designed to be worn externally, resembling a mechanical framework that envelops and amplifies the movements of a user's limbs. Widely applied in medical and rehabilitative contexts, exoskeleton-type rehabilitation robots are tailored to enhance mobility, strength, and coordination for individuals dealing with mobility challenges or neuromuscular impairments (Esquenazi, 2019) . Exoskeleton-type rehabilitation robots provide extra support to specific body parts like arms or legs, helping users perform movements they might find challenging or unfeasible. These robots use special sensors, actuators, and sophisticated control algorithms, to understand and respond to what the user wants to do. This makes it easier for people to move and do things they want, even if their bodies have limitations. These robots are a promising way to improve movement and recovery for those who have trouble moving around.

Meanwhile, an end effector rehabilitation robot is an advanced technological system designed to assist and enhance the rehabilitation process for individuals with impaired motor function, typically due to neurological or musculoskeletal conditions. This innovative device focuses on the manipulation and movement of the distal part of the body, often the hand or foot, which is referred to as the "end effector" (Esquenazi, 2019)

. By providing targeted therapy and exercises, the end effector rehabilitation robot aims to improve joint mobility, muscle strength, coordination, and overall functionality (Dong et al., 2022). This technology offers personalized and adaptable rehabilitation protocols, enabling healthcare professionals to tailor treatment plans to the specific needs and progress of each patient (Eiammanussakul & Sangveraphunsiri, 2018).

However, the structural complexity of both devices can be changed as the degree of freedom increases. Soft robotic devices for lower limb rehabilitation have been developed in response to the inability of conventional hard therapy to keep up with the rising demand. It was chosen due to its safety, ease of construction, and use of lightweight materials.

2.4   Compression Based Rehabilitation Therapy

Compression therapy is a technique that involves applying external pressure to the human body. This therapy will influence the entire deformable structure of the region where the pressure is applied. For example, when pressure is applied to the lower limb, tissue, arteries, veins and lymphatics are compressed (Partsch & Mortimer, 2015). Exerting external pressure on the lower limb causes compression on the leg veins which results in vein vessels constriction and an increase in blood flow velocity (Berszakiewicz et al., 2020). Thus, it decreases the veins reflux and improves the function pumping of veins. As a result, compression of veins and lymphatic capillaries can effectively treat leg oedema and lymphedema by enhancing lymphatic drainage and reducing vascular wall tension (Mosti et al., 2020).

The compression therapy pressure can be explained through Laplace's Law and Pascal's Law. These laws define the relationship between cylindrical and spherical vessel forces. Laplace's Law states that vascular wall tension causes an increase in vessel wall pressure (Srivastava et al., 2010). The surface pressure exerted by bandage of

compression therapy device onto the surface of cylindrical vessel can be computing by using the Laplace's Law in Equation 1.1 (Rotsch et al., 2011). The compression of pressure exerted by the compression of bandage is directly proportional to the tension, inversely proportional to radius of leg. Figure 2.2 shows the relationship between the pressure exerts to the lower extremity through compression bandage and radius of leg. From Laplace's Law, the small radius of leg exerts high pressure, and the big radius of leg exerts low pressure.

$$P = \frac{T}{R}$$

(1.1)

Where P represents pressure under the bandage, T is tension of compression bandage and R represents radius of leg.
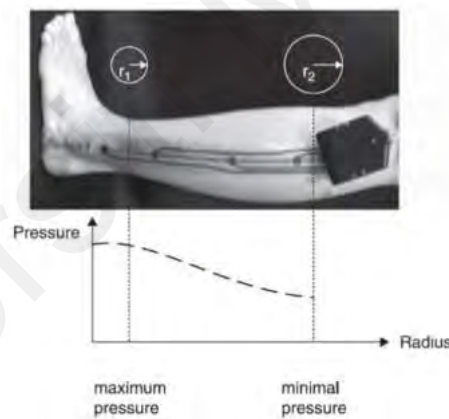
Figure 2.2: Pressure flow on the lower extremity based on Laplace's Law adapted from (Rotsch et al., 2011).

Pascal's Law describes the pressure distribution within the container filled with non-compressible fluid and enclosed by rigid material. Increasing pressure at any point on the leg resulting equal value of pressure at every other point in the leg. For instance, in the covered compartment like bandage, the pressure will be equally distributed on the lower limb during compression therapy. Soft tissues in the human body acts as incompressible fluids (Schuren & Mohr, 2010). The compression applied to one part of the leg will affect

the pressure in all directions, potentially aiding in the redistribution of fluids and improving circulation. Human epidermis is extensible. As a result, it can absorb force generated by functional activity or compression of external pressure distributed equally, thereby enhancing vein flow. However, these factors influence the compression therapy pressure:

a) Stiffness of the bandage

The stiffness of the bandage is the ability to resist deformation under stress. The relationship between the tensile force and bandage stretch is crucial elements in stiffness. It can differentiate between elastic and inelastic substances. The European Centre for Standardisation defines stiffness as the rise in pressure induced by muscle contraction per centimeter of augmentation in leg girth, conveyed in hectopascals per centimeter and/or millimeters of mercury per centimeter. (Partsch et al., 2016). Table 2.1 shows the stiffness categorization as per the European Center for Standardization.

Table 2.1: The stiffness categorization according to the European Centre for Standardization. Retrieved from (Partsch et al., 2016).

Stiffness	Pressure (mm Hg)
Low	0-2
Medium	2-4
High	4-6

a) Elasticity

Elasticity is the ability of bandage to return to its original size after the pressure has been reduced (Whitaker, 2012). The optimal materials utilized for compression treatment are elastic. The contrast between elastic and non-elastic compression materials relies on the maximum extent of stretch. Materials with a stretch capacity exceeding 100% are

consider elastic and less than 100% consider as inelastic (Partsch et al., 2016; Wong et al., 2012). The effect on the pressure of the material elasticity depends on the position either in standing, supine resting, or walking. Muscle tightening and fluctuations in leg circumference result in elevated pressure beneath the compressive material. (Partsch et al., 2006; Rabe et al., 2018).

  b) Interface pressure

The interface of two surfaces between compression device and skin known as interface pressure (Mosti & Partsch, 2010). This pressure is exerted by compression material toward the lower limb. The effectiveness of interface pressure depends on the elasticity of compression materials and muscle activity. However, this relationship is not always linear. Developing the most suitable compression choice for individual clinical scenarios can be refined and contrasted with emerging compression systems. There are two commercially measurement device available which are Picopress and Kikuhime as well as piezoresistive pressure sensor (Chi, 2017). The level of compression for interface pressure can be adjustable depends on the symptoms severity (Rabe et al., 2018). It's crucial to provide just enough compression to effectively manage the injury without causing further harm or impeding circulation. Berszakiewicz et al.,(2020) summarized the optimal compression for interface pressure to ensure the greatest clinical benefit for lower limb therapy in Table 2.2. Pressures ranging from 10-20mmHg and 20-30mmHg have demonstrated effectiveness in reducing edema, enhancing venous flow, and promoting improved microcirculation. In the upright position, external compression must exceed intravenous pressure, which typically falls within the range of 60 to 100 mmHg, to impact venous hemodynamics. Nonetheless, maintaining external pressure above 60 mm Hg for prolonged durations may result in tissue damage. Therefore, there is a

consensus that effective compression therapy should replicate the physiological distribution of pressure, accommodating variations in body position (Partsch et al., 2016).

Table 2.2: Interface pressure and clinical effect for compression therapy for lower limb adapted from (Berszakiewicz et al., 2020).

Clinical effect	Interface pressure (mm Hg)				
	1-10	10-20	20-30	30-40	>40
Oedema reduction	√	√	√	√	√
Increased venous flow		√	√	√	√
Reduced venous diameter in a supine position		√	√	√	√
Improved microcirculation			√	√	√
Improved venous pump function			√	√	√
Improved venous emptying			√	√	√
Reduced vein diameter in a standing position				√	√

√ represents the ability to deliver the compression therapy

Diverse compression techniques have been developed in the form of multi-layered bandage wrapping, compression garments, compression stockings, and adjustable compression (VELCRO) wrap devices (Williams, 2016).

2.4.1   Compression Bandage

Compression bandages are commonly used in clinical settings to treat a variety of circulatory disorders. Application of compression to reduce symptoms of lower limb injuries is now commonplace in sports medicine (Franke et al., 2021). Due to the rising prevalence of venous disorders, compression therapy is commonly utilized to manage and alleviate conditions related to blood vessel issues. This includes the prevention and

treatment of conditions such as varicose veins, deep vein thrombosis, lymphatic edema, wound healing, and the reduction of pain (Youn & Lee, 2019). Bandages are typically composed of a single layer or multilayer with high stretch or low stretch. Figure 2.3 depicts various compression bandage application techniques with their respective overlap percentages.

Figure 2.3:Different application techniques: A - 2-layer spiral pattern (i.e. 50% overlapping); B - 3-layer spiral pattern (i.e. 66% overlapping); C – 3 layer spiral pattern adapted from (Chassagne, 2018).

The interface pressure administered by compression bandages or stockings is the most crucial aspect of the therapy and must be tailored to the pathophysiology of the patient. However, the required amount of pressure for treating various venous diseases is not well characterized. Fukushima et al., (2017) applied a pressure of 40 mmHg, as it is recommended to counteract intravenous pressure in the antigravity position and sub-bandage pressure tends to increase during exercise. Abe & Tsuji, (2021) applied multilayered compression bandages to the lower extremities with approximately 40mmHg pressure to determine the relative benefits of active exercise with compression therapy. Although the pressure levels were identical between the studies, there was a difference in the compression bandage used on the thigh, which was only 12 cm wide.

This limited width of the bandage might have led to a tourniquet effect due to the pressure being concentrated on a small area of the thigh.

The review found that compression bandage focuses mainly on venous leg ulcer treatment and recovery of post injuries. Limited effects on global measures of endurance performance have been observed. Research into the efficacy of compression bandage used in venous leg ulcer treatment has produced beneficial results when tested on patients with non-severe arterial impairment. Previous study investigating compression bandaging for venous leg ulcer patients have shown that high compression ranging from 40mmHg to 60mmHg significantly enhances the rate of full ulcer healing compared to no compression treatment (Conde Montero et al., 2020; Moscicka et al., 2019; Rabe et al., 2018). Treatment of venous disease suggests that higher pressure is more effective than lower pressure, with the efficacy varying depending on the measured parameter.

The use of conventional bandages can be time-consuming due to their multilayer nature and the need for short daily intervals, often requiring the expertise of a lymphedema specialist (Shallwani & Towers, 2018). Additionally, the coarse texture of these bandages may restrict the function of the lower extremity. There was also significant variation in bandage application, particularly when different operators were involved. Despite these differences, it was noted that a bandager tends to maintain consistency and repeatability in bandage application.

2.4.2 Compression Garment

The significance of blood flow in sport and exercise performance has led to an increase in the use of compression garments as an ergogenic aid to enhance performance and facilitate recuperation in the sporting environment. Compression garments are designed to apply progressive external compression to a limb, with pressure typically increasing from the distal to proximal regions of the limb enclosed. Compression garments offered

by manufacturers of athletic apparel include stockings, shorts, tights, and arm sleeves. Different levels of pressure are designed into these garments, which are determined by their mechanical characteristics. The review found that compression garments during exercise have limited effects on global measures of endurance performance but may improve some sport-specific variables. While most muscle proteins/metabolites are unchanged with compression garment use during exercise, blood lactate tends to be lowered. Compression garments for recovery have a positive benefit on cool-down period after endurance and are associated with reductions in lactate dehydrogenase and perceived muscle soreness. All these findings are based on the type of garment and level of compression pressure used. Leabeater et al., (2022) analyzed a total of 160 articles to assess the effectiveness of compression garments (CGs) during and after exercise.

A study conducted by Castilho Junior et al., (2018) reported graduated compression stockings (GCS) improved venous lower limb hemodynamics. This study found that wearing GCS with low-grade compression (20-30 mmHg) enhanced the heamodynamics of a healthy amateur runner during a 10 km treadmill run. Subsequently, Ehrström et al., (2018) reported wearing high pressure compression garment during downhill running provide mechanical protective effects on soft tissue vibration and perceived muscle soreness contributing to enhance muscle recovery. Mechanical protective effect could be an external strategy for runners, particularly to tolerate a high training load or to optimize recovery in multi-stage races.

2.4.3   Pneumatic Compression

Pneumatic compression devices also have been introduced for patients who are unable to use the compression garment (Dunn et al., 2019). A more recent advancement in the application of compression in athletics is the utilization of pneumatic compressive devices as a recovery tool. The popularity of pneumatic compression devices has

increased due to their ability to combine compression with massage. However, despite widespread reports and marketing claims promoting their effectiveness as recovery aids, there is limited scientific evidence to support their actual benefits. Similar to compression garment, intermittent pneumatic compression (IPC) has been used for treatment of lymphedema and posttraumatic edema. However, the key distinction lies in IPC's is the ability to apply much higher levels of pressure to the affected area compared to commercially available compression garments.

Furthermore, IPC simulates the anatomical muscle-venous pump by mechanically squeezing the limb through inflatable cuffs in a sequential pattern from distal to proximal. Ren et al., (2022) reported that intermittent pneumatic compression (IPC) proves to be a successful method for enhancing peripheral circulation in the lower limb. This research recruited 24 participants, some with and some without diabetes mellitus (DM), to undergo three distinct protocols of intermittent pneumatic compression (IPC) applied to the foot at pressures of 60, 90, and 120 mmHg. Laser Doppler flowmetry was used to measure the foot skin blood flow (SBF) responses during and after the IPC interventions. The findings indicate that IPC interventions with pressures of 60, 90, and 120 mmHg can enhance foot skin blood flow responses in individuals without health complications. However, only interventions employing pressures of 90 and 120 mmHg demonstrate efficacy in ameliorating foot microcirculation in individuals diagnosed with type 2 diabetes mellitus.

Moreover, research on evaluating IPC for exercise recovery and performance is limited with various methods used to assess its effectiveness. Zuj et al., (2019) discovered a trend towards increased limb blood flow during cycling exercise with the use of IPC (70mmHg) during recovery when compared to no compression. The authors assessed 12 young healthy individuals to determine superficial femoral artery blood flow responses using doppler ultrasound. This was further supported by Sakai et al., (2021) who reported an

increase in peak velocity of superficial femoral vein measured by doppler ultrasound during active ankle exercise with IPC in 20 healthy subjects. However, both authors did not report on performance measures.

Although IPC is an effective technique for improving circulation, the pressure and duration of the intervention may also contribute to the therapy's effectiveness. Traditional pneumatic compression modalities typically follow a predetermined mode, resulting in limited treatment options for both patients and physicians during practical operation. Rosalia et al., (2021) developed an innovative soft robotic device for lower limb compression therapy, particularly for lymphedema treatment. This breakthrough builds upon the approach first pioneered by Low et al., (2019) enabling the tailoring of actuation intensity and movement according to user input. Recent developments in soft robotics have shown promising capabilities in the field of assistive rehabilitation, including the use of soft pneumatic actuators (SPAs) for compression treatment of human limbs and joints (C. Thalman & Artemiadis, 2020).

Recent studies listed in Table 2.3 demonstrated the effectiveness of compression therapy in recovery in improving blood flow and recovery. However, recent investigation into the effectiveness of compression therapy for promoting recovery have yielded inconsistence result. Struhár et al., (2018) shows the use of medium grade compression garment increase in running performance and decreasing muscle soreness within 24-hour post exercise. Heiss et al., (2018) demonstrated that compression garments can manage muscle rigidity, correlating with delayed-onset muscle soreness (DOMS) and perceived discomfort, but do not seem to influence muscle perfusion; Rosalia et al., (2021) found that wearing compression sleeves after exercise may effectively reduce DOMS, while Butani et al. (Butani & Hima, 2017) showed that wearing compression garments during sleep at night can improve muscle force output, but not sEMG (surface

electromyography). These studies highlight the potential benefits of using compression therapy for managing DOMS and improving muscle function. Although there are differing interpretations regarding the effectiveness of compression garments for muscle recovery, there is potential for these garments to be useful in this area. Three of the studies reported that compression therapy is effective in improving blood flow to the affected areas. These findings suggest that compression therapy can be a valuable treatment option for various medical conditions that benefit from improved circulation, such as venous insufficiency, lymphedema, and deep vein thrombosis. The consistent results across these studies highlight the importance of compression therapy as a non-invasive and cost-effective approach to managing these conditions (Dolibog et al., 2022; Gibbons et al., 2019; K.A. Zuj, Prince, R.L. Hughson, 2019).

In summary, compression therapy has been shown to be a successful way of rehabilitation that focuses on the limb systemic circulation and for preventing deep vein thrombosis. Compression therapy ability to speed up muscle recovery is still unknown, as some researchers have found it beneficial while others have found it to be ineffective. Nevertheless, the therapy still holds some potential as the pressure applied by the garment might not be adequate. Therefore, to better understand the effectiveness of intermittent pneumatic compression, further research is needed to identify optimal protocols for using the treatment for various injuries and medical conditions, as well as to investigate the mechanisms of action involved.

Table 2.3: Compression Therapy for Rehabilitation.

Author/ Year	Compression Therapy	Site of Application	Treatment for	Participants	Variable Analyse	Outcome
(Zuj et al., 2019)	Intermittent Compression therapy (Pressure of ~70 mmHg) applied during the diastolic phase of the cardiac cycle	Lower leg	Exercise and post exercise recovery	8 participants (4 male)	Superficial femoral artery (SFA) blood flow, Hemoglobin concentration, Vascular conductance, Heart rate (HR)	Enhanced vascular conductance during exercise and elevated postexercise SFA blood flow and tissue oxygenation during recovery.
(Struhár et al., 2018)	Compression garments with low, medium grade and high reverse grade compression	Ankle to knee	Performance and recovery for running	10 trained male runners	Creatine kinase, muscle soreness, ankle strength of plantar/dorsal flexors and mean performance time	Increase in running performance and decreasing muscle soreness within 24-hour post exercise with medium grade compression garments.

Table 2.3 continued

Author/ Year	Compression Therapy	Site of Application	Treatment for	Participants	Variable Analyse	Outcome
(Gibbons et al., 2019)	Intermittent compression during local diastolic phase	Leg	Orthostatic stress	7 male and 7 female	Blood circulation in superficial arteries, average arterial pressure, doppler ultrasound cardiac output	Intermittent compression represents a viable therapeutic approach for orthostatic stress.
(Butani & Hima, 2017)	Compression garment during night sleep	Lower Limb	Recovery from muscle fatigue	17 healthy male students	Maximum isometric contraction force for knee extensor, surface electromyograph (sEMG)	Utilizing compression attire while sleeping resulted in increased muscle strength, though there was no notable variance in sEMG
(Dolibog et al., 2022)	Intermittent Pneumatic Compression (IPC)with 12 and 60 mmHg at the ankle	Ankle	Venous ulcers	18 venous ulcers patients	Changes in size of ulcer	IPC is effective against lower limb venous ulcers

2.5   Soft Robotic for Rehabilitation Therapy

Soft robotics is a subfield of robotics that focuses on creating robots made of soft and flexible materials, such as silicone or elastomers, instead of rigid materials like metal (Rus & Tolley, 2015). Soft robotics typically use pneumatic or hydraulic systems to generate movement (James Walker, Thomas Zidek , Cory Harbel , Sanghyun Yoon, F. Sterling Strickland, 2020). It can be designed to mimic the movement of natural organisms or to perform specific tasks in unique environments.

Soft robotics has the potential to enhance the recovery process of patients through the development of novel and inventive techniques. The advantage of soft robotic assisting device over conventional rigid robotic is the ability to interact with human bodies safely (Su et al., 2022). However, the rigid design of conventional rehabilitation robotics makes it challenging for patients to have a positive experience while using them, and if the machine malfunctions, it is likely that the patient would suffer significant damage (Peng & Huang, 2019). Table 2.4 shows the comparison of advantages and disadvantages between soft robotic and conventional rehabilitation robotic.

Table 2.4: The comparison of advantages and disadvantages between soft robotic and conventional rehabilitation robotic.

Type of robotic rehabilitation	Advantages	Disadvantages
Soft robotics	- Made from flexible material and can be operate by continuous deformation (Filippini et al., 2008). - Ability to emulate human body (Shepherd et al., 2011) - Able to distribute forces equally over large contact of surface area (Deimel & Brock, 2013; Majidi, 2014; Polygerinos et al., 2017). - Safe to interact and interface with human as assistive device (Ansari et al., 2017; Manti et al., 2016).	- Do not consist of rigid joints or a fully mechanical system to complete actuation (Lee et al., 2017). - Unable to withstand heavy loads and survive a large quantify of actuation (Ashuri et al., 2020).
Conventional robotics	- Have rigid components connected to discreet joints with relative ease (Ashuri et al., 2020). - Made of hard materials with invariable properties (Alici, 2018).	- Do not have ability to perform in variety condition as it made from hard materials with invariable properties (Rossiter & Hauser, 2016). - Unsafe, intolerable, and unable to function in unknown conditions without proper control systems (Alici, 2018).

Soft robotics can be designed to assist with a variety of rehabilitation tasks, such as providing passive or active movement assistance, improving range of motion, and enhancing kinesthesia (Akbari et al., 2021). For example, soft robotic can be used by patients to aid with walking or arm movements (Bardi et al., 2022; Morris et al., 2023). Soft robotic systems are also regarded as safer for human interaction, as they refrain the use of rigid motors or gears for activation. Instead, they utilize methods such as pneumatic mechanisms, nematic elastomers, magnetorheological elastomers, chemical processes, shape memory alloys (SMAs) and fluid-based activation to regulate the flexibility of their soft components. (Christianson et al., 2018; H. T. Lin et al., 2011; Mazzolai & Mattoli, 2016; Shepherd et al., 2011). A variety of actuation techniques and materials exist, yet there is no established standard protocol for characterization. Consequently, the selection of suitable parameters is crucial to facilitate a deeper understanding and effective benchmarking of these techniques.

2.6   Soft Pneumatic Actuators (SPA)

Soft actuator is an integral part of soft robotic devices. The common mechanisms that activate the soft actuators includes tendon/cable-driven and pneumatic based mechanisms (C. Thalman & Artemiadis, 2020). Recent development shows pneumatic-based soft robotics have a certain advantage compared to the currently available actuation mechanisms (Cappello et al., 2018). Soft pneumatic actuators (SPA) have been widely utilised in the medical field and rehabilitation due to their light weight, flexibility, and good compatibility in human-machine interaction. Pneumatic compression mechanisms commonly utilize singular or multiple pneumatic chambers or bladders to create diverse compression patterns through the control of air during inflation and deflation phases. This encompasses a range of soft pneumatic actuators (SPAs) constructed from linear or non-linear soft materials, intended to deliver a variety of predefined movements or forces.

The power transfer medium for soft pneumatic actuators is air (Pan et al., 2022). Because of its low viscosity, high compressibility, accessibility, and low cost, compressed air is the most often used medium. Compressible air is used in pneumatically powered systems to provide changeable stiffness inside certain actuators (C. Thalman & Artemiadis, 2020). Guan et al., (2020) presented soft pneumatic actuators (SPA) in compression therapy that can expand due to air pressure. This design has shown promise in the treatment of chronic venous insufficiency and lymphedema with proactive pressure delivery at a variety of dosages. C. M. Thalman & Lee (2020) invent a fabric-based pneumatic actuator-driven soft robotic ankle-foot orthosis (SRA-FO) exosuit. This exosuit offers ankle support for inversion and eversion as well as contributes to gait rehabilitation, The findings revealed that exosuit may successfully adjust eversion stiffness at the ankle joint from roughly 20 to 70 Nm/rad at relatively low-pressure level. Each motion of forces on the limbs had its own actuator unit in this device. Shape deposition and 3D printing are two approaches for fabricating this type of actuator (Yap, Lim, et al., 2016).

2.6.1   Fabric-based Soft Pneumatic Actuators

Textile fabrics are compliant, lightweight, and inherently anisotropic by nature, making them promising material for the design of soft pneumatic actuators. Recently, these actuators were proposed for use in the design of soft actuators for assistive gloves (Heung et al., 2019) and neuromuscular rehabilitation devices for upper and lower extremities (Belforte et al., 2014). The actuators utilized knit materials with varying levels of textile stretching to induce specific types of motion, particularly bending motion. Yap et al., (2017) exploited fabric to design actuators for hand assistance and rehabilitation training by offering finger extension and flexion with minimal air pressure. The deformation of the flexion actuators was controlled by a folded chamber structure. The kind of actuators can generate forces and torques to support bidirectional movement

including flexion and extension. Figure 2.4 depicts a fabric-based flexion actuator with a corrugated fold. When pressurized, the corrugated fabric layers expand and unfold. The third fabric layer serves as a strain-limiting layer, constraining the actuator's bottom surface's elongation.

Figure 2.4: A fabric-based flexion actuator with corrugated fold adapted from (Yap et al., 2017).

SPA also known as Pneumatic Artificial Muscles (PAMs) consist of a deformable inflatable chamber that can be reinforced with inextensible fabrics (Cacucciolo et al., 2016), or stiff rings (Manuello Bertetto et al., 2016). The materials utilized differ based on the shape of the inflated chamber and how the reinforcing material is organized on its surface. The pressurization induces chamber expansion in the low stiffness direction, resulting in a pushing or pulling force and axial, bending, or torsional deformations (Kojima et al., 2021) Fabric based actuators are commonly developed to assist hand impaired patients in rehabilitation exercises and performing activities of daily living.

Kojima et al., (2021) developed the straight-fiber-type artificial muscle actuators with a rubber tube that contains reinforcing fibers arranged in the axial direction. Due to the

restraining effect of the reinforcing fiber, when air pressure is applied to the rubber tube, the artificial muscle undergoes radial expansion while contracting in the axial direction. Furthermore, the actuators developed by Deimel et al. (Deimel & Brock, 2013) incorporated radially inserted fibers to stabilize the actuators' shape during inflation, leading to finger bending instead of radial expansion. To maintain the intended configuration of the finger during pressurisation, the base of the finger was constrained with an inelastic material, ensuring that another portion of the finger remained extended.

The inflation of actuators can be challenging for higher force applications, like shoulder and ankle assistance, as it may cause excessive ballooning of the textile at higher pressures, leading to potential failure (O'Neill et al., 2022). Therefore, inextensible woven textiles are a preferable option for systems aiming to deliver higher levels of assistance. The design of these fabric-based actuators usually involves an iterative process due to the complexity of predicting the soft and compliant behavior of the textiles. Thus, suitable techniques to predict behavior and final shape of a range of elastomer-based inflatable actuators is needed.

Finite element modelling has been employed in recent study of knitted textile actuators for wearable applications. Nesler et al., (2018) and Fang et al., (2020) presented an approach to predict behavior of textile-based actuators by modelling the energetics of inflating the actuator. They developed a model that predicted the torque output of the actuator as a function of the fluidic input by assuming that the textile behaved as an inextensible membrane. The advantage of this technique is that it gives a highly general methodology for modeling any fluidic actuator behavior, independent of the exact mechanism of actuation and the actuator's material properties.

2.6.2 Silicone-based Soft Pneumatic Actuators

Silicon-based SPAs have been very popular, since they provide solutions to many applications that require comfort and safety. The unique mechanical properties and good biocompatibility of silicone elastomer have sparked great interest in research for fabrication of soft actuators. Silicone rubber is a highly flexible elastomer with high temperature resistance and low temperature flexibility. Elastomers have the remarkable ability to endure extensive strains exceeding 500% without experiencing permanent deformation or fracture (Xavier et al., 2021). Among the soft robotics community, the silicone rubbers most commonly used include Ecoflex (Shore Hardness 00-10 to 00-50) (Smooth-On, 2015), DragonSkin (Shore Hardness 10–30 A), Smooth-Sil (Shore Hardness 36–60 A) ,Elastosil M4601 (Shore Hardness 28A) (Elastosil et al., 2021) and Sylgard 184. Figure 2.5 show the shore hardness scale for silicone rubbers in soft robotic and Figure 2.6 show uniaxial tensile testing results.
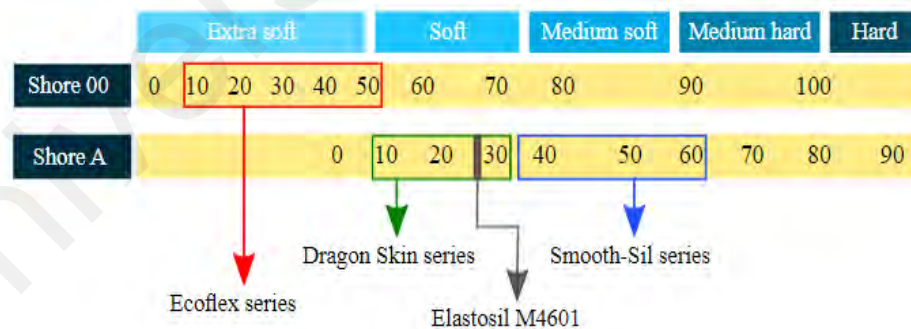
Figure 2.5:Shore hardness scale for silicone rubbers in soft robotics adapted from (Xavier et al., 2021).
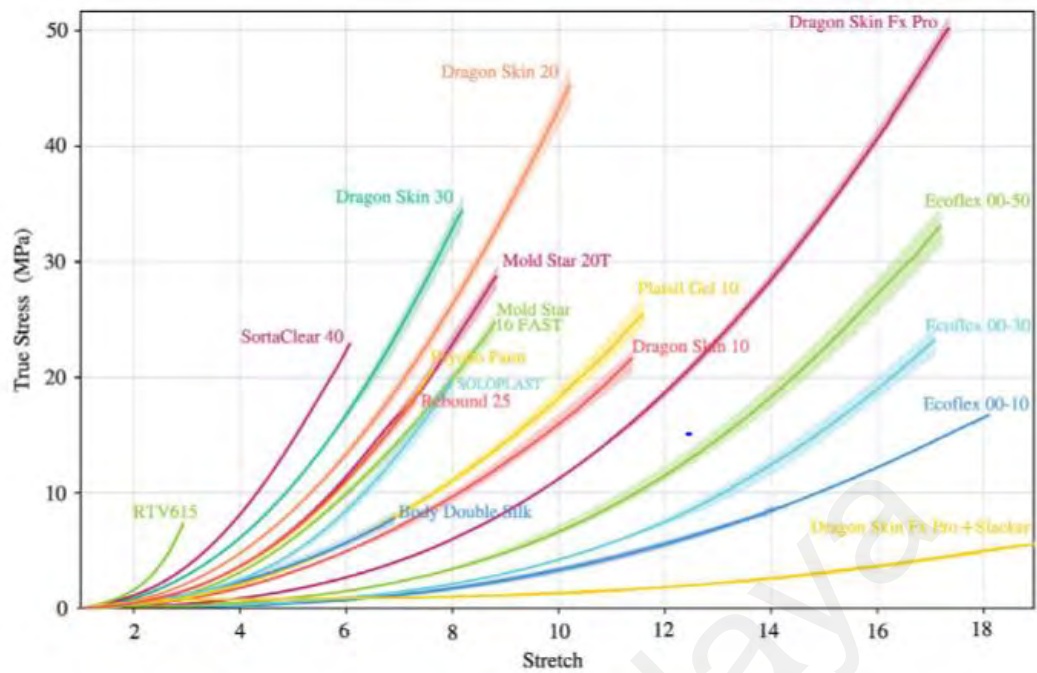
Figure 2.6 : Experimental uniaxial tensile stress–stretch pull to failure responses for a selection of silicone rubbers adapted from (Xavier et al., 2021).

The fabrication process of silicone-based soft pneumatic actuators (SPA) typically involves multi-material fabrication, where different rubber compositions are used. For instance, a silicone rubber with high stiffness might be employed for the bottom layer of the actuator. The subsequent technique is the multi-chambered or PneuNet actuator, where folds on one side of the actuators expand when subjected to pressure (Borman & Koyuncu, 2020). The performance of these actuators can be assessed through a combination of experimental measurements and finite element modeling and analysis.

Agarwal et al., (2016) introduced a new soft pneumatic actuator idea based on shell-reinforced patterns and a single air chamber constructed of a highly elastomeric material to allow bending and linear motions. Finite element analysis was employed to optimize design parameters, anticipated actuator performance and behavior. Despite employing the Ogden model to represent the nonlinear behavior of the air chamber in the actuators, a linear elastic model is used to represent the deformation of the shell. Mohammadi et al., (2020) developed an analytical model to predict the quasi-static bending displacement of

pneumatic actuators comprising discrete pneumatic chambers made of two different elastomeric silicones (Elastosil M4601). The gray box model was utilized and validated using experimental results. Moreover, Sun (2017) fabricated a hybrid type of material combining non stretchable material and silicone with customizable aggregated elasticity. The authors used modelling and tensile test to study the material stiffness distribution. Stiffness distribution is a crucial design factor in SPA engineering. By strategically arranging the material stiffness throughout the SPA body, we can create SPAs with unique and specific properties.

Different fabrication techniques also influence the performance of SPA. Yap, Technologies, et al., (2016) utilized a low-cost printer based on fused deposition modeling to fabricate soft actuators with pneumatic chambers. They used a soft commercial material called Ninjaflex (Shore Hardness 85A) to fabricate soft actuators with pneumatic chambers. The fabricated SPA has low durability and requires high actuation pressure with constant stiffness. While direct fabrication can reduce the time-consuming process of constructing the actuation chamber, the resulting actuator tends to have lower displacement output and, consequently, lower force output. In soft actuators, pressure and durability are couple, the lower the pressure the higher the is the durability. Sparrman et al., (2021) study three types of SPA fabrication technique using silicone elastomer including cone casting, multi-material polyjet printing, and Rapid Liquid Printing (RLP). These actuators are tested for elongation and fatigue behavior through cycling and force. The results demonstrate that RLP actuators have excellent cycling performance, performing better than cast and multi-material polyjet printing actuators in terms of robustness and predictability.

Due to the wide range of fabrication techniques and materials available for soft pneumatic actuators, there is currently no standardized protocol for performance

assessment. As a result, researchers need to choose suitable parameters to gain better insights and to establish benchmark testing procedure for pneumatic soft actuators based on application needed. However, regardless of the SPA's usage in rehabilitation, the challenge of creating it with biocompatible materials and ensuring safety for both people and the ecosystem has proven to be ongoing. Current research aims to create adaptable programmable motion, drawing inspiration from biological features, to seamlessly integrate natural flexibility with controllable actuation (Coyle et al., 2018; Craddock et al., 2022; Miriyev et al., 2017).

Table 2.5 presents a summary of the recent developments in soft pneumatic actuators. The focus of the research primarily revolves around designing and fabricating the SPA, as well as developing dynamic pressure delivery and feedback systems. The outcomes of the studies include the establishment of fluid-structure coupling models to guide SPA designs, validation of dynamic pressure delivery and feedback systems for future compression therapy applications, and clinical trial results demonstrating improved venous blood flow with a robotic sock compared to conventional IPC devices (Guan et al., 2020; Zhao et al., 2019). Moreover, Konishi & Hirata, (2019) concentrate on the integration of temperature sensors with their micro finger soft pneumatic actuator. The successful integration of the flexible temperature sensor into the soft pneumatic actuator is characterized to verify the sensor's functionality remains intact during the deformation and actuation of the micro finger. These studies focus on clinical trials and testing mechanisms of soft pneumatic actuators. On the other hand, .H. T. Lin et al., (2011) designed self-sensing pneumatic actuators for a hand gripper robot and robot joint, using two different membrane materials and positive-negative pressure combined actuation, which effectively resisted and detected impacts. They demonstrated the broad application of this soft actuator by designing a two-digit robotic hand and joint. Another study by Suarez et al., (2018) focuses on designing of a soft pneumatic fabric-polymer bending

actuator. The study aims to create an actuator that can bend by inflating a pre-shaped fabric-based element and to provide a proof-of-concept system for lymphedema treatment. The actuator achieved a free bending of about 1.5 cm in the proof-of-concept system.

Table 2.5: Application of Soft Pneumatic Actuators.

Author/Year	Actuator	Application	Focus	Outcome
(Guan et al., 2020)	Soft pneumatic actuators (SPA)	Intermittent pneumatic compression therapy	Developing and verifying a fluid-structure coupling model that describes the interaction between SPA and the lower limb.	The verified fluid-structure model will prove valuable in informing SPA design processes.
(Guan et al., 2020)	Soft pneumatic actuators (SPA)	Intermittent pneumatic compression therapy	Designing a customizable dynamic pressure delivery and feedback system.	The validated system for delivering dynamic pressure and providing feedback is deemed suitable for leading the way in future compression therapy applications.
(Low et al., 2019)	Soft pneumatic actuator sock	Intermittent pneumatic compression therapy for preventing deep vein thrombosis	Clinical study comparing the robotic sock to traditional IPC devices.	The robot-assisted sock enhances venous blood circulation during ankle joint exercises in the initial stage of usage.
(N. Lin et al., 2020)	Self-Sensing Pneumatic Actuators	Self-sensing vacuum soft actuation for hand gripper robot and robot joint	Designing quasi-static models for actuators composed of two distinct types of membrane materials utilizing combined positive-negative pressure actuation	The actuators demonstrate efficient resistance and detection of impacts. The utilization of this elastic actuator in designing a robotic hand and robotic joint underscores its extensive utility.

Table 2.5 continued.

References	Actuator	Application	Focus	Outcome
(Suarez et al., 2018)	Soft Pneumatic Fabric-Polymer Actuators	Soft Pneumatic fabric-polymer bending actuator as a base component for a robotic device for lymphedema treatment	Designing actuator capable of bending by inflating pre-shaped fabric-based element and proof-of-concept system for lymphedema treatment	The actuator achieved a free bending of about 1.5 cm in the proof-of-concept system to treat lymphedema
(Irshaidat et al., 2019)	Pneumatic Muscle Actuators (pMA)	pMA for Exoskeleton Arm in Post-Stroke Rehabilitation	Analysis, design, integration, and characterisation of the exoskeleton arm using Model Reference Adaptive Control (MRAC)	Portable exoskeleton arm can offer more effective intense rehabilitation therapies at home without the need to therapists
(Konishi & Hirata, 2019)	Soft pneumatic micro actuators with flexible temperature sensor.	Micro finger for biomedical applications	Fabrication and and analysis of soft pneumatic actuators with incorporated temperature sensors.	The successful integration of a flexible temperature sensor into the soft pneumatic actuator is confirmed through characterization, ensuring its functionality.

The optimal resolution for compression therapy should maintain optimal pressure levels, ensure adherence, and permit the user to live a virtually normal life while wearing the device. Recent research has proposed flexible pneumatic actuators for a variety of applications, but most studies focus on their implementation for compression therapy. Guan et al., (2020) conducted a study to explore the operational mechanisms between soft pneumatic actuators and the lower limb. to increase the efficacy of dynamic compression therapy in practice for the promotion of venous hemodynamics. This research produced fluid-structure coupling models and an intermittent pneumatic compression testing system, as well as an intermittent pneumatic compression testing system. The system comprised an SPA unit with numerous textile-laminated chambers, a pneumatic controller, and various types of pressure sensors and accessory components for real-time monitoring. The devised coupling model was able to characterize the SPA unit's dynamic behaviour. The model illustrated that the initial thickness, flexibility, and airflow of the SPA unit, along with the firmness of the limb tissues, influenced the interactions between the SPA and the lower limb, as well as the magnitude of pressure exertedIn alignment with data obtained from the IPC testing setup, these results expanded our understanding of the interplay between the soft pneumatic actuator and the lower limb.

Based on these investigations, one can deduce that the predominant emphasis of current research on soft pneumatic actuators lies in the design and production of the actuators themselves. Although some studies suggest potential applications for their designs, there is a lack of validation of their performance in specific applications.

2.7   Identification of Research Gaps

In conclusion, the works provide a comprehensive review of the existing research on compression-based rehabilitation therapy, soft pneumatic actuators, and potential methods for determining the efficacy of rehabilitation therapy. Currently, the

physiological effects of compression therapy on injured or fatigued muscles are inconclusive. Some studies have demonstrated that static compression via compression garments is beneficial to the localized circulatory system. However, other studies have suggested that dynamic compression via intermittent pneumatic compression devices may be more effective in providing pain relief and reducing the duration of delayed-onset muscle soreness (DOMS). However, there are presently insufficient studies in this field to support these claims. Based on the recent review, most of these studies focused on fabricating SPA using commercial silicone elastomer with reinforced fabric. As discussed in Section 2.5, the development of the SPA by integrating biocompatible components is elusive. To bridge this gap, this study will explore a food-grade silicone soft pneumatic actuator (SPA) model with varying actuation strength and motion. This innovative approach aims to achieve improved performance of soft actuators while ensuring safety for human use.

Furthermore, while there is ongoing research in developing soft pneumatic actuators for compression therapy, the suitable materials and design in developing this device to delivere compression therapy is still poorly understood. Several studies have recommended using FEM to optimize design parameters and anticipated actuator performance and behaviour. To address this recommendation, the numerical analysis of SPA pressure performance will be conducted through FEM, guiding the selection of SPA material design and pressure dosage for therapeutic purposes.

The existing SPA models in previous works primarily focused on designing and fabricating the actuators themselves. Although some studies suggest potential applications for their designs, there is a lack of validation of their performance in specific applications. Experiment validation of these devices for lower limb musculoskeletal injury rehabilitation through compression therapy could provide valuable insights and aid

in strengthening the conclusions in this field of study. Therefore, this study explores the potential benefits and limitations of PSA for muscle recovery and injury rehabilitation.

To conclude this chapter, this thesis aims to propose a novel approach to enhance the performance of SPA and provide a valuable impact in lower limb rehabilitation therapy. With the implementation of Finite element modeling (FEM) for modeling and simulating soft robotic components. Numerical analysis of SPA pressure performance offers the potential to guide the selection of SPA material designs and therapeutic pressure dosages. These simulations can facilitate rapid and efficient iterations across diverse designs and materials, thereby contributing to the enhancement of their functionalities (Mourtzis, 2020) This impacts the treatment's efficacy, user comfort, and the frequency of its application. The main gap lies in the potential application of SPA for providing therapy for lower limb injuries. By employing an appropriate method to evaluate the efficacy of SPA that can interact safely with humans, it is possible to obtain valid and reliable results for evaluating the performance of soft actuators in musculoskeletal injury recovery.

CHAPTER 3: METHODOLOGY

3.1   Introduction

This chapter describes the development of the proposed Soft Pneumatic Actuator (SPA) systems. SPA has been widely utilized in the medical field and rehabilitation due to their light weight, flexibility, and good compatibility in human-machine interaction. Most of the research has utilized SPA as a method for applying compression to human limbs and joints. However, there are challenges in developing SPA using biocompatible materials and exploring their potential applications in rehabilitation. In this study, the efficiency of the proposed SPA was assessed through simulation analysis and experimental testing conducted on healthy participants. These validation methods were employed to evaluate the performance and effectiveness of the SPA. Section 3.2 explains the development of the SPA covers the materials and method used for the 3D modelling construction and simulation. Section 3.3 focused on the design testing of the SPA for lower limb rehabilitation, where fabricated SPA chambers were used to conduct experimental analysis simulating actual compression on a mannequin leg. Section 3.4 outlines the process of conducting experimental analysis and experimental validation on healthy participants to assess the efficiency of the SPA system for treating fatigue in calf muscles induced by exercise. In this section, the criteria for the selection of participants, the instrument used, and the experimental procedure are explained. Lastly, Section 3.5 explains the statistical analysis that was utilized to evaluate the patterns and trends of various parameters, such as muscle stiffness, calf circumference, and Mc Gill pain scores, for all subjects in both the control and intervention groups.

3.2   3D Modelling of the Proposed SPA

The soft robotic toolkit was employed to create the conceptual framework of the SPA (Soft Robotics Toolkit, 2017). The actuators were made up of two silicone parts: the main body and the bottom layer as shown in Figure 3.1(a). The main body was composed of

several chambers powered by a pressure source and inflated upon actuation as depicted in Figure 3.1(b). The actuators were configured to have one extendable side (top layer), while the opposite side remained restricted or non-expandable (bottom layer) as depicted in Figure 3.1. The bottom layer of the silicone incorporated a non-extendable mesh fabric to limit deformation. Polyester plain English net mesh fabric with a thickness of 0.008 was employed. The fabric's thickness adequately restrained the deformation of the external layer. The fabric was selected based on various criteria, including its mesh structure designed to offer flexibility and breathability, ideal for accommodating the soft actuator's movements. Furthermore, the fabric's thin thickness was specifically chosen to mitigate the effects of extra pressure generated by the stretching of the fabric. Thus, a fabric with a comparatively lower extension capability than the silicone layer was chosen. This fabric has an insignificant effect on the soft actuator's deformation due to its location at the bottom layer of the SPA. This study focused on the deformation of the upper layer (chamber). This research primarily concentrated on the deformation of the upper layer (chamber). This reinforcement directs significant expansion to the upper part, where inflation is intended, effectively controlling the actuator's inflation. By strategically placing the fabric, the functionality of the actuator is enhanced, ensuring deformation is focused on the desired area while reducing unwanted movement elsewhere.

(a)

(b)
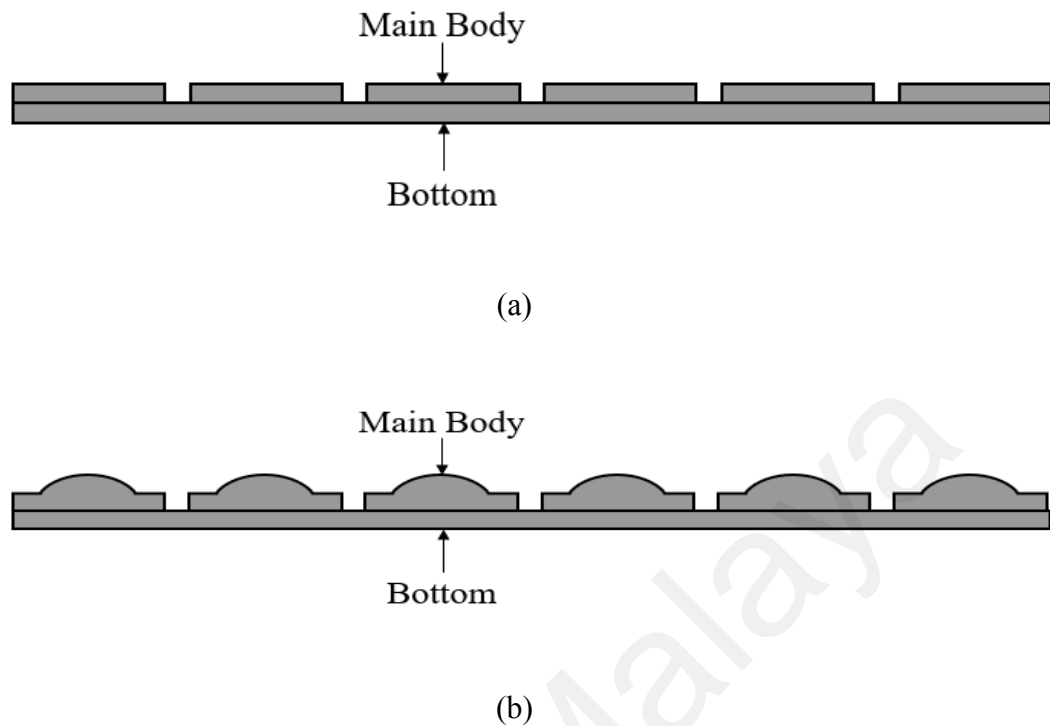
Figure 3.1: Schematic diagram of SPA with six airtight chambers in two states: (a)the resting state and (b) the state when they are inflated.

An investigation was conducted using a SPA model to assess the amount of pressure and the inflation time required by each chamber. Two distinct SPA models, referred to as Model A and Model B, were introduced to examine the amount of pressure and inflation time of each chamber. Model A featured six chambers and a single air inlet in Figure 3.2, whereas Model B was designed with six chambers with six separate inlets. The chambers for Model B were divided by a 10 mm gap and had a side wall thickness of 1 mm. as shown in Figure 3.3. Their configuration was adapted to the lower limb's anatomy, with the six chambers applying compression along both the posterior and anterior sections of the lower leg, thus minimizing dead volume. The integration of six vertically aligned chambers in both models was due to the complexity of the lower limb's anatomy, where diverse muscle groups and tissues are distributed across distinct regions. By dividing the compression into six chambers, each chamber can target specific areas more precisely.

This allows for tailored compression to address various muscle groups and areas of concern along both the anterior and posterior sections of the leg. Each chamber measured 65 mm in width and 190 mm in height, based on the average size of a man's calf circumference and height. A 6 mm-diameter air inlet was incorporated into the cuff shell to enable the chamber to be filled with adequate airflow from the pressure and maintain compatibility with standard fittings. As illustrated in Figure 3.2, each chamber was linked by a channel to facilitate fluid flow. The non-expandable layer of each actuator possessed a thickness of 3 mm. The bottom layer was flexible to reduce the overall rigidity of the actuators. Upon the application of pressure, the upper layer of the chambers achieved complete inflation, while the lower layer experienced minimal to no inflation.
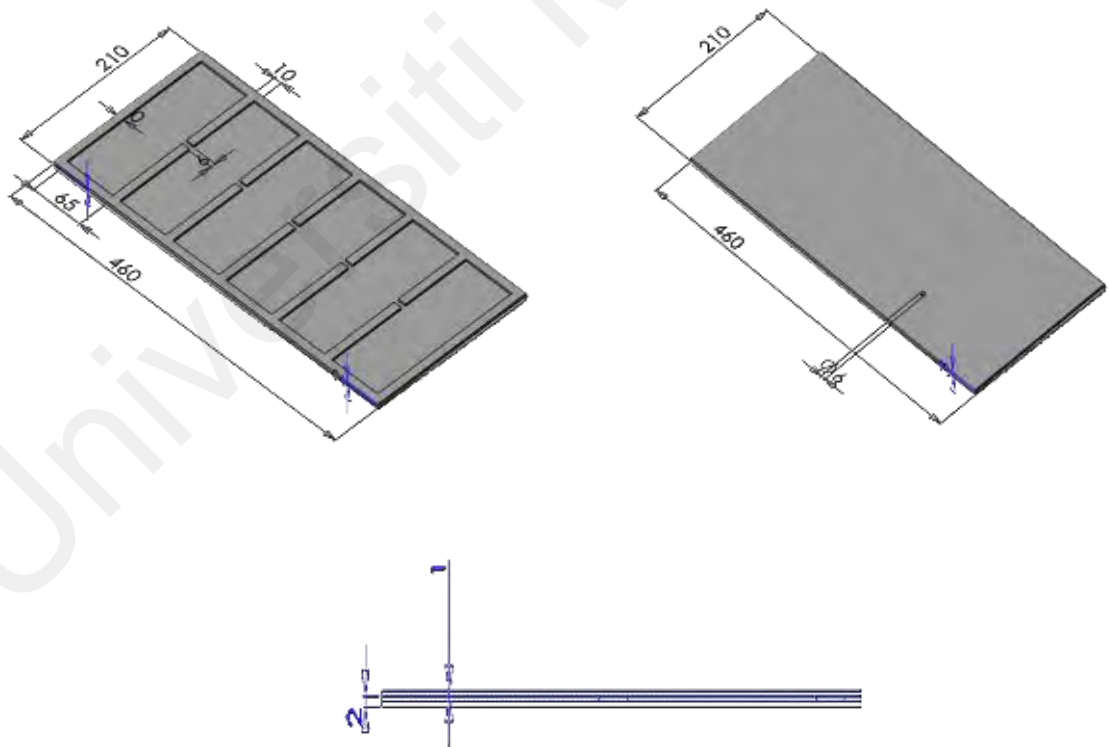
Figure 3.2: Dimension of 3D model construction of the proposed Model A SPA in mm: (a) top layer (b) nonexpendable bottom layer; and (c) side view.
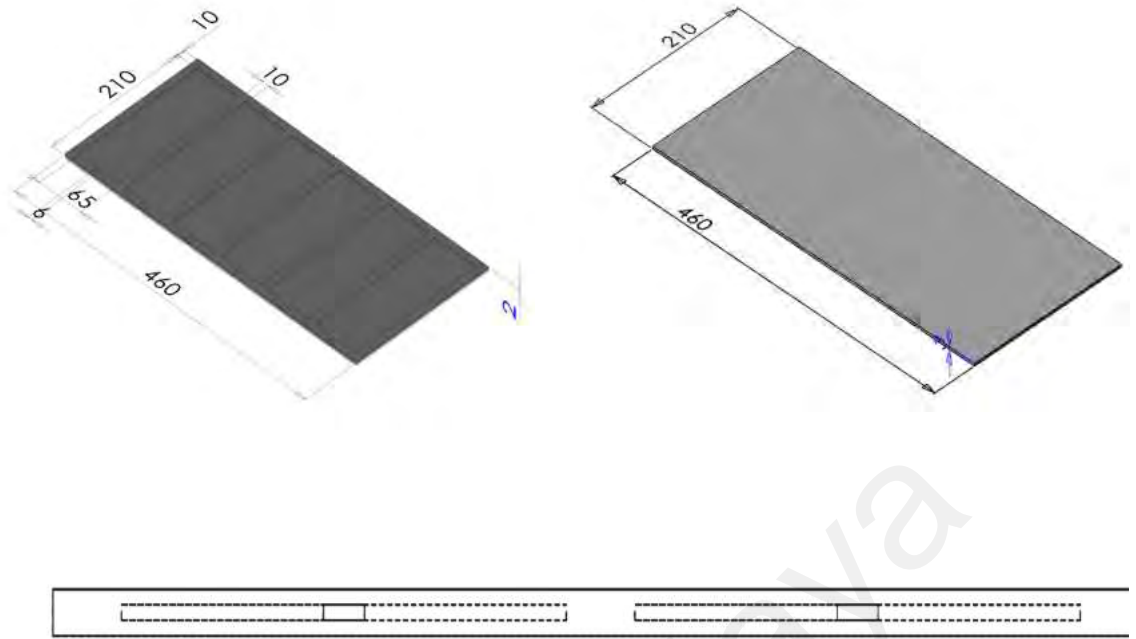
Figure 3.3: Dimension of 3D model construction of the proposed Model B in mm: (a) top layer (b) nonexpendable bottom layer; and (c) side view.

3.2.1 Material Properties and Characteristics

Selecting appropriate materials was a vital aspect of creating SPAs that were both biocompatible and non-hazardous. The common choice of materials for the 3D molding process in creating soft actuators is silicone elastomeric rubber. In this study, the properties of three different silicone-based materials were examined as exhibited in Table 3.1.

The elastomeric materials model was used to describe the behavior of the selected silicone, with the characteristic of absorbing large deformation without permanent distortion. The silicone elastomeric rubber demonstrated resilience against considerable strains, reaching up to 500%(Maruthavanan et al., 2021). Silicone rubber exhibits an elastic stress-strain curve with a non-linear relationship, displaying isotropic qualities, incompressibility, and a general insensitivity to strain rate. The most common non-linear constitutive model with incompressibility constraints, including the Neo-Hookean,

Ogden, Mooney-Rivlin, and Yeoh models, have been explored for hyperelastic material (Steck et al., 2019). the Mooney-Rivlin model primarily addresses small deformation ranges in rubber studies, whereas the Yeoh model takes precedence in wide deformation range investigations and is recommended for significant deformations (Xavier et al., 2021)

The Yeoh model stands out due to its simplicity and high accuracy, and the material properties can be determined through uniaxial compression tests. The strain energy density function for Yeoh's 3rd model is given by:

$$W = C_1(I_1 - 3) + C_2(I_2 - 3)^2 + C_3(I_3 - 3)^3 \qquad (3.1)$$

where C_1, C_2, and C_3 are model parameters, while I_1, I_2 and I_3 are strain invariants of Cauchy–Green deformation tensors, respectively. In this study, A15 Shore, A10 Shore, and Sylgard 184 were examined as the material of the proposed SPA system based on their noted characteristics, including flexibility, durability, biocompatibility, and tunability of mechanical properties, alongside their classification as non-hazardous food-grade silicone. These materials were selected for their suitability in soft robotics applications, offering desirable traits such as elasticity, resistance to fatigue, compatibility with biomedical settings, and the capacity for mechanical behavior customization. The constitutive model parameters for three silicone elastomers and their properties are tabulated Table 3.1. The Sylgard 184 model parameter was sourced from Laura et al. (2020) where the researchers where uniaxial tensile tests were employed to determine the parameters of the Yeoh models. In the ANSYS software (ANSYS 2019 R3), the A15 Shore is an elastomer. The model parameter values for A15 Shore were obtained from the ANSYS database ((Product, 2022) for the elastomer sample. A10 Shore shares characteristics with Dragon Skin 10 medium. The model parameters for A10 Shore were

acquired from Michele Di Lecce et al. (2022), who utilized Evolutionary Inverse Material

Identification (EIMI) for the parameter identification of Yeoh models.

The three-materials exhibit flexibility, stretchability, and affordability. These silicone

variants are remarkably robust against the effects of extreme temperatures and resistant

to deterioration, non-toxic, and biodegradable (Miriyev et al., 2017). However, to ensure

the most effective inflation and deflation of the proposed SPA, a lower tensile strength

was favored to mitigate potential prolonged discomfort during compression.

Table 3.1: Material properties and constitutive model parameters of silicone elastomer.

	Slygard 184	A15 Shore	A10 Shore
Manufacturer	Dow Corning	Clay Art	Clay Art
Color	Colourless	Translucent	Grey
Shore Hardness	A50	A15	A10
Tensile Strength	980 psi	537psi	475psi
Density	1.04 g/cm3	1.35 g/cm3	1.35 g/cm3
Elongation at Break	150%	771%	1000%
Durometer Shore	50	15	10
Young's Modulus	1.32–2.97 MPa	0.74 MPa	0.25 MPa
Model Parameter	$C_1 = 0.42480$MPa $C_2 = -0.15880$MPa $C_3 = 0.24350$MPa (Pini, 2020)	$C_1 = 0.69760$ MPa $C_2 = -0.24484$ MPa $C_3 = 0.12629$ MPa (Product, 2022)	$C_1 = 0.00204$ Mpa $C_2 = -0.17070$MPa $C_3 = 2.05000$ MPa (Di Lecce et al., 2022)

3.2.2   Simulation Parameters of The Proposed Soft Pneumatic Actuators

To ensure the optimal deformation of the proposed SPA, the pressure distribution of

the proposed 3D model and the proposed elastomeric materials (A15 Shore, A10 Shore,

and Sylgard 184) was analyzed using the finite element method (FEM). The 3D model of

the SPA was designed in Solidworks (Dassault Systèmes SOLIDWORKS Corp.,

Waltham, MA, USA) and then imported to ANSYS 2019 R3 for FEM analysis. It was

assumed that the proposed compression system with a chamber should be able to provide

homogeneous pressure regardless of the location of the cuff. For ensuring a balanced pressure, the air pressure was observed on the inner wall of the chamber. The SPA system for the analysis is shown in Figure 3.4 (a) with fixed supports surrounding all edges highlighted in blue to imitate real-life behavior. Gravity was also considered for the solid domain, and it acted in the negative y direction.

Since this study employed elastomeric material, a physics nonlinear mechanics mesh with linear element order was adopted. The mesh method used for the SPA system was a hex-dominated element shape. Curvature and proximity capturing were activated. The experimental element size was set at 1 mm for all simulations which resulted in a total number of 300,196 elements. This choice provides sufficient accuracy for capturing actuator geometry, resolving stress concentrations, and representing material properties in most soft pneumatic actuator simulations, while also striking a crucial balance with computational efficiency. Material properties in soft actuators are often heterogeneous and anisotropic. The use of 1 mm elements allows for a reasonable representation of these properties while remaining computationally feasible. The minimum element quality based on skewness was 0.90.

In this study, a controlled condition of 23 s of inflates, 7 s of hold, and 7 s of deflate (23–7–7 s) in one cycle cumulating in 37 s was simulated. The inflation and deflation of the SPA can be referenced respectively to Figure 3.4(b) and Figure 3.4(c). This method is a recommended treatment cycle by a commercially available intermittent pneumatic compression (IPC) device for daily home care of the lower limb (Guan et al., 2020). The pressure was applied using the ramp function, with the gradual increment of the pressure from 0 to 120 mmHg from t = 0s to t = 23 s. Furthermore, in each simulation, the pressure was applied progressively throughout 44 sub-steps. This was a crucial variable because it prevents the load from being delivered entirely at once, which often leads to convergence

problems, particularly when working with soft materials that have a low Young's modulus (Tawk & Alici, 2020).
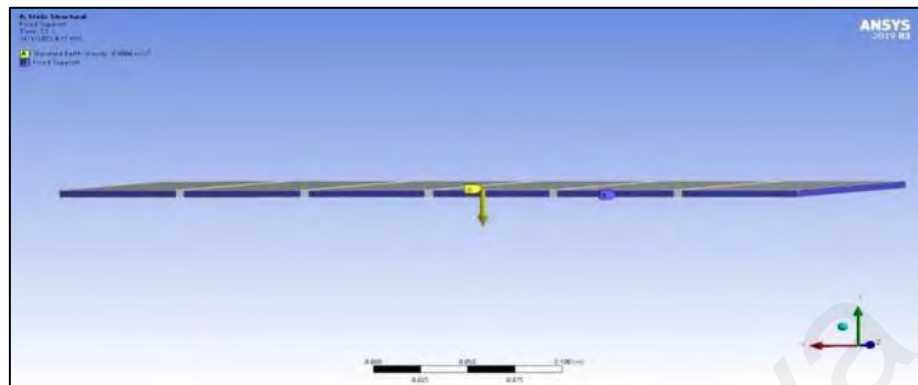
(a)
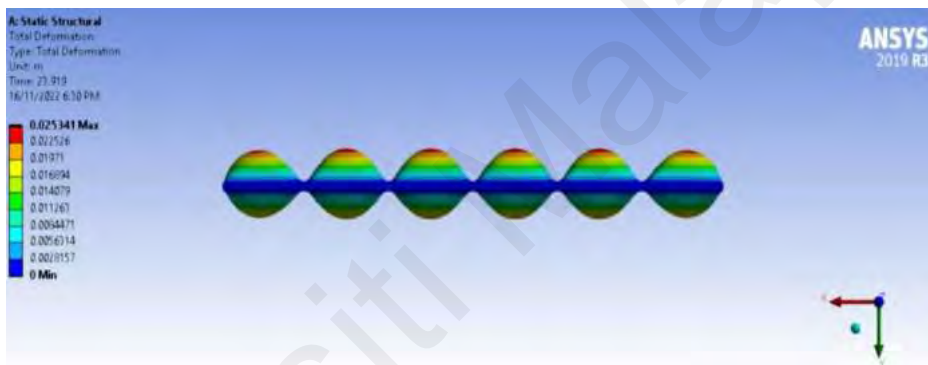
(b)
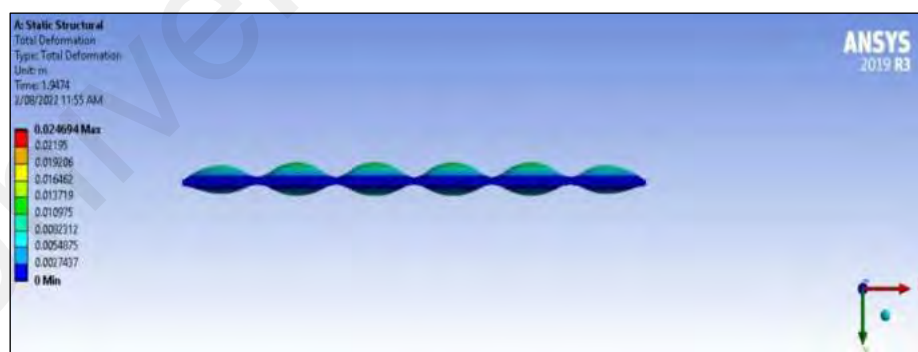
(c)

Figure 3.4: FEM simulation (a) setting for SPA chamber with fixed support surrounding the object and earth gravity applied in the negative y direction, (b) inflation and (c) deflation cycle of SPA chamber.

3.3   Design and Evaluation of SPA for Lower Limb Rehabilitation

After the 3D model design and simulation stages, the SPA chambers were fabricated for the experimental analysis. The experiment was conducted using the SPA chamber unit to resemble the actual compression. SPA made of food grade silicone A10 Shore and A15 Shore were used for compression therapy. The actuators comprise six chambers and a single air inlet. For the validation of the SPA system model, the obtained simulated and experimental results were compared for a better understanding of the fabricated SPA chambers. A sensor-based SPA system was developed, consisting of SPA, a SPA controller, and monitoring software as shown in Figure 3.5 and 3.6. The exterior layer of the chambers was laminated with a woven-based textile shell with a dimension of 210 (width) × 460 (length) to form the main part of the SPA unit. This was wrapped onto a mannequin leg for compression treatment simulation as depicted in Figure 3.5(a). According to Li et al., (2022) the mannequin leg demonstrated similar contact pressure patterns to the human leg. The force applied to the mannequin leg was measured to provide an accurate pressure reading. Force-sensitive resistor (FSR) was attached to the medial side of the lower leg, about 20 cm above the ankle, where the gastrocnemius muscle's tendinous and muscular parts separate as shown in Figure 3.5(b). Next, the pressure exerted on the skin by the SPA system on the force sensor was assessed using the formula below:

$$P = \frac{F}{A} \tag{3.2}$$

Where, F is the bio-mechanical force between the chamber and the skin surface. P is the pressure exerted on the skin, and A is the contact area between the chamber and the skin. In this study, the contact area was the area of the force sensor that in contact with the skin, which is:

$$A = \pi r^2 \tag{3.3}$$

Where, r is radius of the force sensor obtained from the FSR datasheet (Electronics, n.d.). A portable air compressor was attached to the pressure sensor and solenoid valve to operate the SPA system. Pressure sensors (model no. MPS20N0040D, Soldered Electronics, Osijek, Croatia) were used to monitor the supply pressure. The SPA controller comprised an air pump, Step-Down voltage regulator (LM2596 SIMPLE Switcher Power Converter 150-kHz, Digi-Key Electronics, Thief River Falls, MN, USA), pressure sensor, data acquisition control board (Arduino Pro Mini, Digi-Key Electronics, Thief River Falls, MN, USA), and solenoid valve. The hardware working model was built as shown in Figure 3.6 (c).

(a)

(b)

(c)
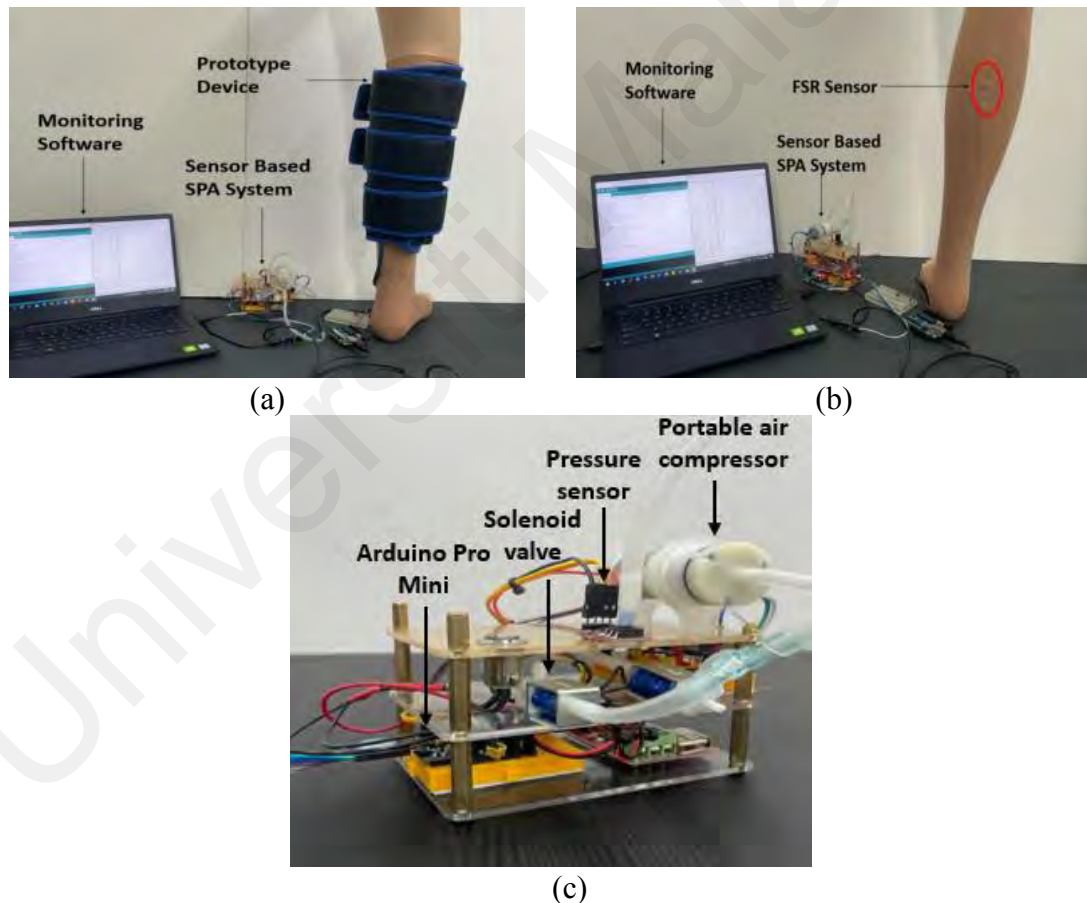
Figure 3.5: The experimental setup to evaluate pressure transmission: (a) monitoring system for mannequin leg with SPA chamber; (b) the FSR sensor embedded inside the skin layer at gastrocnemius muscle and (c) component of the SPA based system.
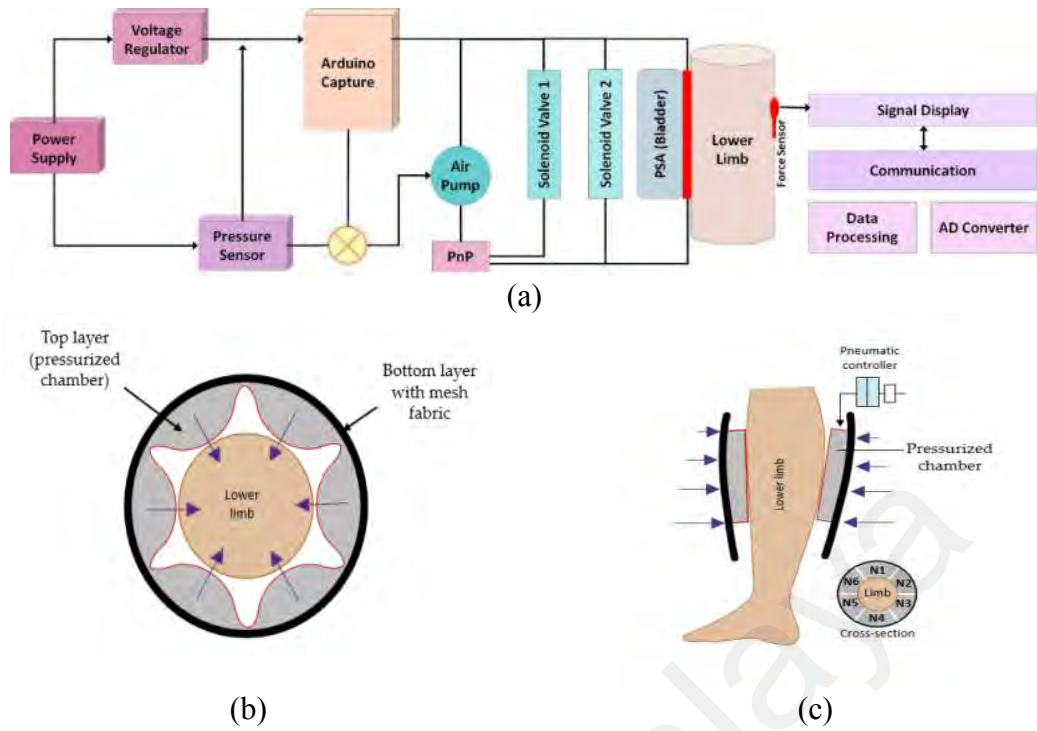
Figure 3.6: The schematic diagram of (a)SPA testing system, pressure transmission monitor; (b) schematic diagram of SPA with six airtight chambers; and (c) schematic diagram of lower-limb SPA system.

3.3.1 Deformation and Stress of the SPA Chambers

The experimental setup designed for calculating the 3D deformation profile of the chamber concerning its inflation height is depicted in Figure 3.7. The testing apparatus comprises a distance laser meter (Class 2,635 nm, <1 mV, Accuracy ± 1 mm) affixed vertically to a retort stand to secure its position. Since the most significant deformation for uniformly distributed pressure occurred at the center of the simulation result, the laser head was directed toward the chamber's center. The SPA chamber was placed horizontally on a flat table to measure the deformation with the laser point coinciding with the chamber's center. The position of the SPA was fixed by placing load cells at every corner of the SPA before air was supplied inside the chamber. This approach ensured stability and provided reference points for accurately monitoring any deformations or changes in position throughout the experiment. The initial height, h_0 of the chamber was measured. The SPA chambers underwent inflation in 1.0 mL air volume

increments for 23 seconds of inflation, followed by 7 seconds of holding, and subsequently 7 seconds of deflation. The deformed height, h_i was recorded at every 1 second interval. This testing protocol was conducted for five complete cycles at the specified location, and the average deformation values were included in the results.
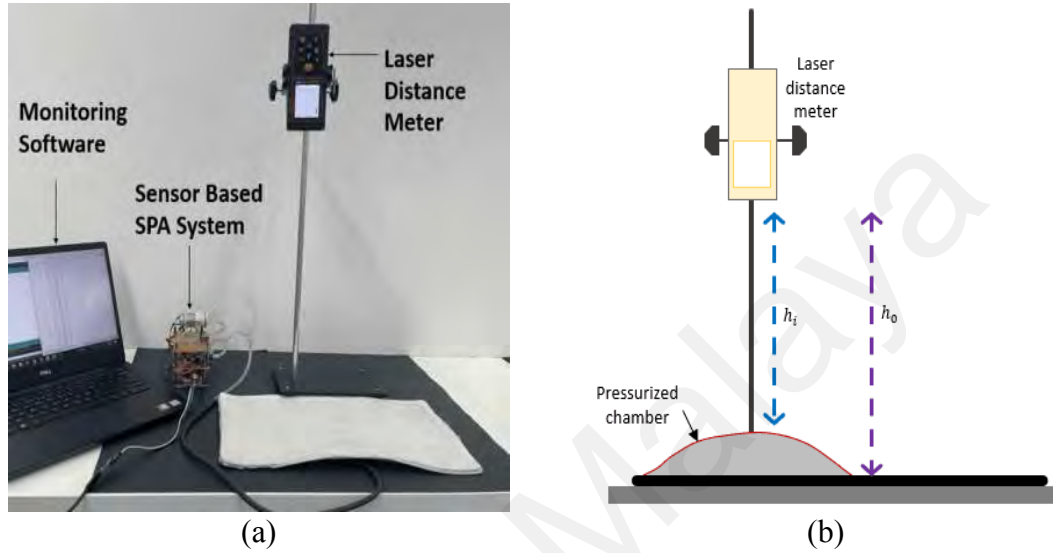
Figure 3.7: Experimental setup: (a) real-time arrangement and (b) schematic diagram for measuring the inflation height.

The actual relation between the stress and deformation for an incompressible material under tension/compression is given by (Rackl, 2017):

$$\sigma_e = 2 \cdot (\lambda - \lambda^{-2}) \cdot \left(\frac{\delta W}{\delta I_1} + \frac{1}{\lambda} \cdot \frac{\delta W}{\delta I_2} \right) \tag{3.4}$$

where:
σ_e: Engineering stress
λ: Deformation ratio, parallel to
W: Strain energy
I_1, I_2: Strain invariant

The deformation ratios λ defined as the ratio of the deformed height, to the undeformed height, (Equation 3.5). The deformation ratio equals to 1 in undeformed state (Rackl, 2017).

$$\lambda = \frac{h_i}{h_0} \tag{3.5}$$

Equation 3.6 was derived from combination of equation 3.1, 3.4 and 3.5, where the yields a stress-strain relation for the elastomeric model

$$\sigma_e = \sum_{i=1}^{n} 2 \cdot C_i \cdot i \cdot \left(\frac{h_i}{h_0} - \left(\frac{h_i}{h_0} \right)^{-2} \right) \cdot \left(\left(\frac{h_i}{h_0} \right)^2 + 2 \left(\frac{h_i}{h_0} \right)^{-1} - 3 \right)^{i-1} \tag{3.6}$$

To assess the reliability between simulated and experimental conditions, the intraclass correlation coefficient (ICC) was used. With this, 95% confidence intervals were calculated using Microsoft Excel based on an absolute agreement: specifically, a mixed-effect model (ICC 3,1). The classification of ICC defined the degree of consistency used to interpret ICC value: excellent (>0.9), good (0.76–0.9), moderate (0.5–0.75), and poor (lower than 0.50) (Fernández-González et al., 2020). Bland–Altman analysis with 95% limits of agreement (LoA) was performed to access the agreements between datasets obtained during the two conditions. The scatterplot was constructed with partiality and the LoA is shown in the plot for the parameters registered. The mean score is represented on the x-axis, and the difference between two measurements (mean of the differences) is plotted on the y-axis. The 95% LoA is defined as ±1.96 standard deviation (SD). The average difference (Diff), the standard deviation of the differences (SD), and lower and upper 95% confidence level (CI) were from the formula: upper 95% CI = Diff − 1.96 × SD; lower 95% CI = Diff + 1.96 × SD (Liu et al., 2021). The width of the boundaries of agreement and the distance of the mean through these differences were used to interpret measurement errors. An acceptable agreement between these two measurements was indicated when 95% of the data fell inside the LoA (Gerke, 2020). No significant difference between the measurements was reflected in case the line of equality was within the interval (Lau, 2020).

3.4 Experimental Validation on Healthy Participants

3.4.1 Sample Size

The calculation of the appropriate sample size calculation was performed using the G*Power software. To achieve an effect size of 0.50 and an 80% power level, a minimum

of 26 participants were required. The anticipated effect size based on previous study on muscle damage of r = 0.4 (small to moderate effect) (Lateef & Earp, 2023). Therefore, to account for possible dropouts, thirty (30) healthy male participants spanning in age 24.8 ± 2.4 years and body mass index (BMI) from 23.1 ± 3.6 kg/m2 were recruited.

3.4.1.1   Control Group (without compression therapy)

In the control group, participants went through assessments independently from the SPA system. After the initial measurements, fatigue was induced following the established guidelines. In the case of pre-treatment and post-treatment measurements, the control group was advised to take a 30-minute rest before proceeding with the post-treatment evaluation. The post-24 hours measurement occurred after a 24-hour period of rest. During those measurements, no SPA system intervention was used in the control group.

3.4.1.2   Intervention Group (with compression therapy)

In the intervention group the pressure sensor was placed in the upper central area of the calf, while the pneumatic actuator was fitted around the participant's leg, leaving a 2.5-centimeter gap for inflation as shown in Figure 3.8(a). Gradual and consistent inflation of the pneumatic actuator took place after readiness was confirmed. Participants were regularly monitored for comfort and asked to indicate if they reached their maximum pain threshold. Maximum pressure values were logged from both the skin pressure readings and the compressor's pressure sensor. These measurements were iterated thrice to ensure uniformity. The intermittent compression therapy began once the pressure sensor and pneumatic actuator were in position as shown in Figure 3.8(b). The pneumatic actuator inflated to the maximum pressure, maintained it for 7 seconds, and then released the pressure for 10 seconds, constituting one compression cycle. This compression cycle was repeated for a duration of 30 minutes.
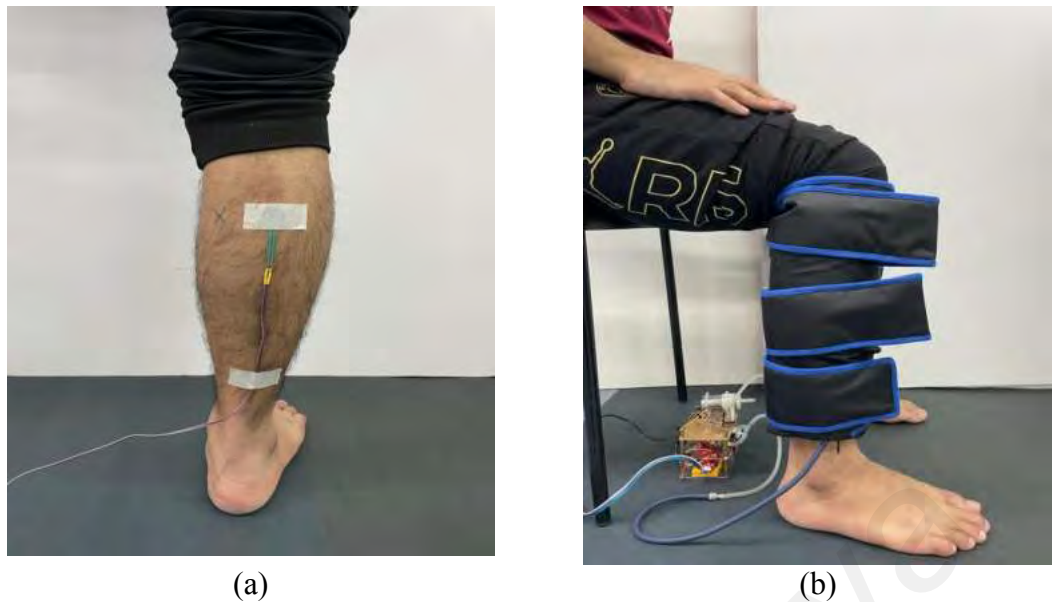
(a)   (b)
**Figure 3.8: Experimental setup (a) position of FSR at medial side of the lower
leg and (b) SPA cuff wrapped around the participant's leg.**

3.4.2   Experimental Procedure

Assessing alterations in muscle stiffness provides insight into the effectiveness of
using soft pneumatic actuators (SPA) for addressing lower limb injuries following fatigue
induction exercise. However, there is limited scholarly research on soft actuators tailored
for musculoskeletal injuries. Thus, a study was carried out to examine the effectiveness
of using SPA after calf raise exercise in healthy individuals. The assessment of muscle
stiffness played a crucial role in this investigation, enabling us to explore the potential
advantages of SPA therapy. The flow of the experimental procedure is illustrated in
Figure 3.9.
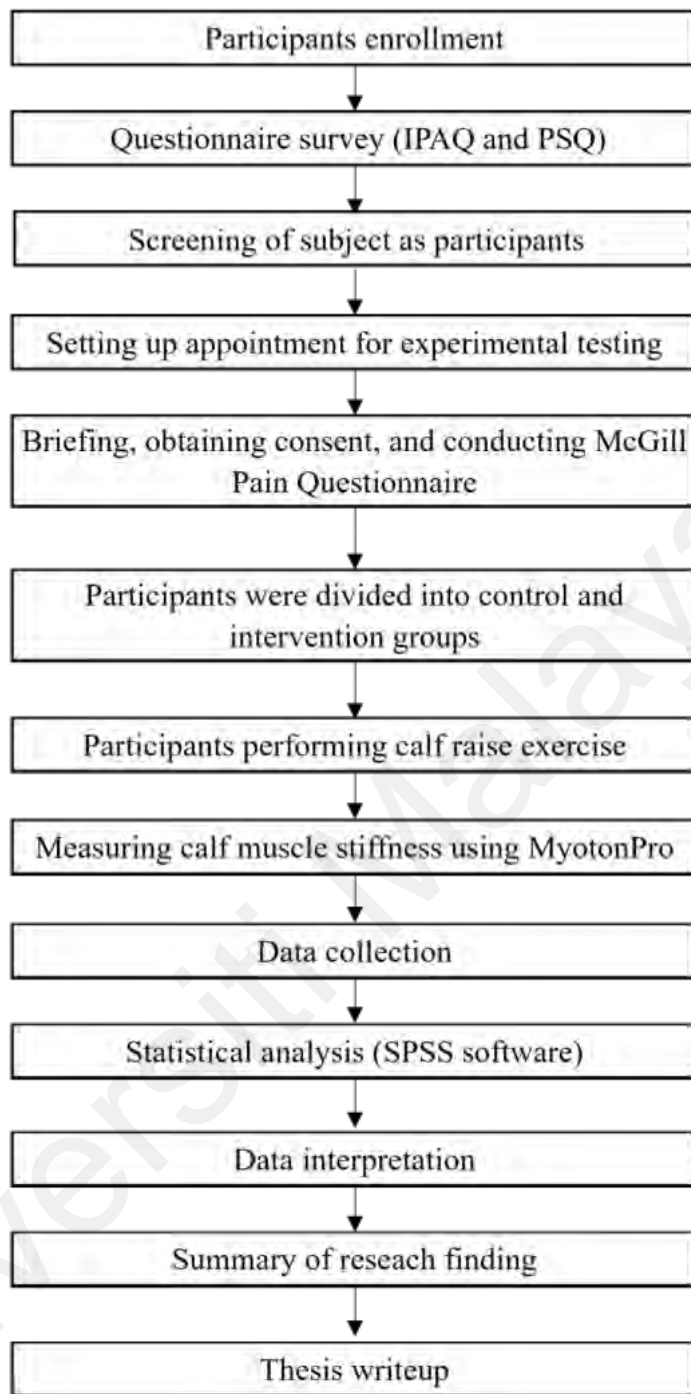
Figure 3.9:Experimental procedure on healthy participants flow chart.

3.4.2.1 Participants Selection

The participants were recruited from the student community. Inclusion criteria were healthy male aged more than 18 years old with no previous or current injury record, had achieved moderate to high score in both the International Physical Activity Questionnaire (IPAQ) (Kurth & Klenosky, 2021) and Pain Sensitivity Questionnaire (PSQ) (Ruscheweyh et al., 2009). This gender-specific approach was chosen to streamline the study's focus on assessing the efficiency of soft pneumatic actuators in reducing muscle stiffness following fatigue induction exercise. By concentrating on one gender, the study aimed to eliminate potential confounding variables related to gender differences. Furthermore, selecting adults over 18 years of age eliminated the need for parental consent and ensured participants were legally capable of providing informed consent. Additionally, adults were deemed more relevant to the study's objectives due to their exercise experience and higher likelihood of experiencing muscle soreness and fatigue, aligning closely with the intended user demographic of soft pneumatic actuators for muscle recovery. These selection criteria were strategically chosen to enhance the study's relevance, applicability, and ethical considerations within the methodology while distinguishing the effects of soft pneumatic actuators (SPA) from regular physical activity and assessing SPA effectiveness in individuals more likely to benefit from pain relief. The exclusion criteria for the study include individuals with chronic pain or history of neuromuscular injury as well as those who have had less than 5 hours of sleep prior to the experiment and individuals with a leg circumference less than 30 cm. Throughout the study, participants were requested not to utilize any medications or therapies or involve themselves in additional physical exercises following the intervention. The participants' Body Mass Index (BMI) was gathered for further analysis. Prior to the testing, all participants were given detailed information about the study and voluntarily agreed to participate, as authorized by University Malaya Research Ethics Committee (Non-

Medical) with the reference number (UM.TNC2/UMREC_2397). The ethics form can be referred to Appendix D. The participants also provided written consent by signing agreement forms.

3.4.2.2 Testing Procedure

This study implemented a crossover study design, where the participants were randomly assigned to start with control group (without compression therapy) or intervention group (with compression therapy). Participants who started with control group then switched to intervention group and vice versa. Correspondingly, the study was structured into two different groups where the participants' roles were reversed after 7 days of wash-out period. Figure 3.10 shows the cross over testing protocol flow chart. The participants underwent preliminary measurement, fatigue induction, pre-treatment measurement and post-treatment measurement was recorded 30 minutes and 24 hours after fatigue induction exercise.

Participants' preliminary measurements for calf muscle stiffness were measured as a baseline in two distinct positions, sitting and standing. Prior to starting, participants will need to wear leggings to minimize heat dispersion, perform stretching exercises, and acquaint themselves with standing calf raises. The stiffness of participants' calf muscles will be gauged using MyotonPRO, and their pain intensity will be evaluated using the McGill Questionnaire and documented as the initial measurement (Melzack, 1975). The participants were required to stand barefoot and do a fatigue induction exercise continuously at steady pace until their muscle fatigue. After completion of fatigue induction, the rigidity of participants' calf muscles was evaluated in both sitting and standing positions and their pain level were assessed using McGill Questionnaire and recorded as pre-treatment readings. Next, the participants were then assigned to either the control group or the intervention group. For the control group, participants were required

to rest in a seated position for 30 minutes. Meanwhile, for the intervention group, participants were instructed to wear an SPA cuff while remaining seated for 30 minutes. After 30 minutes, the stiffness of participants' calf muscles was measured using MyotonPRO and their pain level were assessed using McGill Questionnaire and recorded as post-treatment readings. Following the session, the participants were excused and instructed to return after a period of 24 hours. They were advised to rest and avoid engaging in any physical exercise during this duration. After the 24-hour period, the stiffness of their calf muscles was assessed using MyotonPRO, their pain levels were evaluated using the McGill Questionnaire and recorded as post 24 hours readings.
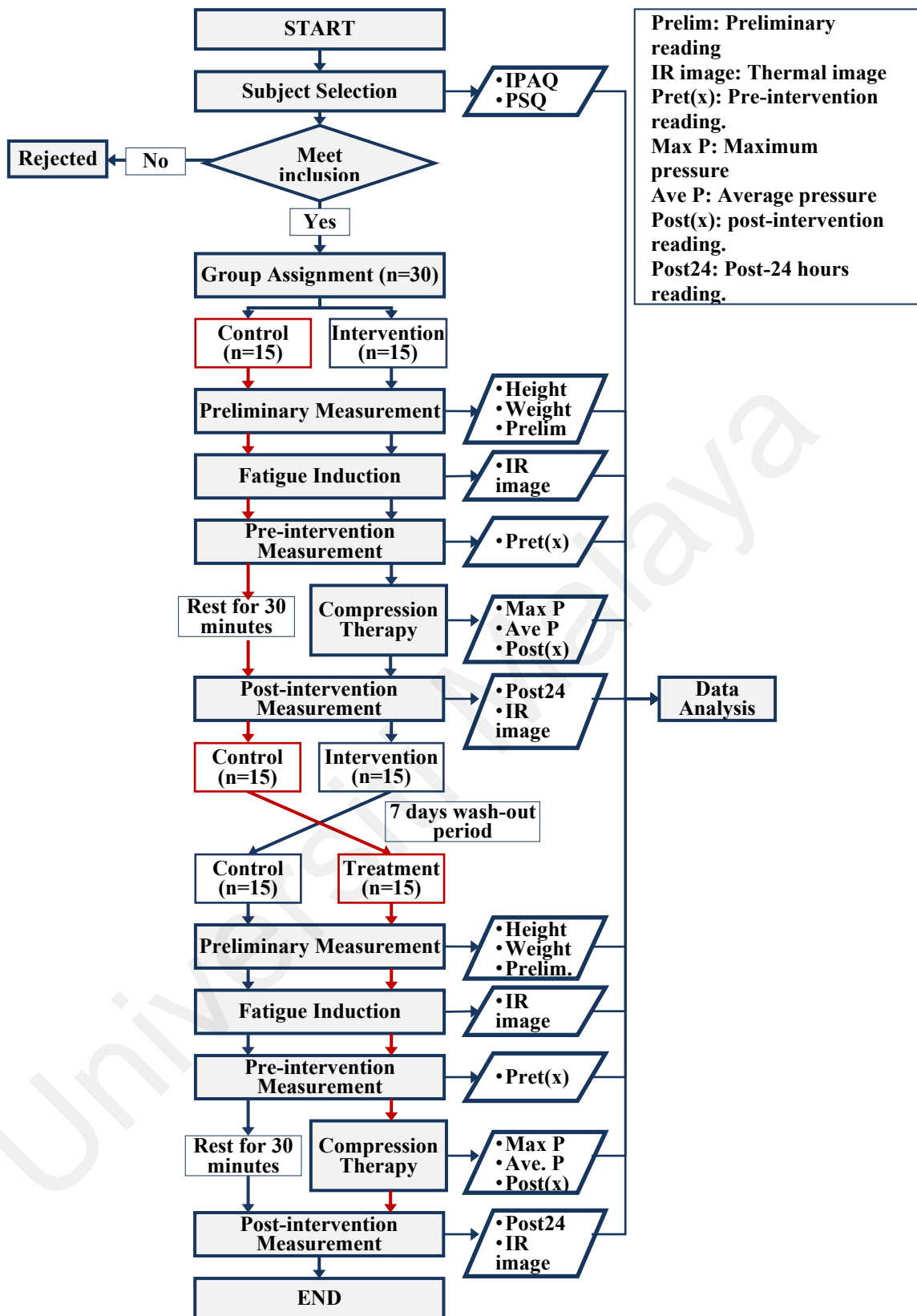
Figure 3.10: Cross over testing protocol flow chart.

3.4.2.3 Pressure Measurement

Before proceeding with the application of the SPA cuff, the maximum pressure that participants were comfortable with was measured. This measurement was accomplished by utilizing a circular 2.5 cm force sensitive resistor (FSR) in a voltage divider circuit. The voltage reading obtained was then converted into a pressure reading using an Arduino UNO, which incorporated a built-in ADC (Analog-to-Digital Converter). The calibration process involves applying increasing pressure to the cuff which is then detected by the FSR, until the participant indicates discomfort or reaches their maximum tolerance level. This process is repeated three times to ensure consistency and accuracy in determining each participant's comfort threshold. The pressure level on the SPA system is then set based on the average of these three measurements, ensuring that it remains within the participant's comfort range during the experiment. This process ensured that the pressure exerted on the skin during the compression therapy was within the participants' comfort level and optimized for effectiveness. To obtain precise pressure measurements, the force applied to the leg was measured. A force-sensitive resistor (FSR) was attached to the medial side of the lower leg, specifically around 20 cm above the ankle, in an area where the tendinous and muscular sections of the gastrocnemius muscle separate. Subsequently, the pressure exerted on the skin by the SPA system was evaluated through the force sensor.

3.4.2.4 Fatigue Induction Exercise

Muscle fatigue in the calf muscles was induced through the execution of standing calf raises exercises to replicate muscle soreness, as illustrated in Figure 3.11(a). Following initial measurements, participants were instructed to stand in front of the IR camera and perform standing calf raises continuously at a steady pace (100 beats per minute) until instructed to stop. Infrared (IR) thermal imaging was employed to identify and locate thermal variations, characterized by fluctuations in skin temperature in the calf region, as

depicted in Figure 3.11(c). FLIR One Pro LT IR (Teledyne FLIR, Oregon, US) thermal imaging camera which has working range of -20 ˚C to 120 ˚C at ±3 ˚C was used in this study as shown in Figure 3.11(b). Upon an increase of 1 degree Celsius in the temperature of the calf muscles, participants were requested to stop their activity, indicating that their calf muscles had reached a state of fatigue (Al-Nakhli et al., 2012; Hadžić et al., 2019; Ramamoorthy, 2018). The FLIR was used to monitor changes in muscle temperature during fatigued induction exercise. Moreover, the MyotonPRO device was employed to validate the occurrence of muscle fatigue by assessing muscle stiffness in both sitting and standing positions. While engaging in physical activity, the human body faces the task of maintaining core temperature within acceptable limits to avoid overheating caused by the heat generated from contracting muscles. Initially, at the onset of exercise, there is a reduction in skin blood flow due to the increased circulation to the contracting muscles. However, as exercise continues and core temperature rises, the body's central regulatory mechanisms prompt vasodilation, facilitating heat dissipation through the skin (Abbiss et al., 2010; Hadžić et al., 2019).

(a)   (b)

(c)

Figure 3.11: Fatigue Induction Exercise (a) standing calf raise, (b) FLIR One PRO and (c) thermal imaging of the calf area in °F.

3.4.2.5 Muscle Stiffness Measurement

The calf muscle's left and right positions were marked using a VISCOT medical skin marker, as depicted in Figure 3.12(a). Muscle stiffness was assessed using the MyotonPRO device (Myoton AS,Estonia,US) by recording the natural oscillation of the muscle upon an external mechanical stimulus. Throughout the measurement procedure, the multiscan mode was utilized to acquire five successive readings for the mean muscle stiffness at every designated position. The participant underwent measurements in both standing and sitting position as shown in Figure 3.12(b) and (c). For maintaining uniform and accurate measurements, the MyotonPRO probe was positioned directly in contact with the skin at the specified location. The apparatus was kept parallel to the ground with the screen facing upwards and securely held, as illustrated in the Figure 3.12(b). Stability was maintained throughout the measurement, ensuring accurate results.

The Coefficient of Variation (CV) was evaluated prior to preserving the measurement; if the CV exceeds 3%, the reading will be remeasured. The choice of a 3% threshold for the CV in muscle stiffness measurement was based on established standards in biomechanical research and clinical practice (Khan et al., 2018). This threshold ensures that the measurements are sufficiently stable and reproducible, enabling reliable

68

assessment of muscle stiffness over time. Previous studies utilizing similar measurement techniques have also supported the use of a 3% CV threshold for ensuring measurement stability and reproducibility (Jones et al., 2016; Smith et al., 2019). Adhering to this criterion enhances the validity and reliability of muscle stiffness measurements obtained from the Myoton Pro. After an intense exercise session that induces muscle fatigue, there is a subsequent increase in muscle stiffness. This stiffness reaches its peak 24 hours after exercise and then gradually diminishes within 48 hours. This pattern of stiffness corresponds to the occurrence of delayed onset muscle soreness (DOMS), which is characterized by feelings of discomfort and pain (Marathamuthu et al., 2022). Consequently, the measurement of muscle stiffness will serve as a variable to assess the efficacy of the compression therapy, indicating its effectiveness in mitigating the symptoms associated with DOMS.

(a)   (b)

(c)

Figure 3.12: (a) positions marking using a VISCOT medical skin marker, measurement of mucle stiffness in (b) standing and (c) sitting position using MyotonPRO.

3.4.3   Qualitative Survey based on Questionnaire.

3.4.3.1   International Physical Activity Questionnaire (IPAQ)

Prior to the testing, participants were asked to complete a study questionnaire which included questions regarding their demographic characteristics (gender, age, highest educational attainment) the IPAQ (short form). The IPAQ (short form) consists of 7 questions which reflect on the previous 7 days' activities. The sample of the questionnaire can be referred to Appendix A. The information about the minutes per day or days per week, at any time of the day, spent doing activities was assessed. Participants reported their frequency and duration of different types of activity: vigorous (*i.e.* using bike, treadmill, performing intense exercise), moderate (*i.e.* carrying light loads, bicycling at a regular pace, or doubles tennis), walking activities, and time spent sitting. Responses were translated to Metabolic Equivalent Task minutes per week (METmin/week) based on continuous scoring of the IPAQ (short form) (Maugeri et al., 2020). Based on IPAQ guidelines for scoring protocol, participants physical activity was classified in three different groups of physical activity considering the METmin/week of sum of vigorous intensity, moderate intensity, and walking: low active (< 600 METmin/week); moderate active (≥600 METmin/week) and high active (≥3000 METmin/week). The choice of these

IPAQ thresholds is to examine the potential interaction between SPA application and participants' existing levels of physical activity. By specifically enrolling individuals with moderate to high IPAQ scores, the study explores how SPA affects muscle stiffness in individuals who are already engaged in regular physical activity. This approach helps to assess muscle stiffness in contexts commonly associated with an active lifestyle, sports, and exercise. The collected data from the International Physical Activity Questionnaire (IPAQ) were quantified as a continuous measure and communicated as the median MET-minute value using equation 3.7 to 3.10:

$$Walking\ MET = 3.3 \times walking\ minutes \times walking\ days \tag{3.7}$$

$$Moderate\ MET = 4.0 \times moderate\ minutes \times moderate\ days \tag{3.8}$$

$$Vigorous\ MET = 8.0 \times vigorous\ minutes \times vigorous\ days \tag{3.9}$$

$$Total\ MET = (Walking\ MET) + (Moderate\ MET) + (Vigorous\ MET) \tag{3.10}$$

3.4.3.2 Pain Sensitivity Questionnaire (PSQ)

The participants' pain sensitivity was accessed prior to the experimental testing using Pain Sensitivity Questionnaire (PSQ). PSQ is a self-evaluation tool designed to gauge pain perception through hypothetical painful scenarios encountered in everyday activities. The questionnaire comprises 17 items depicting typical pain scenarios experienced in daily life. Participants will responses to hypothetical pain scenarios based on their subjective experiences and perceptions. Several studies have demonstrated the significant impact of psychological factors, such as pain catastrophizing and fear of pain, on pain perception and tolerance. It is suggested that the intensity ratings of imagined painful scenarios may closely resemble those of actual clinical pain (Ruscheweyh et al., 2009). Therefore, despite the absence of direct physiological measurements, PSQ is valuable for understanding individuals' cognitive and emotional reactions to pain. These responses will then be analyzed to explore potential associations between participants' reported pain sensitivity and other variables of interest, such as demographic characteristics or clinical

outcomes. The sample of the questionnaire can be referred to Appendix B. Before taking part in the experiment, the participants will be asked to rate their pain level on numeric rating scale (NRS) ranging from 0 (no pain) to 10 (worst pain imaginable) with a higher score indicates greater pain sensitivity (Fu et al., 2023). The questionnaire covers a wide range of pain modalities such as hot, cold, sharp, and blunt, as well as different areas of the body such as the head, upper extremities, and lower limb. The PSQ can be quantified using scales such as the PSQ-total, moderate subscale (PSQ-moderate), and minor subscale (PSQ-minor). The moderate subscale comprises the sum of items 1, 2, 4, 8, 15, 16, and 17, which depict scenarios involving moderate pain. The minor subscale encompasses the sum of items 3, 6, 7, 10, 11, 12, and 14, representing situations of mild pain. Items 5, 9, and 13 were excluded from analysis as they portray non-painful scenarios, such as taking a warm shower (Ibancos-Losada et al., 2022). Figure 3.13 shows an example of PSQ questionnaire.

3.4.3.3 Short-Form McGill Pain Questionnaire (SF-MPG)

The Short-Form McGill Pain Questionnaire (SF-MPG) is a multidimensional measure of current perceived pain among adults with chronic pain (Velez et al., 2022). The primary component of the SF-MPG consists of a questionnaire containing 15 items, divided into 2 subcategories: 1) a sensory segment comprising 11 items, and 2) an affective segment comprising 4 items. Each item employs a Likert intensity scale, with ratings ranging from 0 for none, 1 for mild, 2 for moderate, to 3 for severe. The questionnaire sample can be found in Appendix C. The total SF-MPG score is derived by summing the scores of individual items, with a range of 0 to 45. The sensory segment ranges from 0 to 33, while the affective segment ranges from 0 to 12. Figure 3.14 shows an example of SF-MPG questionnaire.

Figure 3.14: Example of SF-MPG questionnaire and scoring level.

3.5 Statistical Analysis

The statistical analyses were conducted with Statistical Package for the Social Sciences (SPSS) version 27 (SPSS Inc., Chicago, IL., USA). The average of muscle stiffness data (s), IPAQ scores and Mc Gill Pain score were established in the SPSS. The normality of the parameters for all subjects was assessed by conducting the Shapiro-Wilk test on the data of muscle stiffness, IPAQ, PSQ, and Mc Gill Pain, to examine the distribution characteristics. Bonferroni adjustment for multiple comparisons was used as a post hoc test. In all tests, p-value < 0.05 was considered significant. In order to assess the normal distribution of the data, Quantile-Quantile (Q-Q) plots were utilized. Q-Q plots compare the quantiles of the observed data against the quantiles of a theoretical normal distribution. Deviations from a straight diagonal line in the plot suggest departures from normality. This method provides a visual assessment of the data's distributional assumptions, aiding in determining the appropriateness of parametric statistical tests used in the analysis.

3.5.1 Intraclass Analysis

Significant differences of muscle stiffness between two measurements position and timepoint; baseline, pre-treatment, post treatment and post 24 hours of the physiological data, were statistically analyzed using two-way repeated measure ANOVA test (for normally distributed data). This study consists of two categorical independent groups in two factors. The independent variables include treatment position and treatment timepoint, while the dependent variable of interest was muscle stiffness. A two-way repeated measure ANOVA was performed to evaluate the effect of measurement position and treatment timepoint on muscle stiffness. In this study, three sets of null and alternative hypothesis, H_1 were formulated and tested. These hypotheses are summarized in Table 3.2.

Table 3.2: The null hypotheses of two-way repeated measure ANOVA.

Null hypothesis (H_0)	Alternative hypothesis (H_1)
The means of measurement position are equal.	The mean of at least one measurement position is different.
The means of treatment timepoint are equal.	The mean of at least one treatment timepoint is different
There is no interaction effect between the measurement position and treatment timepoint on muscle stiffness.	There is interaction effect between the measurement position and treatment timepoint on muscle stiffness.

The ANOVA coefficient, F score was used to determine the significance of effects in the two-way ANOVA, which examined the differences between measurement positions and treatment timepoints on muscle stiffness. The formula for F used for the analysis was as follows:

$$F = \frac{Mean\ Square}{Mean\ Square\ Residuals} \qquad (3.11)$$

The ANOVA coefficient F score was used to determine the significance of the effects in the two-way repeated measures ANOVA. A higher F score value indicated a larger difference between groups relative to the within-group variability. In reporting the results, the F score, degrees of freedom (df), and p-value were examined.

The Wilcoxon Signed rank test was performed to measure the significant differences between treatment timepoint in Mc Gill Pain score. The Wilcoxon signed-rank test was chosen to analyze this data, since the data was not normally distributed. According to Gracht (2012), the Wilcoxon signed-ranks test is recommended for analyzing paired data within the same group of individuals, such as in a "before and after" scenario. This test is utilized to determine whether there is a statistically significant difference between the data collected in four different timepoint of the pain score measurement. This test will

provide the sum of each of the positive and negative rank of the differences between any consecutive timepoint of Mc Gill Pain score with a Z statistic and p-value. The formula for the Wilcoxon Signed rank test is as follows:

$$W = \sum_{i=1}^{N_r}[sgn(x_2 - x_1)x \; R_i] \tag{3.12}$$

Where:
W = test statistic (sum of signed rank)
N_r = sample size, excluding pairs where $x_2 = x_1$
Sgn = sign function
x_2, x_1 = corresponding ranked pairs from two distribution
R_i = the ranks assigned to the absolute values of the differences.

The null hypothesis, H_0 assumed median difference between treatment timepoint and McGill pain score on muscle stiffness is equal to zero. The alternative hypothesis, H_1 proposed the median difference between treatment timepoint and McGill pain score on muscle stiffness is not equal to zero. To interpret the results, the test statistic W was compared to the critical values from the Wilcoxon Signed rank table, and the p-value associated with the test statistic was calculated. The p-value indicated the probability of observing the observed differences under the null hypothesis of no difference between the treatment timepoints. By using the Wilcoxon signed rank test, the possible differences between the McGill Pain Score and the importance of SPA for the participants can be detected.

3.5.2 Interclass Analysis

The Mann–Whitney U test was utilized to compare the Mc Gill Pain scores between the groups, considering the non-normally distributed data. The Mann-Whitney U test is typically used to compare two independent samples of ordinal (ranked) data. In this study, the null hypothesis, H_0 assumed no significant difference in the distribution of pain scores between Control Group and Intervention Group. Meanwhile, the alternative

hypothesis, H_1 proposed that there would be a significant difference in the pain scores between the two group. This test was conducted by ranking all the pain scores from both groups together. The U statistic was calculated using formula:

$$U = R_1 - \frac{n_1(n_1+1)}{2} \tag{3.13}$$

where U represents the Mann-Whitney U statistic, R_1 is the sum of the ranks for the smaller group and n_1 is the sample size of Group. The resulting U statistic was then compared to the critical values from the Mann-Whitney U distribution, or a p-value was calculated to determine the statistical significance. A $p < 0.05$ value is considered statistically significant. Cohen's r measure was calculated to find out the extent of the difference between two groups mean (Wassertheil & Cohen, 1970). Effect size between McGill pain score value in control group and intervention group are categorized as r=0.1(small), r = 0.3(medium) and r = 0.5 (large).

Additionally, the two-sample t-test was employed to compare means of the muscle stiffness value between control and intervention groups. This parametric test was used for continuous variables that approximate a normal distribution. It allows for the investigation of whether there exists a significant difference between the means of the two groups. The test involves calculating the t-statistic, which is determined using the following formula:

$$t = \frac{x_1 - x_2}{\sqrt{\frac{s_1^2}{n_1} + \frac{s_2^2}{n_2}}} \tag{3.14}$$

where t represent the t-statistic, $x_1 \, and \, x_2$ are the sample means of control group and intervention group, respectively, $s_1 \, and \, s_2$ are the sample standard deviation of control group and intervention group and $n_1 \, and \, n_2$ are the sample size of control group and intervention group respectively.

The hypothesis for this two-sample t test can be define as; The null hypothesis, H_0 assumed no significant difference between the means of Control Group and Intervention Group, while alternative hypothesis, H_1 proposed that there is a significant different between the means of control and intervention group. The calculated t-statistic was compared to critical values from the t-distribution, or a p-value was computed. A $p < 0.05$ value is considered statistically significant. Cohen's d measure was calculated to find out the extent of the difference between two groups mean (Wassertheil & Cohen, 1970). Effect size between participants muscle stiffness value in control group and intervention group are categorized as d=0.2(small), d=0.5 (medium) and d=0.8 (large).

3.5.3 Correlation Analysis

To investigate whether there is correlation between maximum pressure and leg circumference Pearson's Correlation analysis was performed. The purpose of this analysis was to determine the strength and direction of the linear relationship between these two variables. Pearson's correlation coefficient (r) for maximum pressure and calf circumference were calculated using the following formula:

$$r = \frac{\sum (x_i - \bar{x})(y_i - \bar{y})}{\sqrt{\sum (x_i - \bar{x})^2 \sum (y_i - \bar{y})^2}} \tag{3.15}$$

Where:
r = correlation coefficient
x_i = x-variable parameters values in the dataset
$\bar{x}$ = mean of the values of the parameters
y_i = y-variable parameters values in the dataset
$\bar{y}$ = mean of values of the parameters

The strength and direction of the linear relationship between maximum pressure and calf circumference was quantified based on the r value. Positive r value indicates a positive linear relationship, meanwhile a negative r value indicates negative linear relationship. The correlation coefficient's magnitude represented the strength of the relationship, with values closer to -1 or +1 suggesting a stronger linear association. The

correlation coefficient 'r' will be presented as the effect magnitude, with r < 0.30 indicating a minor effect, 0.3 < r < 0.5 indicating a moderate effect, and r > 0.5 indicating a substantial effect (Maurer et al., 2020). The calculated r and the p-value was observed to determine the statistical significance of the correlation between maximum pressure and calf circumference. A p-value ≤ 0.05 indicated a statistically significant correlation.

3.6   Summary

This chapter describes the methodology that was used in this study. It included the conceptual model, hypotheses, setting and participants, instrumentation, research design and procedures, and data analysis procedures. The development of the SPA begins with the conceptual model development, followed by the materials testing and simulation using FEM and fabrication of the SPA using silicone elastomer. The experimental phase proceeded with integration of sensor-based SPA system for monitoring pressure transmission.

Thirty healthy male participants were recruited to predict the effect of SPA on muscle stiffness following a fatigue-inducing exercise. The participants were divided into a control group and an intervention group for the study. The control group underwent assessments without receiving any compression therapy, while the intervention group received compression therapy using the SPA system. The study aimed to provide insights into the effects of compression therapy using SPA on healthy participants and contribute to the understanding of its potential benefits in muscle recovery and pain management.

Next, the statistical analysis was conducted using the Statistical Package for the Social Sciences (SPSS) version 23. The mean values of muscle stiffness, IPAQ scores, and Mc Gill Pain scores were calculated. The normality of the data was assessed using the Shapiro-Wilk test. Parametric tests, such as two-way repeated measure ANOVA and two-sample t test, were used to analyze normally distributed data. Non-parametric tests,

including the Wilcoxon signed-rank test, Mann-Whitney U test, and Spearman's rank-order correlation analysis, were employed for non-normally distributed data. The methodology presented in this chapter provides a solid framework for the subsequent research and analysis of the SPA system's efficacy in the context of lower limb rehabilitation.

CHAPTER 4: RESULTS AND DISCUSSION

4.1 Introduction

This chapter discusses the findings of the performance of the proposed SPA system based on an analysis of simulation results and data collected from surveys and experimental measurements. The experimental measurement was analyzed using several statistical analyses.

Section 4.2 explains the outcomes of the SPA performance based on FEM analysis using three different silicone-based materials in predicting the deformation and stress of the SPA chamber. In Section 4.3, the simulation and experimental deformation and stress outcomes were compared and discussed to assess the feasibility of the SPA system in replicating real-world compression conditions in applying pressure. Next, the analysis of the data collected from experimental validation on healthy participants was presented in section 4.4. This section presents an analysis of the survey data, which includes the distribution of demographic information and the pain levels reported by the respondents. Moreover, this section also discusses the findings on how the presence of SPA affected muscle stiffness. The relationship between the participants demographic, pain level, and maximum tolerable pressure with muscle stiffness is also stated in this section. The relationship was analyzed using five statistical methods; two-way repeated measure ANOVA, Wilcoxon Signed rank test, two sample t-test, Mann–Whitney U test, and Pearson's r Correlation analysis. Finally, Section 4.5 concludes the thesis by highlighting the research contributions and recommending a comprehensive theoretical and practical contributions of the proposed SPA.

4.2 Simulated 3D Deformation Results of the Proposed Chamber Using Three Different Materials

Pressure variation was employed to comprehend the interrelated mechanisms of the SPA performance design parameter throughout its inflation–deflation cycle. This pressure variation also serves to assess the functionality of the developed prototype model. Figure 4.1 shows the simulation result of the SPA chamber's detected operating rhythms using the three silicone rubber materials. This outcome effectively illustrates the practicality of the developed 3D model in predicting the pneumatic pressure and its fluctuations during the inflation-deflation cycles within the SPA system for three different materials. The variation profile was based on the pressure supply at the inner wall of the SPA chamber.
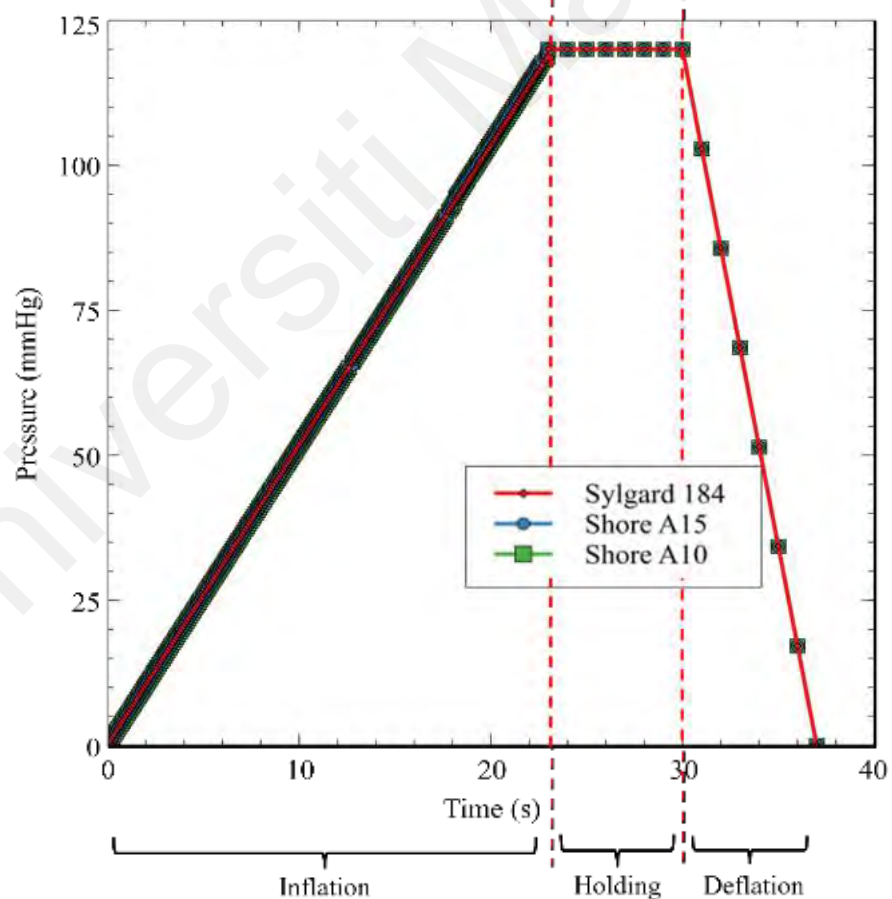
Figure 4.1: Detected pneumatic pressure during simulated inflation–holding–deflation cycle for three different materials by the SPA system.

Simulations of the SPA were conducted across a range of 0 to 120 mmHg. The deformation outcomes throughout the inflation-holding-deflation phases of the SPA system were acquired and subsequently compared across the three different silicone-based materials. The contour of deformation during the 27-second inflation period for the three materials is visualized in Figure 4.2, with a focus on the y direction deformation. At the initial state, the deformation started at approximately 14 to 16 mm for each material. The deformation within each chamber is illustrated using a color map, with red signifying high pressure and blue indicating low pressure. Notably, the upper part of the chamber exhibited more pronounced deformation compared to the lower part. This observation can be attributed to the material and thickness differences between its components. Specifically, the upper part utilized food-grade silicone with a shore hardness of A10, while the lower part employed food-grade silicone with a shore hardness of A15. This variation in shore hardness influenced the overall flexibility and deformability of the chamber. This variation can be attributed to the different thickness inputs for the upper and lower part. The thickness inputs contributed to differences in deformation. Thicker inputs generally resulted in reduced deformation due to increased stiffness and resistance to compression, while thinner inputs allowed for greater flexibility and deformation under applied pressure. Hence, the combination of material properties and thickness variations between the upper and lower parts of the chamber led to the observed differences in deformation. The center of the chamber experienced the highest-pressure concentration in contrast to the areas closer to the surrounding edges.

(a)   (b)

(c)   (d)

(e)   (f)
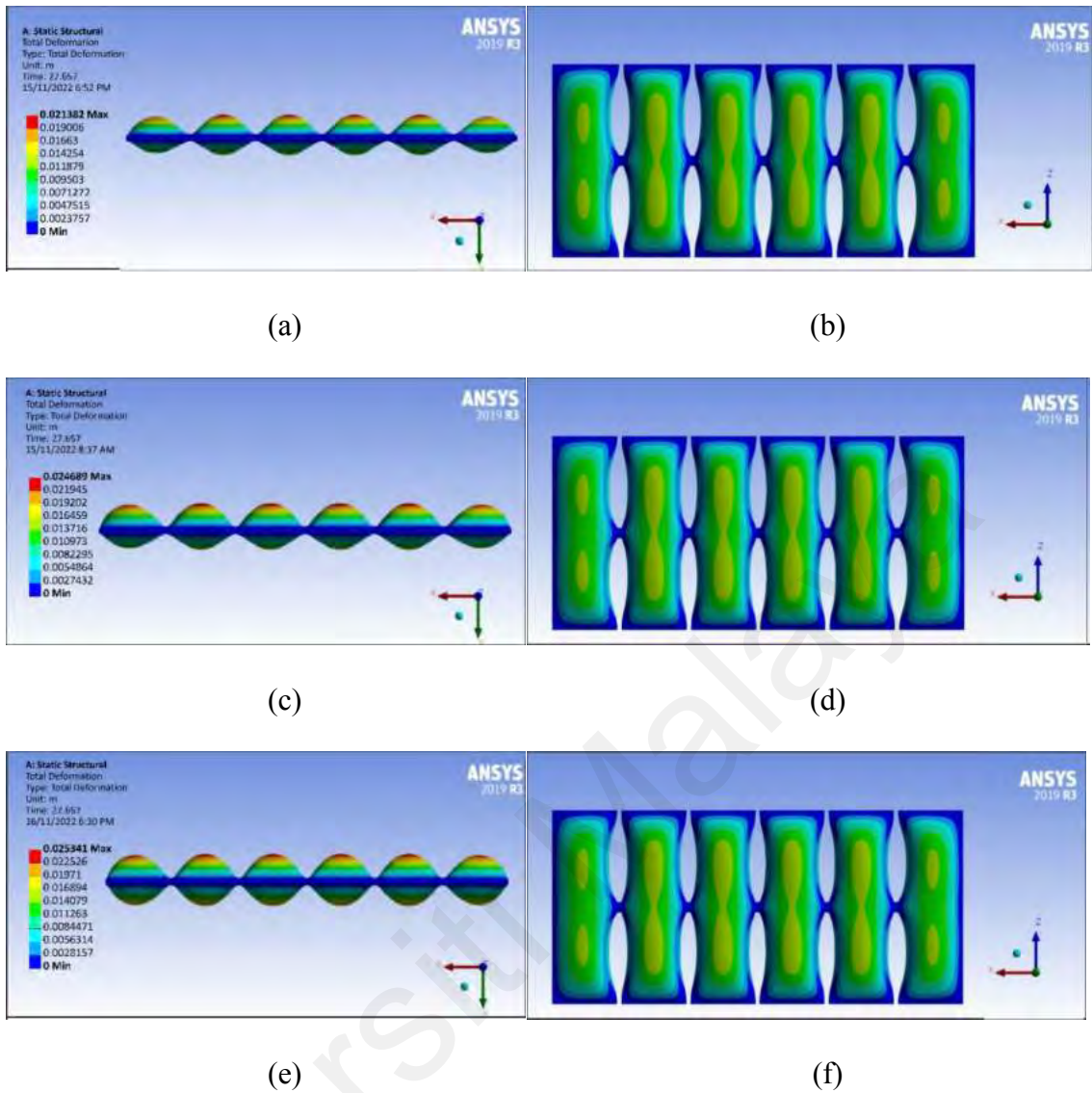
Figure 4.2: Deformation comparison of three different silicone rubber of the SPA chamber from the FEM simulation models. Slygard 184: (a) side view and (b) bottom view. Food-grade silicone (A15 Shore): (c) side view and (d) bottom view. Food-grade silicone (A10 Shore): (e) side view and (f) bottom view.

The average deformation varied between 0 to 23mm, A10 Shore silicone had the highest inflation with maximum deformation of 25.34mm, followed by A15 Shore with maximum deformation at 24.68mm, and Sylgard 184 with maximum deformation of 21.38mm. Figure 4.3(a) indicates that A10 Shore silicone could perform higher deformation under the same air pressure as compared to A15 Shore and Sylgard 184. Material with higher deformation is used to produce the main part of the SPA. As discussed by Xavier et al.(2021), in their comprehensive exploration of recent

advancements in soft actuators, it was noted that lower silicone hardness results in greater deformation at lower pressure levels. This will reduce the time required to achieve the shape transition and provide the desired force towards the leg.

To avoid catastrophic failure during deformation, stretchable devices such as soft actuators should have high elongation at break values (Park et al., 2018). Figure 4.3(b) displays material stress in relation to pressure. The various mechanical characteristics of silicone elastomers causes variations in the resultant stress. A10 Shore silicone, 3598.5 kPa, was the most extensible at mild stress, followed by A15 Shore silicone, 3630.6 kPa. Sylgard 184, on the other hand, required a larger stress to deform, which was 25047.0 kPa. The low elongation at break makes Sylgard 184 unsuitable for emerging mechanically demanding applications of soft actuators (Park et al., 2018).
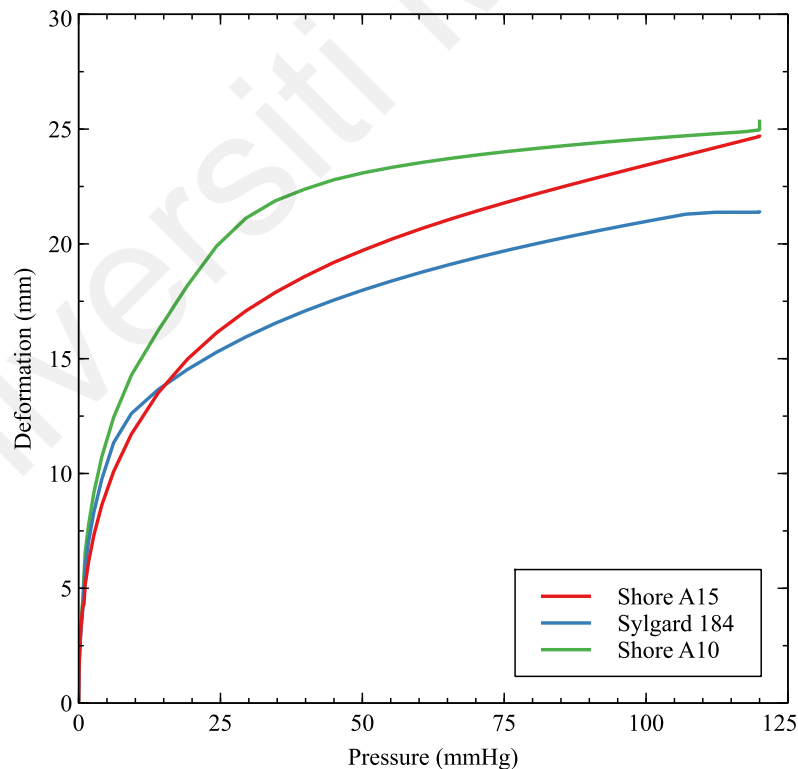
(a)
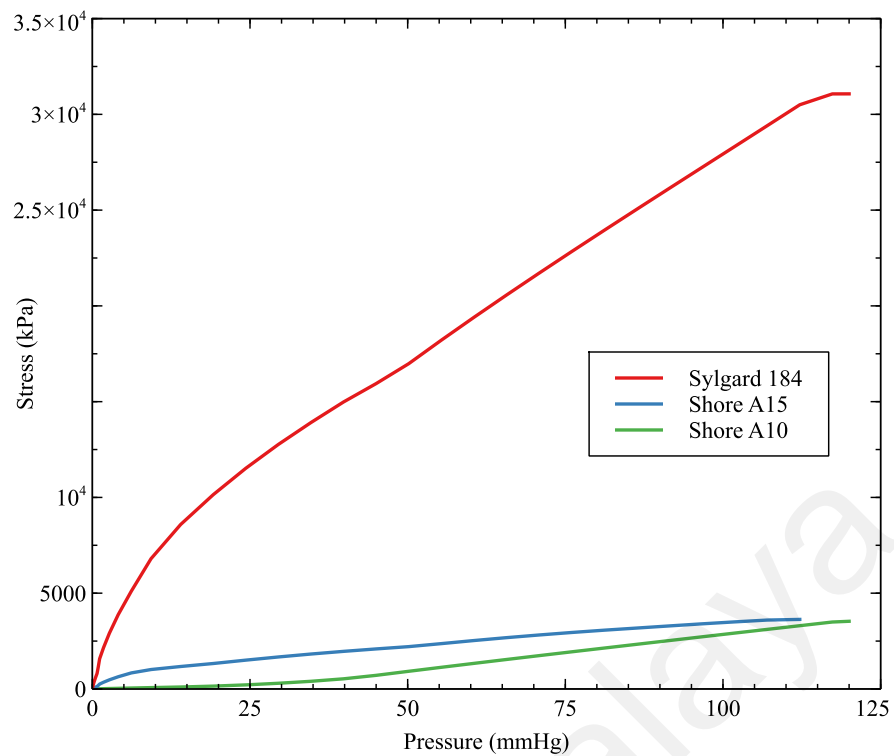
(b)

Figure 4.3:The behavior of three silicone elastomers from the simulation results (a). Deformation vs. pressure and (b) Stress vs. pressure.

The evaluation of the SPA's behavior has been conducted through FEM analysis to optimize its design. The efficacy of the SPA is significantly influenced by the choice of design parameters and materials employed (Maruthavanan et al., 2021). Considering that food-grade silicone has the same properties as commercial silicone, including the ability to provide effective pressure transmission and non-hazardous characteristics, this study aimed to evaluate the potential impact of material selection on three silicone elastomeric rubbers composed of commercial and food grade silicone. The study findings revealed that A10 Shore silicone exhibited the most considerable deformation in comparison to A15 Shore and Sylgard 184. These outcomes align with the properties of A10 Shore, characterized by a lower shore hardness than A15 Shore and Sylgard 184(Smooth-On, n.d.). Gorissen et al., (2017) stated that the significant deformation encountered by inflatable actuators prompts a preference for elastomers with lower shore hardness to prevent increased pressure levels.

Silicone is characterized as an isotropic material, demonstrating unique mechanical attributes encompassing Young's Modulus, Poisson's ratio, and shear modulus, which collectively influence varying deformations during inflation. In comparison to A15 Shore and Sylgard 184, A10 Shore boasts the lowest Young's Modulus. Due to its softer nature, A10 Shore requires lower pressure levels to achieve the desired deformation in soft actuators. s. In a study on the characterization of pneumatic muscle actuators, Carvalho et al., (2022) discovered that materials featuring a lower Young's modulus yield greater deformation and force upon stimulation. The quantity of compressed gas needed to attain the requisite pressure is dictated by the deformations of the elastomeric material within the chamber (Mosadegh et al., 2014).

Based on FEM analysis, A10 Shore is the most extendable under mild stress, followed by A15 Shore silicone. Sylgard 184 requires a larger stress to deform. Murphy et al., (2020) in the study of tailoring properties and processing of silicone found that materials having a low modulus can absorb and delocalize stress. From the findings, A10 Shore and A15 Shore are suitable for the fabrication of SPA, since Sylgard requires higher pressure to work and has lower elongation to prevent it from reaching the limit. Sylgard 184 is widely used in the fabrication of soft actuator applications, particularly microfluidic actuators (Pagoli et al., 2022). However, Sylgard 184 is not robust enough for applications that require stretchability and deformation due to its low elongation at break. Nevertheless, Sylgard is deemed ideal for hard components due to its resistance to deformation. According to Doss & Sharma, (2021) research, silicone with higher elongation is a better material to be used as actuators in rehabilitation.

4.3 Comparison and Validation of Simulation and Experimental Results

To facilitate a comparison and validation process between simulation and experimental findings, an experiment was performed on a mannequin leg. It was important to calculate

the pressure transferred by the SPA chamber onto the leg surface and assess the effectiveness of the SPA chamber's performance based on the selected material. This will depict the inflatable SPA chamber in contact with human skin in delivering the required pressure. Based on the simulation results, the SPA chamber was fabricated using food-grade silicone, specifically A10 Shore and A15 Shore. The upper layer employed A10 Shore food-grade silicone, while the lower layer was comprised of A15 Shore food-grade silicone. The experimental setup discussed at Section 3.3 was utilized to measure the transmission of pressure from the SPA chamber. Interface pressure was quantified as a function of force exerted on skin measured using FSR sensor. To validate the experimental outcomes, a comparison was made between the maximum deformation and stress experienced by the SPA chamber during inflation against FEM results for the maximum deformation and stress in relation to the supplied pressure. Bland–Altman analysis with 95% limits of agreement (LoA) was performed to access the agreements between datasets obtained during the two conditions.

The assessment of reliability demonstrated a strong correlation for both material deformation and stress, with an ICC greater than 0.9 for both parameters, as outlined in Table 4.1. A higher ICC value indicates a greater proportion of variability in measurements attributed to true differences between method. Thus, higher ICC values signify stronger agreement between the methods or observers being compared, reflecting greater reliability in the measurements. The classification of ICC defined the degree of consistency used to interpret ICC value: excellent (>0.9), good (0.76–0.9), moderate (0.5–0.75), and poor (lower than 0.50) (Fernández-González et al., 2020). The average deformation and stress exhibited no significant difference between the two testing methods ($p > 0.05$). The Bland-Altman plot visualizes the differences between simulation and experimental outcomes for the two material parameters (i.e. deformation and stress) in Figure 4.4(a) and (b). The data point in Figure 4.4 represents the comparison between

simulated and experimental values of deformation and stress recorded at one-second intervals over a duration of 20 seconds. The LoA for material deformation and stress was (95% CI 2.83 to -1.33) and (95% CI 438.67 to -330.84), respectively. The LoA were determined as the mean difference (bias) between the two methods, with a range of ±1.96 times the standard deviation of the differences. These lines, drawn parallel to the mean difference line, encompass the range within which 95% of the differences between the two methods are expected to lie. The scatterplot in the graph also reveals a uniform distribution of points within the interval for both material deformation and stress, with only a single outlier detected beyond the interval. However, most of the deformation and stress data points fell within the limits of the agreement.

Table 4.1: Inter-rater reliability of material parameters.

	95% CI	ICC	p-values
Simulation vs Experimental			
Deformation	-1.33 to 2.88	0.98949	>0.05
Stress	-330.84 to 438.67	0.99141	>0.05
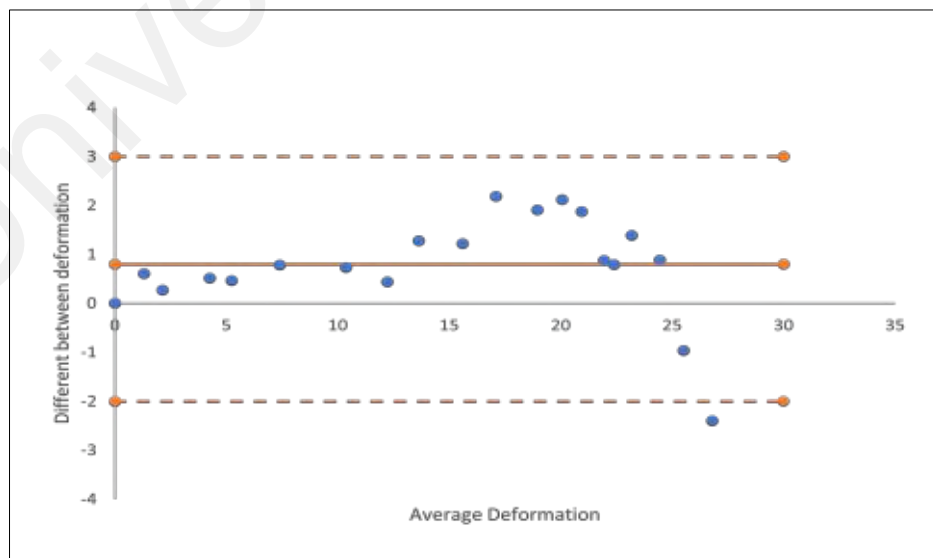
(a)
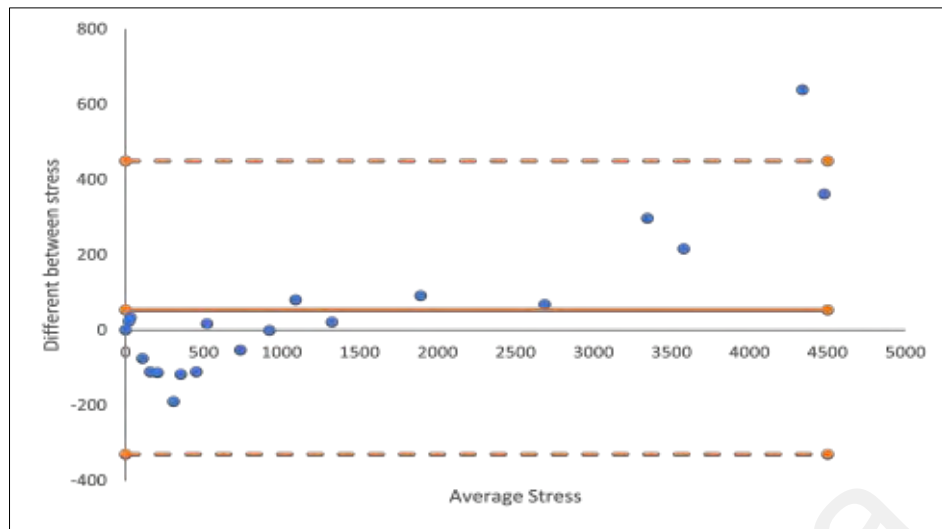
(b)

Figure 4.4: Bland-Altman plot of the SPA unit for simulation and experimental. (a)Bland-Altman plot for SPA unit deformation and (b)Bland-Altman plot for SPA unit stress.

According to the Bland-Altman plot, both the deformation and stress points from simulation and experimental data fell within the interval and limits of agreement (LoA). The outcomes indicated a satisfactory level of agreement between the deformation and stress testing methods employed in simulation and experimental conditions. No apparent systematic bias was observed, suggesting that the differences between the two testing methods were distributed randomly across the pressure range. A study conducted by Yang Song et al., (2022) validating a 3D Finite Element (FE) coupled model of the foot and sports shoe reported that most points scattering between $\pm$ 1.96SD signified a favorable agreement between the two approaches.. In another study by Leitner et al., (2022), Bland-Altman and correlation analysis were utilized to evaluate two blood pressure measurement methods. The Bland-Altman plot method was employed to illustrate and analyze the mean difference between the two conditions in their research.

The high ICC values for both parameters signified the reliability of the SPA unit. Nevertheless, a consensus on universally accepted standard values for assessing reliability using ICC remains elusive. Fleiss' study categorized ICC values as excellent

when ≥ 0.75, good to moderate within the range of 0.75 to 0.40, and poor when < 0.40 (Stable, 2014).

4.4   Experimental validation results on healthy participants

4.4.1   Muscle stiffness measurement for control and intervention group

   The significant difference within each group measurement position, treatment timepoint and pain levels score were investigated. Parametric analysis was used for normally distributed data; measurement position and treatment timepoint. Meanwhile nonparametric analysis was used for non-normally distributed data. In this study, the dataset includes measurements of three variables: BMI, age, and calf circumference. Each of these variables exhibits a distinct distribution and characteristics across the population. The diverse range of body compositions and ages contributes to the variability in BMI, age, and calf circumference readings. The violin plot is an effective graphic tool to depict the distribution and features of the dataset, providing a comprehensive visual representation of data distribution and facilitating comparisons across variables. Figure 4.5 depicts the violin plot on the distribution of the participants' age, BMI, and calf circumference. Meanwhile, Table 4.2 illustrates the statistical analysis of the participants parameters. From the figure we can see that the calf circumference and age have two different modes whereas the BMI has one mode. The box plot shows the median for BMI is lower than ages and calf circumference. Lower median BMI compared to age or calf circumference suggests potential variations in body composition among participants. The narrowness with a wide center observed for calf circumference highlights a uniform distribution among individuals. The recognition of these subtle patterns within the dataset, especially the consistency of calf circumference, plays a pivotal role in understanding the correlation between calf size and the maximum tolerance of SPA pressure. This understanding is crucial for determining appropriate SPA pressure levels.

Additionally, it offers valuable insights into the effects of SPA on muscle stiffness measurements following fatigue-inducing exercise.
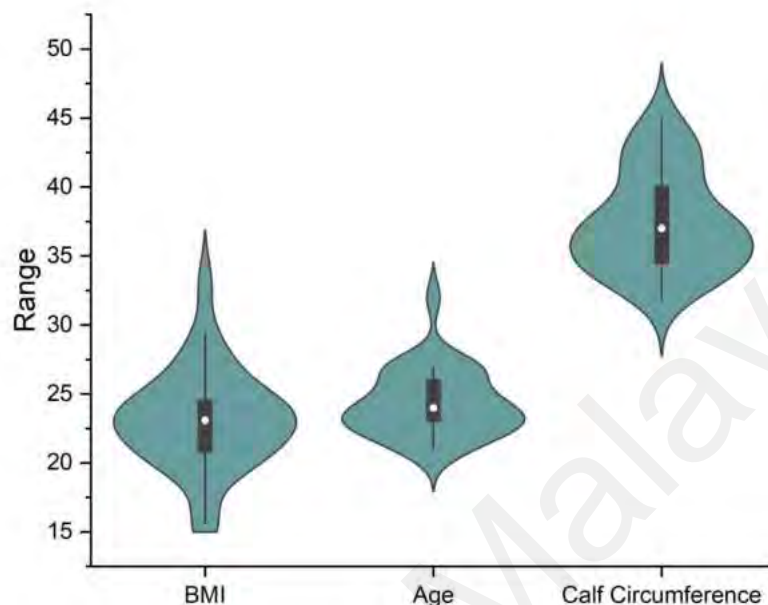
Figure 4.5: Violin plot of the participants BMI, age, and calf circumference.

Table 4.2 : Statistical analysis of the participants parameters.

	Min	Max	Mean	SD
BMI	19.7	33.1	23.1	3.56
Age	21	32	24	2.38
Calf Circumference	31.7	44.2	37	3.53

4.4.1.1 Participants Position and Treatment Timepoint for Intraclass Analysis

The significant difference between the treatment timepoint and participants position during muscle stiffness measurements were investigated. The Q-Q Plot normality test was used to see the distribution of data for participants muscle stiffness. The data distribution

is normally distributed as shown by Figure 4.6. Two-way repeated measure ANOVA test was used for the analysis.
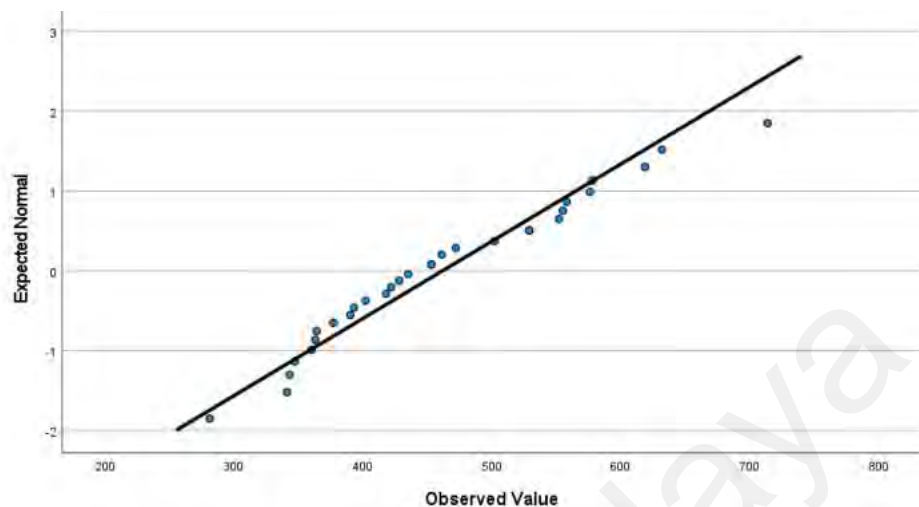
Figure 4.6 Q-Q plot for the participants muscle stiffness.

In the control group, a decreased in muscle stiffness value was recorded at post-treatment as compared to pre-treatment in for both standing (post-treatment: 431.96 ± 15.00; pre-treatment: 461.56 ± 18.90, $p > 0.05$) and sitting (post-treatment: 264.53 ± 5.89; pre-treatment: 270.00 ± 6.27, $p > 0.05$) during measurement. However, these reductions in stiffness were not found to be statistically significant p-values for both sitting and standing were greater than 0.05. The results of the muscle stiffness at pre-treatment and post-treatment for control group on dominant leg calf muscle were tabulated in Table 4.3.

Table 4.3: Calf muscle stiffness (N/m^2) for control group before and after treatment during sitting and standing.

Calf muscle stiffness on the dominant leg			
Measurement condition	Pre-Treatment	Post-Treatment	p-value
Sitting	270.00 ± 6.27	264.53 ± 5.89	0.98
Standing	461.56 ± 18.90	431.96 ± 15.00	0.35

In Table 4.4, the calf muscle stiffness for the control group is examined at baseline and 24 hours post-treatment during sitting and standing. Similar findings were observed

during sitting, where the baseline muscles stiffness was $269.57 \pm 10.72 \ N/m^2$, and it slightly decreased to $266.16 \pm 7.25 \ N/m^2$ after 24 hours of post treatment. However, the change was not statistically significant (p-value = 0.99). Meanwhile, for standing, the baseline of the muscle stiffness was $444.46 \pm 19.31 \ N/m^2$, and it increased to $457.33 \pm 18.67 \ N/m^2$ after 24 hours, but once again, the change was not statistically significant (p-value = 0.89).

Table 4.4: Calf muscle stiffness (N/m^2) for control group at baseline and 24 hours post treatment during sitting and standing.

Calf muscle stiffness on the dominant leg			
Measurement condition	Baseline	Post 24 hours	p-value
Sitting	269.57±10.72	266.16 ± 7.25	0.99
Standing	444.46 ± 19.31	457.33 ± 18.67	0.89

Table 4.5 focuses on the calf muscle stiffness for the control group at post-treatment and 24 hours after treatment during sitting and standing. An increased in muscle stiffness value was recorded after 24 hours of treatment as compared to post-treatment in both standing (post 24 hours: $457.33 \pm 18.67 N/m^2$); post-treatment: $431.96 \pm 15.00 \ N/m^2$), p > 0.05) and sitting (post 24 hours: $266.16 \pm 7.25 \ N/m^2$); post-treatment: 264.53 ± 5.89 N/m^2), p>0.05) during measurement. However, these increases in muscle stiffness were not found to be statistically significant p-values for both sitting and standing were greater than 0.05.

The comparison of the muscle stiffness value between different timepoint in both standing and sitting for control group is illustrated more clearly in the bar graph in Figure 4.7. The variations observed might be due to natural fluctuations or other factors unrelated to the treatment..Further analysis and larger sample sizes may be needed to draw more conclusive results.

Calf muscle on the dominant leg			
Measurement condition	Post-Treatment	Post 24 hours	p-value
Sitting	264.53 ± 5.89	266.16 ± 7.25	0.99
Standing	431.96 ± 15.00	457.33 ± 18.67	0.49
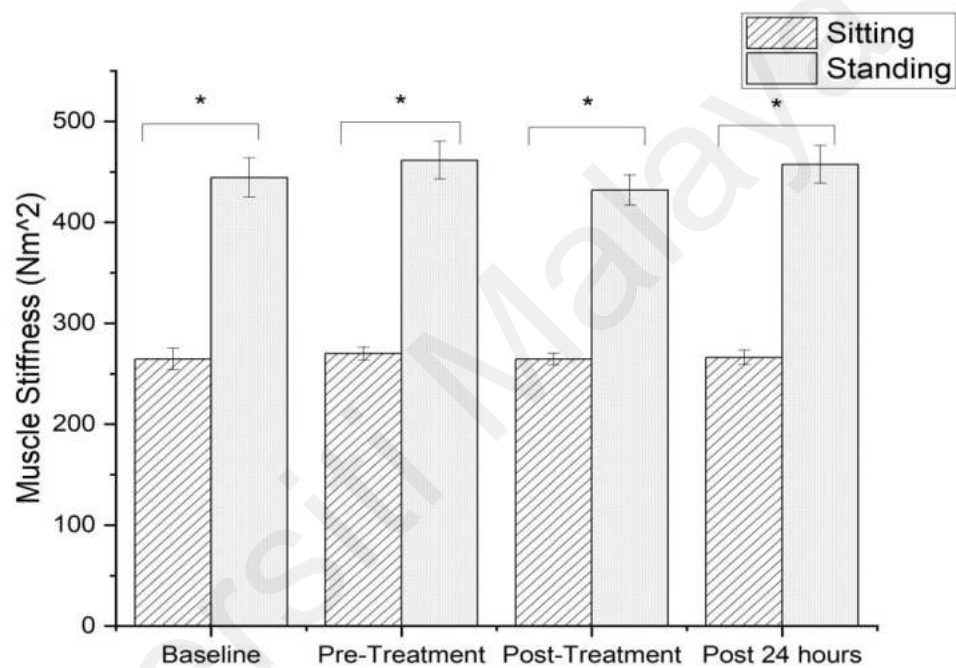
Figure 4.7: The comparison of the muscle stiffness value between different timepoint in both standing and sitting position for control group.

For the intervention group, a decreased in muscle stiffness value was recorded at post-treatment as compared to pre-treatment for standing (post-treatment; 382.30 ± 19.72 N/m^2; pre-treatment: 496.26 ± 24.70 N/m^2, $p < 0.05$), indicating a highly significant reduction in stiffness during standing after the intervention. However, for sitting, the pre-treatment stiffness was 281.30 ± 6.07 N/m^2, and it decreased to 237.53 ± 6.38 N/m^2 post-treatment. The p-value associated with this reduction is $p > 0.05$, which suggests that the decrease in stiffness during sitting was not statistically significant. The

result of the muscle stiffness at pre-treatment and post-treatment for intervention group

on dominant leg calf muscle were tabulated in Table 4.6.

Table 4.6: Calf muscle stiffness (N/m^2) for intervention group before and after treatment during sitting and standing.

	Calf muscle on the dominant leg		
Measurement condition	Pre-Treatment	Post-Treatment	p-value
Sitting	281.30 ± 6.07	237.53 ± 6.38	0.0640
Standing	496.26 ± 24.70	382.30 ± 19.72	**<0.0001**

Table 4.7 presents the calf muscle stiffness for the intervention group at baseline and

24 hours post-treatment during sitting and standing. A decreased in muscle stiffness value

was recorded after 24 hours of intervention as compared to baseline in for both standing

(post 24 hours: 433.90 ± 15.28 N/m^2; baseline: 450.46 ± 19.98 N/m^2, p > 0.05) and

sitting (post 24 hours: 259.10 ± 6.05 N/m^2; baseline: 263.83 ± 6.07 N/m^2, p >0.05)

during measurement. The p-value associated with this change is p>0.05 for both

measurement positions, suggesting that the difference in stiffness during sitting and

standing between baseline and 24 hours post-treatment was not statistically significant.

Table 4.7: Calf muscle stiffness (N/m^2) for intervention group at baseline and 24 hours post treatment during sitting and standing.

	Calf muscle on the dominant leg		
Measurement condition	Baseline	Post 24 hours	p-value
Sitting	263.83 ± 6.07	259.10 ± 6.05	0.99
Standing	450.46 ± 19.98	433.90 ± 15.28	0.77

A significantly increased in muscle stiffness value was observed after 24 hours of

intervention compared to post-treatment in both sitting (post 24 hours: 259.10 ± 6.05

N/m^2; post-treatment: $237.53 \pm 6.38 \ N/m^2$, p < 0.05) and standing (post 24 hours: $433.90 \pm 15.28 \ N/m^2$; post-treatment: $382.30 \pm 19.72 \ N/m^2$, p < 0.05). The results were summarized in Table 4.8. The comparison of the muscle stiffness value between different timepoint in both standing and sitting for intervention group is illustrated more clearly in the bar graph in Figure 4.8.

Table 4.8: Calf muscle stiffness (N/m^2) for intervention group at post treatment and post 24 hours after treatment during sitting and standing.

|	Calf muscle on the dominant leg		
Measurement condition	Post-treatment	Post 24 hours	p-value
Sitting	237.53 ± 6.38	259.10 ± 6.05	**0.01**
Standing	382.30 ± 19.72	433.90 ± 15.28	**0.02**
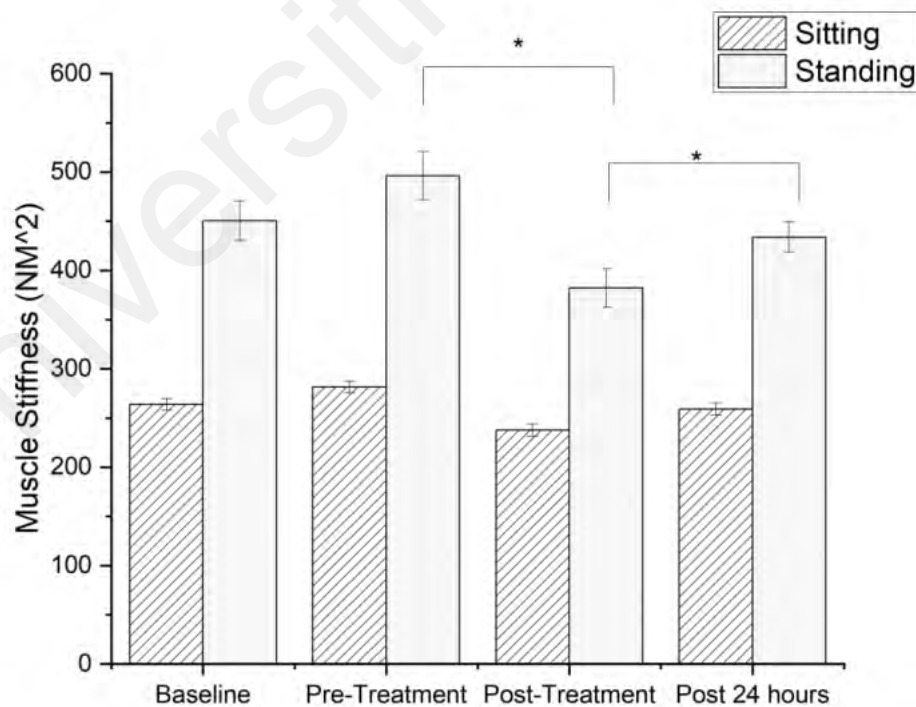
Figure 4.8: The comparison of the muscle stiffness value between different timepoint in both standing and sitting positions for intervention group.

Due to factors such as muscle fatigue and exercise-induced muscle damage (EIMD), engaging in repetitive and strenuous exercise can contribute to a reduction in exercise performance predominantly caused by changes in muscle architecture, including variations in muscle thickness (MT), fascicle length (FL), and pentation angle, as well as stiffness (Kato & Mariko Nakamura, 2018). Most of previous studies were able to establish a correlation between alterations in muscle rigidity and functional impairments. Muscle soreness can sometimes result in muscle rigidity. This study aimed to determine how SPA influences muscle stiffness following intense exercise at different time intervals.

The results demonstrate no significant changes in calf muscle stiffness between standing and sitting timepoints for the control group in. In contrast, the intervention group exhibited significant decreases in calf muscle stiffness between pre-treatment and post-treatment, indicating potential benefits for this condition. Our results suggest that PSA is effective in temporarily decreasing exercise induced stiffness. These findings are consistent with previous research indicating that compression can effectively reduce posttraumatic edoema and increase range of motion in patients with lower leg fractures and ankle sprains. (Franke et al., 2021; Kumar et al., 2019). They also offer valuable insights on the prevalent use of lower extremity compression garments (CGs) among athletes, particularly endurance athletes, for injury prevention and symptom management. The high proportion of athletes reporting CG usage during both training sessions and competitions underscores their perceived significance in supporting performance and recovery. Futhermore, Kumar et al., (2019) compared pneumatic compression therapy (PCT), lymphatic drainage exercises (LDE), and a control group in lower limb lymphedema patients. After four weeks of treatment, all groups showed significant improvement, with Group A (PCT and LDE) demonstrating outcomes comparable to Group B manual lymphatic drainage (MLD) and LDE) and superior to the control group

(MLD alone). Even though the type of injury and injured tissues vary, the present data demonstrate that the compressive effect is time dependent.

In addition, the intervention group demonstrated a significant increase in calf muscle stiffness between post treatment and post 24 hours were observed in intervention group. Previous studies were able to establish a correlation between alterations in muscle rigidity and functional impairments. Muscle soreness can sometimes result in muscle rigidity. Delayed onset muscle soreness (DOMS) is a type of muscle soreness that typically develops between 24 and 48 hours after exercise, especially when conducting new or intense exercises. The inflammation and pain associated with DOMS can cause stiffness and tightness in the muscles. Muscle rigidity is a crucial indicator of muscle health. After performing calf raises, repeated muscle contractions induced an increase in muscle rigidity (Kristensen et al., 2021). The study revealed the emergence of non-dominant calf pain two days after the induction of delayed onset muscle soreness (DOMS), alongside diminished isometric force production and pressure pain thresholds. Regression analyses uncovered key predictors of DOMS pain intensity variation, including cuff pressure pain tolerance threshold, temporal summation of pain, and participant age. These findings suggest that age, psychological factors, and central pain mechanisms are consistently associated with pain following acute muscle injury.

This is also supported by Stožer et al., (2020) on the study of pathophysiology of exercise induced muscle damage where muscle passive stiffness increased within 1 hour of exercise and peaked typically at 24 hours. It is recommended to strive for maintaining muscle condition as much as possible during exercise to sustain muscle performance.

4.4.1.2 Treatment Timepoint for Interclass Analysis.

A parametric test, the two-sample t-test, was used to investigate the significance of differences in calf muscle stiffness between the intervention and control groups at

different time points. At Baseline, there was no statistically significant difference in calf muscle stiffness between the intervention group (M = 450.46, SD = 19.98) and the control group (M = 444.46, SD = 19.30); degree of freedom (df)(58) = 0.34, p = 0.829.

Similar findings have been observed at pre-treatment and 24 hours after treatment, where there was no statistically significant difference in calf muscle stiffness between the intervention group and control group. The pre-treatment muscle stiffness value for intervention (M = 496.27 N/m^2, SD = 24.70) and the control group (M = 461.57 N/m^2, SD = 18.90); DoF(58) = 1.22, p = 0.269, while the muscle stiffness value after 24 hours of treatment for intervention (M = 433.90 N/m^2, SD = 15.28) and the control group (M = 457.33 N/m^2, SD = 18.67); t(58) = 0.79, p = 0.829.

However, a statistically significant difference was observed in calf muscle stiffness was observed at post treatment between the intervention group (M = 382.30 N/m^2, SD = 108.06) and the control group (M = 431.96 N/m^2, SD = 82.21); df(58) = 2.10, p = 0.049. The p-value of 0.049 indicates that the difference in calf muscle stiffness between the two groups at this timepoint is statistically significant. Table 4.9 summarizes the comparison between control group and intervention group. The comparison between group is illustrated more clearly in the bar chat in Figure 4.9

Table 4.9: Calf muscle stiffness, N/m^2 for intervention and control group in four different timepoint.

Muscle Stiffness (N/m^2)	Calf muscle on the dominant leg			
	Baseline	Pre-Treatment	Post-Treatment	Post 24 hours
Control Group	444.46±19.30	461.57 ± 18.90	431.96 ± 82.21	457.33 ± 18.67
Intervention Group	450.46±19.98	496.27 ± 24.70	382.30 ±108.06	433.90 ± 15.28
p-value (comparison between group)	0.829	0.269	**0.049**	0.829
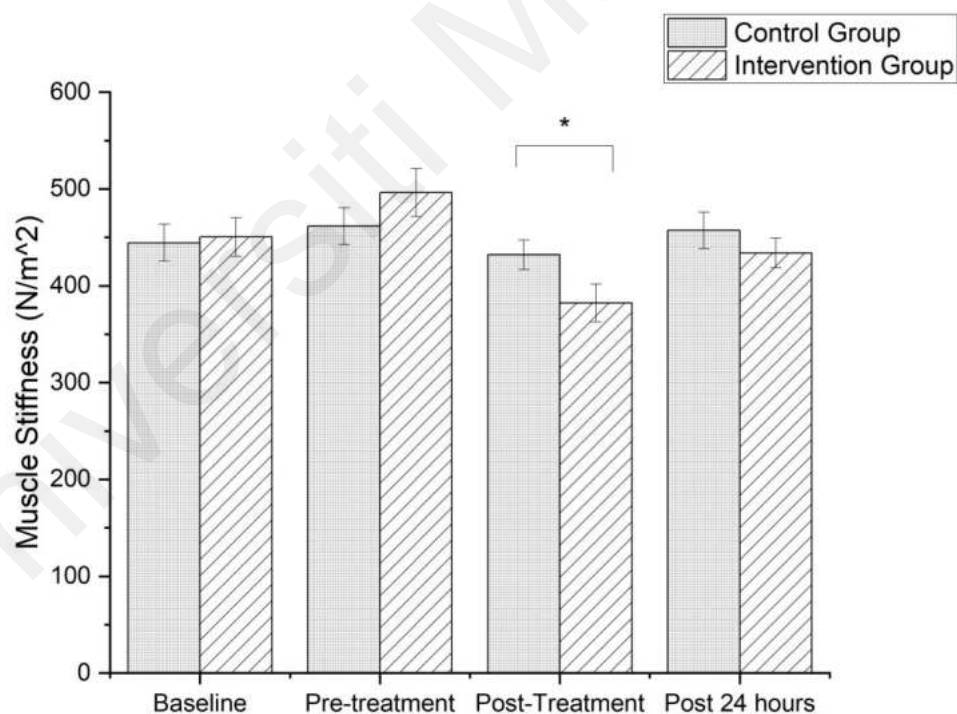
Figure 4.9: Mean ± SD calf muscle stiffness (N/m^2,) for intervention and control group between four different timepoint.

The purpose of this study was to examine the effects of SPA on muscle stiffness after strenuous exercise. The findings suggest that muscle stiffness is reduced significantly at

post treatment in the intervention group compared to control group. In the study on the effect of compression garments on the development of delayed-onset muscle soreness by Heiss et al., (2018), discover continuous wearing of compression garments during the inflammation phase of DOMS may play an important role in regulating muscle stiffness. The findings form study by Sugahara et al., (2018) on the effect of wearing compression stockings on muscle stiffness measured using ultrasound shear-wave elastography also found a decrease in muscle stiffness following application of compression stocking, suggesting that this reduction may be associated with the removal of interstitial fluid. In this study, a decrease in gastrocnemius muscle stiffness could be a common potential outcome of compression therapy. Compression is effective in reducing muscle stiffness by decreasing interstitial fluid production and can delay or prevent muscle fatigue during exercises by reducing muscle oscillation and energy consumption, thus creating an optimal neuromuscular environment (Yun et al., 2023). However, study by Utput et al., (2018) conclude that wearing compression garment during exercise did not change muscle architecture and muscle stiffness significantly. The disparity in findings between the studies may be attributable to a number of factors, including differences in study design, participant characteristics, and compression therapy type.

Since this study follows a crossover study design, no significant differences in muscle stiffness at the baseline and pre-treatment timepoints between the groups may imply that the participants' muscle stiffness was approximately equal when they conducted the experiment for each group.

4.4.1.3 Short-Form McGill Pain Questionnaire (SF-MPG) score for Intraclass Analysis

The significant difference of McGill pain score between the treatment timepoint; pre-treatment and post-treatment were investigated. The Q-Q Plot normality test was used to

see the distribution of data for McGill pain score. The data distribution was not normally distributed as shown by Figure 4.10. The Wilcoxon Signed rank test was used to measure the analysis.
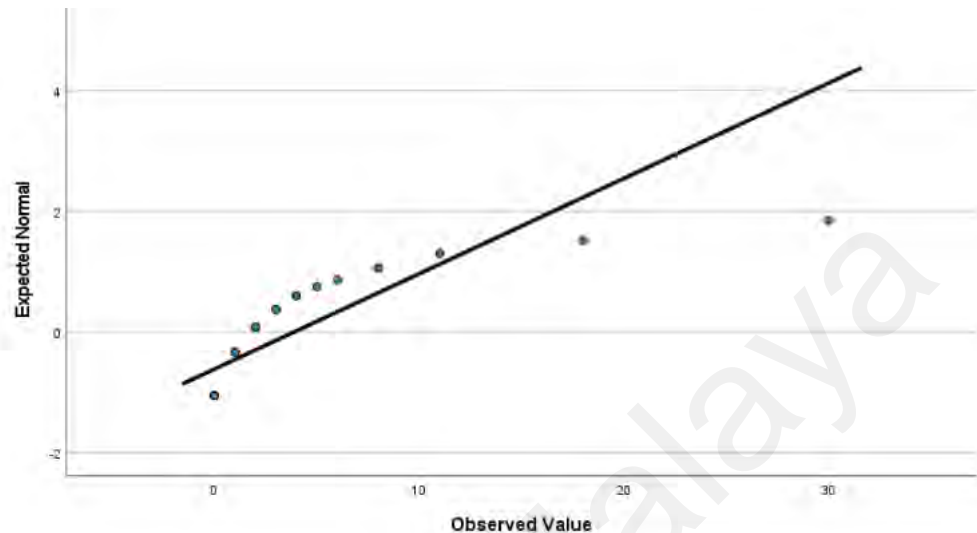
Figure 4.10: Q-Q plot for McGill pain score

Table 4.10 presents the McGill Pain Score data for the control group, comparing the pain scores pre and post treatment. A Wilcoxon signed rank test indicated change in treatment timepoint of the control group after 30 minutes of treatment without SPA does not influence the pain score, $T = 96.50$, $z = -0.1533$ (corrected for ties), N-Ties = 24, $p = 0.125$, two tailed. The test statistic (z) for the comparison between pre-treatment and post-treatment pain scores in the control group and the associated two-tailed p-value is tabulated in Table 4.11. Since the p-value is greater than the typical significance level of 0.05, the change in pain score for the control group is not considered statistically significant.

Relative to their pain score ranking, 15 participants ranked 30 minutes of treatment without SPA as more influential with a decrease in pain score (negative ranks) with a sum of rank of 203.50, and 9 participants ranked them as less influential with an increase in pain score (positive ranks) with a sum of rank of 96.50. Additionally, 6 participants have the pain scores remained unchanged. This effect can be considered as "small", $r = 0.027$.

Table 4.10: McGill Pain Score for control group at pre-treatment and post treatment.

		N	Mean Rank	Sum of Ranks
Pre-Treatment (rank) – Post Treatment (rank)	Negative Rank	15	13.75	203.50
	Positive Rank	9	10.72	96.50
	Unchanged	6	-	-
	Total	30	-	-

Table 4.11: Test Statistic, z for McGill pain score in control group.

	Pre-Treatment (rank) – Post Treatment (rank)
Z	-1.533
Asymp Sig. (2-tailed)	0.125

A Wilcoxon signed rank test for the intervention group, comparing the pain scores pre and post treatment indicated change in score after 30 minutes of treatment with SPA influence the pain score, T = 35.00, z = -3.315 (corrected for ties), N-Ties = 23, p = 0.020, two tailed as tabulated in Table 4.12 and 4.13. Since the p-value is lower than 0.05, the change in pain score for the intervention group is considered statistically significant.

There were 21 participants ranked 30 minutes of treatment with SPA as more influential with a decrement in pain score (negative ranks) with a sum of rank of 241.00, while 2 participants ranked them as less influential with an increment in pain score (positive ranks) with a sum of rank of 35.00. Additionally, seven participants reported no change in pain scores. This effect can be considered as "large", r = 0.605.

Table 4.12: McGill Pain Score for intervention group at pre-treatment and post treatment.

		N	Mean Rank	Sum of Ranks
Pre-Treatment (rank) – Post Treatment (rank)	Negative Rank	21	11.48	241.00
	Positive Rank	2	17.50	35.00
	Unchanged	7	-	-
	Total	30	-	-

Table 4.13: Test Statistic, z for McGill pain score in intervention group.

	Pre-Treatment (rank) – Post Treatment (rank)
Z	-3.315
Asymp Sig. (2-tailed)	**0.020**

The Wilcoxon signed rank test revealed that the pain scores for the control group did not change significantly after 30 minutes of treatment without SPA. This finding suggests that the treatment without SPA had no significant effect on the pain experience of the control group during this specific time. The absence of a significant change in pain scores suggests that factors other than the treatment may be influencing pain perception in the control group at this time. El Tumi et al., (2017) conducted a review on age-related changes in pain sensitivity in healthy humans and the findings suggest that pain perception diminishes in old age.

On the other hand, the Wilcoxon signed rank test conducted in the intervention group indicated that there was a significant influence on the pain score after 30 minutes of treatment with SPA. This suggests that the inclusion of SPA during same time interval had a measurable effect on reducing pain in the intervention group. The pain-relieving properties of SPA, such as its ability to promote relaxation, reduce muscle tension, and increase blood flow, might have contributed to the observed decrease in pain scores

during this specific treatment timepoint (K.A. Zuj, Prince, R.L. Hughson, 2019; Yanaoka et al., 2022). Haun et al., (2017) investigate the intermittent pneumatic compression (IPC) with resistance training, the findings include IPC can increased pressure to pain threshold (PPT).

However, it is crucial to interpret the results with caution and consider several factors. First, the observed effect in the intervention group might be transient, and further evaluations at different timepoints are needed to ascertain the duration of pain relief. Second, individual differences in response to SPA should be considered, as some participants may be more responsive than others.

4.4.1.4 Short-Form McGill Pain Questionnaire (SF-MPG) score for Interclass Analysis

The Mann-Whitney U test was conducted to compare the McGill pain scores between the control and intervention groups at pre-treatment and post-treatment. Table 4.14 and 4.15 present the McGill Pain Score data for both the control and intervention groups at pre-treatment. The participants' pain scores were ranked, and the mean ranks were calculated for each group. This analysis indicated that the pain score in intervention group (Mean Rank = 33.10, n = 30) were higher than in the control group (Mean Rank = 27.90, n = 30), U = 372.00, z = -1.162 (corrected for ties), p = 0.245 (two-tailed). The mean ranks and sum of ranks are lower in the control group compared to the intervention group, suggesting that participants in the control group tended to have slightly lower pain scores at this time point. However, since the p value > 0.05 the difference in pain score is considered not statistically significant. This effect can be described as "small" (r = 0.212).

Table 4.14: McGill Pain Score at pre-treatment between control and intervention group.

Ranks	Group	N	Mean Rank	Sum of Ranks
McGill Pain Score	Control Group	30	27.90	837.00
	Intervention Group	30	33.10	993.50
	Total	60		

Table 4.15: Test Statistic, Z for McGill pain score at pre-treatment between control and intervention group.

Test Statistics	McGill Pain Score
Mann-Whitney U	372.000
Wilcoxon W	837.000
Z	-1.162
p-value	0.245

Table 4.16 and 4.17 display the McGill pain score data for both control and intervention groups at post-treatment. Each group had 30 participants. The participants' pain scores were ranked, resulting in a mean rank for the control group (Mean Rank = 37.82, n = 30) and the intervention group (Mean Rank = 23.18, n = 30), U = 230.500, z = -3.275 (corrected for ties), p = 0.001 (two-tailed). The mean ranks and sum of ranks are considerably higher in the control group compared to the intervention group, indicating that participants in the control group tended to have higher pain scores at this time point. The low p-value of 0.001 confirms that this difference is statistically significant. This effect can be described as "large" (r = 0.597).

Table 4.16: McGill Pain Score at post-treatment between control and intervention group.

	Ranks			
	Group	N	Mean Rank	Sum of Ranks
McGill Pain Score	Control Group	30	37.82	1134.50
	Intervention Group	30	23.18	695.50
	Total	60		

Table 4.17: Test Statistic, Z for McGill pain score at post-treatment between control and intervention group.

Test Statistics	
	McGill Pain Score
Mann-Whitney U	230.500
Wilcoxon W	695.500
Z	-3.275
p-value	**0.001**

Based on the Mann-Whitney analysis, there was no statistically significant difference in pain scores between the control and intervention groups at pre-treatment. However, following the intervention, a significant difference in pain scores emerged between the two groups. The intervention group reported significantly lower pain scores compared to the control group. This finding aligns with previous research, indicating that compression therapy can effectively reduce pain in certain conditions (Stedge & Armstrong, 2021).

Several factors may have contributed to the observed reduction in pain scores in the intervention group. Firstly, SPA's ability to improve circulation might have alleviated pain by minimizing pressure on nerves and tissues. The implementation of SPA enhances circulation through rhythmic compression and decompression, facilitating blood flow to specific regions. This augmented circulation helps in alleviating pressure on nerves and tissues by ensuring efficient delivery of oxygen and nutrients while aiding in the removal

of metabolic waste products. Zuj et al., (2019) determine if intermittent compression could be used during exercise to augment the actions of the muscle pump. The result shows that intermittent compression applied during exercise and recovery from exercise results in increased limb blood flow, potentially contributing to changes in exercise performance and recovery. Furthermore, psychological factors might have played a role in the pain reduction. The study by Draper et al., (2020) in which they tested the physiological and psychological effects of intermittent pneumatic compression (IPC) on DOMS concludes the IPC may provide psychological benefits as it reduces the intensity of soreness which is commonly associated with. The sense of reassurance and comfort provided by compression therapy could have positively influenced the intervention group's pain experience.

4.4.2 Pearson's r Correlation analysis between Maximum Pressure and Calf Circumference

The Q-Q Plot normality test was used to see the distribution of the data measurements for calf circumference and participants' maximum tolerable pressure. Both show that the data distribution is normally as shown by Figure 4.11 and 4.12. Therefore, Pearson's r correlation analysis was conducted to determine the size and direction of the linear relationship between participants' calf circumference and maximum tolerable pressure. Table 4.18 presents the results of Pearson's correlation analysis between two variables: maximum pressure and calf circumference. The bivariate correlation between these two variables was positive and strong, $r(28) = 0.95$, $p < 0.001$. The distribution of the calf circumference and maximum pressure is illustrated more clearly in the scatter plot in Figure 4.13.
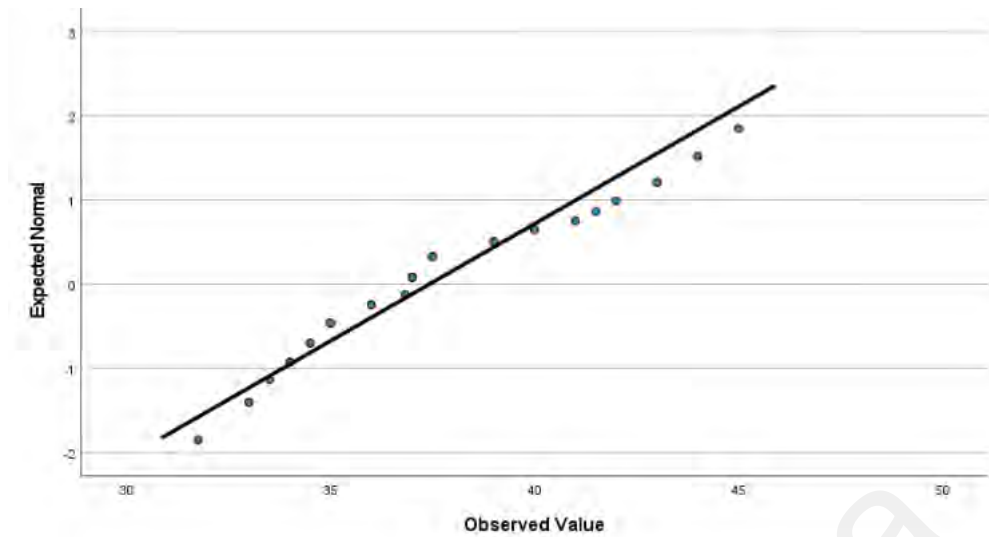
Figure 4.11: Q-Q Plot for calf circumference.
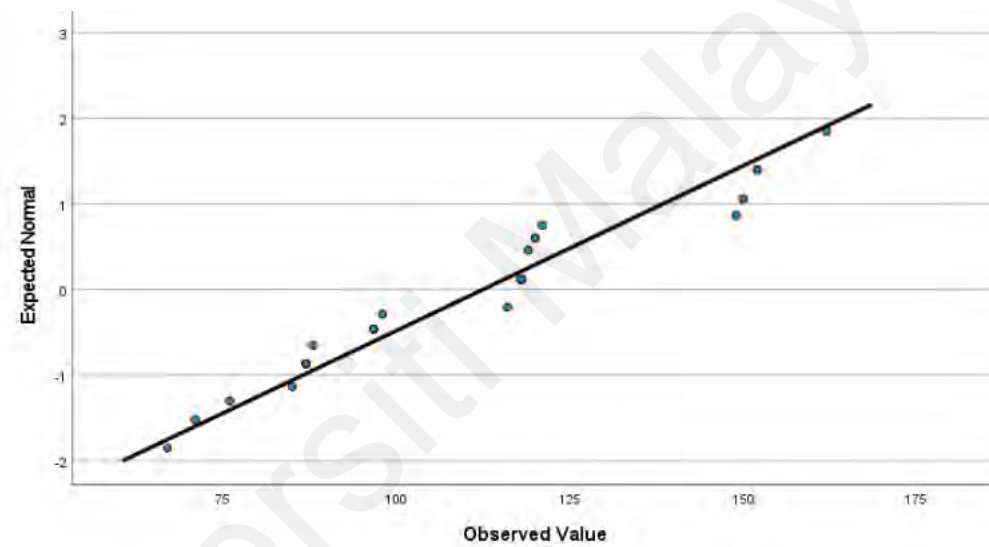
Figure 4.12: Q-Q Plot for maximum pressure participants can tolerate.

Table 4.18: Pearson's r correlation coefficient of the calf circumference and maximum pressure.

	Pearson's r correlation coefficient (r)	p-value
Maximum pressure and calf circumference	0.958	**0.000**
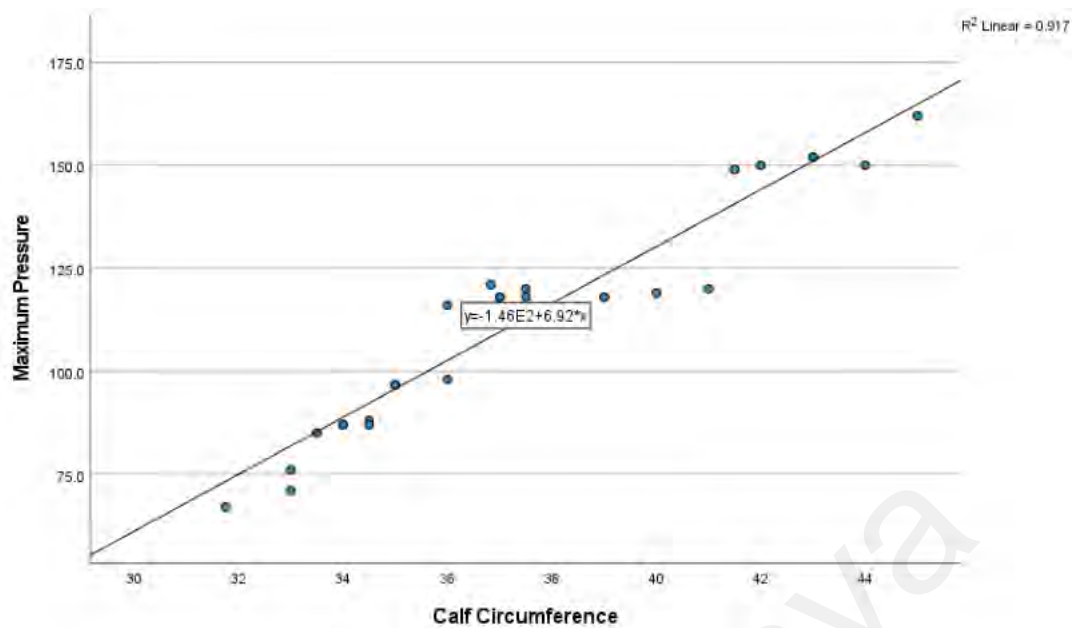
Figure 4.13: Positive linear trend between maximum pressure variation and calf circumference.

The maximum pressure for compression therapy was evaluated based on the circumference of the leg before applying the SPA cuff to ensure maximum therapy effectiveness. The findings show that positive linear trend between pressure variation and leg circumference. Participants with bigger leg circumference can tolerate higher compression pressure compared to participants with smaller circumference. The physiological characteristic of the participants calf muscle and surrounding tissue may attribute the positive linear correlation. A larger calf circumference typically indicates a greater muscle mass and potentially more developed connective tissue. Therefore, individual with larger calf muscles may have a higher capacity to withstand pressure due to the increased muscle volume and support from the surrounding structures.

This finding is in agreement with study by Gianesini et al., (2020) where it concludes that different lower limb circumference variations influence the interface pressure gradient. Mosti et al.(2010) compare the haemodynamic efficiency of a multi-component graduated compression bandage versus a negative graduated compression bandage with higher pressure over the calf. The result demonstrates higher pressure is required at the

calf compared to distal leg in both compression techniques. Moreover, larger calf muscles might have a larger surface area, distributing the applied compression pressure over a larger region. This can reduce the pressure per unit area, making it more tolerable for participants with bigger calf circumferences.

4.5   Summary

4.5.1   Technical Contribution

This research has made significant technical contributions in the field of soft pneumatic actuators (SPAs) for lower limb rehabilitation. First, a detailed modeling and simulation of SPAs using food grade silicone was conducted. The study revealed that A10 Shore food grade silicone exhibited higher deformation under mild stress and low-pressure conditions. This finding underscores the material's suitability for SPA applications, particularly in scenarios where gentle pressure transmission and controlled deformation are crucial. This technique is emphasized as a fundamental step in the fabrication of SPAs, as it offers a widely applicable approach for modeling the behavior of various actuators. This approach remains independent of the actuator's specific actuation mechanism or material properties.

In pursuit of enhancing real-life applications, a significant technical contribution of this study involves conducting a comprehensive comparison between collected simulation and experimental data. Specifically, the study undertook a thorough assessment of the SPA chamber's performance by closely examining the agreement between simulated and experimental pressure transmission on the mannequin leg. Furthermore, employing the Bland-Altman plot, this research extended its technical contribution by evaluating deformation and stress points in both simulation and experimental conditions. The outcomes indicated a favorable agreement between the two methods, as evidenced by the deformation and stress points falling within the interval and limits of agreement (LoA). The lack of consistent bias means that any variations between

the testing methods happened randomly as pressure changed. This careful examination shows that the developed SPA model is strong and dependable, accurately predicting how things deform and handle stress. Altogether, these insights help to better grasp how the SPA works, making it more reliable for helping people recover from lower limb injuries.

Moreover, it is suggested to evaluate the performance of the fabricated SPA on varying human leg profiles, taking into account different skin stiffness and fat layers. This assessment aims to analyze the effectiveness of pressure transmission of SPA across different human subjects. The results showed a significant decrease in muscle stiffness among the intervention group after treatment compared to control group, highlighting the SPA's potential to alleviate stiffness. Additionally, the intervention group reported notably lower pain scores after treatment, further indicating the SPA's effectiveness. This highlights the potential of the SPA as a therapeutic tool for musculoskeletal injury recovery and lower limb rehabilitation. Furthermore, the significant reduction in muscle stiffness and pain scores underscores the SPA's ability to deliver precise and targeted pressure, which is essential for effective treatment. These insights provide valuable information for the design and application of SPAs in the field of soft robotics, specifically for enhancing recovery and performance in individuals with lower limb injuries.

4.5.2 Practical Contribution

Consequently, this investigation has implications for applications in the real world. The purpose of this investigation was to develop an SPA system capable of accelerating recovery and preventing lower limb injuries. Our study's primary objective was to examine the potential of SPAs made of silicone elastomer to reduce muscle rigidity after intense exercise. Based on the experimental testing, the proposed SPA system can deliver the desired pressure for treating musculoskeletal injuries. The soft actuator model

exhibited remarkable properties, including softness, robustness, biocompatibility, and non-hazardous characteristics, with elasticity comparable to commercial silicone. It allowed for substantial deformation in response to pressure changes while maintaining high tensile strength for excellent tear resistance and proper compression pressure on the calf. The sensor-based design of the proposed system is basic and lightweight, and it offers adjustable cycle time and pressure settings for individual comfort.

Furthermore, based on the comprehensive analysis, comparing simulation and experimental data, validated the system's reliability for pressure distribution within the range of 0-120mmHg. These findings present a promising step towards practical and effective compression therapy options, potentially reducing lower limb muscle injuries following intensive exercise in a safe and accessible manner.

In addition, the observed correlation between maximum pressure and calf circumference suggests that the SPA system can be customized to satisfy the individual needs and preferred pressure settings of each subject, thereby increasing its overall efficacy. This adaptability makes the SPA system a valuable and practical addition to the treatment options available to physiotherapists, sports medicine specialists, and other healthcare professionals, empowering them with an accessible and modifiable instrument to address lower limb muscle stiffness and promote patient recovery.

CHAPTER 5: CONCLUSION AND FUTURE WORKS

5.1   Conclusion

In this study, a SPA system was designed and developed to detect and visualize the interface pressure induced by the SPA chamber as well as to perform experimental validation of a soft pneumatic actuators to treat lower limb musculoskeletal injuries focusing on muscle stiffness. This chapter provides a summary of the significant findings presented earlier, aiming to grasp the contributions of the results obtained throughout the course of this research.

Finite element method was used in the selection of design parameters and suitable silicone rubber materials for SPA applications, requiring at least 1N of force. The inclusion of A10 Shore food grade silicone, in the modeling of soft actuators, highlights its capacity as a fundamental element for soft actuator construction. This type of silicone exhibits notable deformability, achieving up to 28 mm of deformation upon inflation and deformed under mild stress.

Subsequently, a comparison was drawn between the simulation model and the SPA system, allowing for the observation of deformation behavior. The reliability demonstrated a strong correlation in terms of material deformation and stress, with an interclass correlation coefficient (ICC>0.9) for both scenarios. Remarkably, the simulation and experimental findings exhibited remarkable consistency in terms of pressure transmission onto the skin within the 0–120 mmHg pressure range. This pressure range aligns with the therapeutic interest in managing lower limb lymphedema through compression therapy. The developed model is useful for FEM simulation-based design optimization of soft actuators, by investigating the relationship between pressure and deformation. Excellent agreement between simulation and experiment demonstrates the

accuracy and dependability of the SPA system in transmitting pressure to the epidermis, making it a promising rehabilitation and recovery tool.

The developed model is then used to conduct a study for the SPA treatment, to evaluate the feasibility of using SPA as a treatment for fatigue induction exercise focusing on muscle stiffness. The correlation between maximum pressure and calf circumference has also been observed in 30 healthy male subjects to determine the necessary pressure needed. The findings show positive linear trends on the pressure variation and calf circumference, r=0.958. This concludes that variations in lower limb circumference have been found to impact the interface pressure gradient, indicating that greater pressure is needed at the calf as opposed to the distal leg.

Moreover, the findings from this study outline the role of SPA made up from food grade silicone in reducing muscle stiffness after fatigue induction exercise. The result presented significant reduction in muscle stiffness between pre-treatment and post treatment for interventions from an initial value of 496.26 ± 24.70 Nm^{-2} to a subsequent value of 382.30 ± 19.72 Nm^{-2} immediately following the application of pneumatic compression. This decrement corresponds to a percentage reduction of 22.96%, with p-value of 0.0001. There was no statistically significant difference seen between the pre-treatment and post-treatment measurements in the control group, with a p-value of 0.3500. In addition, following the intervention, a significant difference in pain scores emerged between the two groups. The intervention group reported significantly lower pain scores compared to the control group. The results are indication for the proposed SPA system can deliver the desired pressure for treating musculoskeletal injuries. The system can operate according to the specific pressure settings required for each subject, which makes it a promising tool for rehabilitation and recovery. This study provides strong evidence for the prospective use of SPA systems constructed from food-grade silicone in the

treatment of lower limb musculoskeletal injuries, specifically muscle stiffness caused by fatigue induction exercise.

5.2 Limitation

The present study had some limitations. Notably, the 3D model simulation did not incorporate fluid-structure interaction (FSI) between the fluid and solid, which would have allowed for analysis of the pressure flow behavior within the SPA. The absence of fluid-structure interaction (FSI) in the 3D model simulation limits the analysis of pressure flow behavior within the SPA. FSI accounts for the interaction between fluid flow and deformable structures, crucial for capturing dynamic coupling effects. Its absence may lead to inaccuracies in predicting fluid-induced vibrations, oscillations, or changes in geometry. In addition, one limitation of conducting experiments on the stress–pressure relationships of soft pneumatic actuator are the challenge of precisely measuring the internal pressure of the actuator. Initially, the experimental pressure was indirectly acquired using the FSR sensor. To establish the stress-strain curve of the SPA, direct uniaxial tension tests using a tensometer should be carried out.

. On the other hand, the study in investigating the SPA treatment's feasibility after fatigue-inducing exercise does not account for potential confounding effects from external factors, such as participants' pre-existing physical activity or lifestyle habits. These uncontrollable variables could add uncertainty to the outcomes, making it harder to confidently link observed effects solely to the SPA treatment.

Furthermore, a significant constraint arises from the small sample size and the narrow age range of participants in the study. The limited sample size may hinder the generalizability of the findings to broader populations, while the restricted age group could limit the applicability of the results to individuals outside the specified age range.

Therefore, caution should be exercised when extending the conclusions of the study to other demographic groups or age categories.

5.3 Future Work

The proposed SPA system has successfully produced a promising result in the treatment of lower limb musculoskeletal injuries, specifically muscle stiffness caused by fatigue induction exercise. Nevertheless, there are few possible future works that can be considered as following:

- Future studies should include a simulation of the pressure originating from the SPA inlet through a fluid-structure interaction (FSI) analysis. This approach could aid in determining the optimal pressure for application on the skin surface.

- Measuring internal pressure within soft pneumatic actuators, future studies could explore and implement advanced pressure measurement techniques, such as using advanced pressure sensors or other innovative methods to directly quantify the pressure distribution within the actuator during various conditions.

- The study investigating the SPA treatment's feasibility could include comprehensive participant profiling. This would involve collecting detailed information about participants' pre-existing physical activity, lifestyle habits, and other relevant variables. By controlling these factors in the study design, researchers can enhance the reliability and validity of the results, providing a clearer understanding of the true impact of SPA treatment on fatigue induction.

- The inclusion of actual patients undergoing lower limb rehabilitation to enhance the clinical relevance and applicability of the findings. This inclusion would allow for a more comprehensive understanding of the SPA system's effectiveness and usability in real-world rehabilitation settings.

- Since this study only evaluates muscle stiffness in healthy male participant cohorts, research exploring between genders might present interesting findings. Generally, males and females have different lower limb muscle activation.

REFERENCES

Abbiss, C. R., Burnett, A., Nosaka, K., Green, J. P., Foster, J. K., & Laursen, P. B. (2010). Effect of hot versus cold climates on power output, muscle activation, and perceived fatigue during a dynamic 100-km cycling trial. *Journal of Sports Sciences*, *28*(2), 117–125. https://doi.org/10.1080/02640410903406216

Abe, K., & Tsuji, T. (2021). *Postural differences in the immediate effects of active exercise with compression therapy on lower limb lymphedema*. 6535–6543.

Agarwal, G., Besuchet, N., Audergon, B., & Paik, J. (2016). Stretchable Materials for Robust Soft Actuators towards Assistive Wearable Devices. *Nature Publishing Group*, *September*, 1–8. https://doi.org/10.1038/srep34224

Akbari, A., Haghverd, F., & Behbahani, S. (2021). Robotic Home-Based Rehabilitation Systems Design: From a Literature Review to a Conceptual Framework for Community-Based Remote Therapy During COVID-19 Pandemic. *Frontiers in Robotics and AI*, *8*. https://doi.org/10.3389/FROBT.2021.612331

Al-Nakhli, H. H., Petrofsky, J. S., Laymon, M. S., & Berk, L. S. (2012). The use of thermal infra-red imaging to detect delayed onset muscle soreness. *Journal of Visualized Experiments*, *59*, 1–9. https://doi.org/10.3791/3551

Alici, G. (2018). Softer is harder: What differentiates soft robotics from hard robotics? *MRS Advances*, *3*(28), 1557–1568. https://doi.org/10.1557/adv.2018.159

Ansari, Y., Manti, M., Falotico, E., Mollard, Y., Cianchetti, M., & Laschi, C. (2017). Towards the development of a soft manipulator as an assistive robot for personal care of elderly people. *International Journal of Advanced Robotic Systems*, *14*(2). https://doi.org/10.1177/1729881416687132

Ashuri, T., Armani, A., Jalilzadeh Hamidi, R., Reasnor, T., Ahmadi, S., & Iqbal, K. (2020). Biomedical soft robots: current status and perspective. *Biomedical Engineering Letters*, *10*(3), 369. https://doi.org/10.1007/S13534-020-00157-6

Baldoli, I., Mazzocchi, T., Paoletti, C., Ricotti, L., Salvo, P., Dini, V., Laschi, C., Di Francesco, F., & Menciassi, A. (2016). Pressure mapping with textile sensors for compression therapy monitoring. *Proceedings of the Institution of Mechanical Engineers, Part H: Journal of Engineering in Medicine*, *230*(8), 795–808. https://doi.org/10.1177/0954411916655184

Baoge, L., Van Den Steen, E., Rimbaut, S., Philips, N., Witvrouw, E., Almqvist, K. F., Vanderstraeten, G., & Vanden Bossche, L. C. (2012). Treatment of Skeletal Muscle Injury: A Review. *ISRN Orthopedics*, *2012*, 1–7. https://doi.org/10.5402/2012/689012

Barassi, G., Obrero-Gaitan, E., Irace, G., Crudeli, M., Campobasso, G., Palano, F., Trivisano, L., & Piazzolla, V. (2020). Integrated Thermal Rehabilitation: A New Therapeutic Approach for Disabilities. *Advances in Experimental Medicine and Biology*, *1251*, 29–38. https://doi.org/10.1007/5584_2019_465/COVER/

Bardi, E., Gandolla, M., Braghin, F., Resta, F., Pedrocchi, A. L. G., & Ambrosini, E. (2022). Upper limb soft robotic wearable devices: a systematic review. *Journal of NeuroEngineering and Rehabilitation*, *19*(1), 87. https://doi.org/10.1186/S12984-022-01065-9

Belfer, I. (2013). Nature and Nurture of Human Pain. *Scientifica*, *2013*, 1–19. https://doi.org/10.1155/2013/415279

Belforte, G., Eula, G., Ivanov, A., & Sirolli, S. (2014). Soft pneumatic actuators for rehabilitation. *Actuators*, *3*(2), 84–106. https://doi.org/10.3390/act3020084

Berszakiewicz, A., Sieroń, A., Krasiński, Z., Cholewka, A., & Stanek, A. (2020). Compression therapy in venous diseases: physical assumptions and clinical effects. *Advances in Dermatology and Allergology/Postępy Dermatologii i Alergologii*, *37*(6), 842. https://doi.org/10.5114/ADA.2019.86990

Bhardwaj, S., Khan, A. A., & Muzammil, M. (2021). Lower limb rehabilitation robotics: The current understanding and technology. *Work*, *69*(3), 775–793. https://doi.org/10.3233/WOR-205012

Bisciotti, G. N., Volpi, P., Amato, M., Alberti, G., & Allegra, F. (2018). Italian consensus conference on guidelines for conservative treatment on lower limb muscle injuries in athlete. *BMJ Open Sport and Exercise Medicine*, *4*(1). https://doi.org/10.1136/bmjsem-2017-000323

Borman, P., & Koyuncu, E. G. (2020). *The Comparative Efficacy of Conventional Short-Stretch Multilayer Bandages and Velcro Adjustable Compression Wraps in Active Treatment Phase of Patients with Lower Limb Lymphedema*. *00*(00), 1–9. https://doi.org/10.1089/lrb.2020.0088

Broderick, P., Horgan, F., Blake, C., Ehrensberger, M., Simpson, D., & Monaghan, K. (2018). Mirror therapy for improving lower limb motor function and mobility after stroke: A systematic review and meta-analysis. *Gait and Posture*, *63*(November 2017), 208–220. https://doi.org/10.1016/j.gaitpost.2018.05.017

Butani, H. I. A., & Hima, N. O. S. (2017). *Effects of Wearing a Compression Garment During Night Sleep on Recovery from High-intencity Eccentric-Concentric Quadriceps Muscle Fatigue*. *2*, 2816–2824.

Cacucciolo, V., Renda, F., Poccia, E., Laschi, C., & Cianchetti, M. (2016). Modelling the nonlinear response of fibre-reinforced bending fluidic actuators. *Smart Materials and Structures*, *25*(10). https://doi.org/10.1088/0964-1726/25/10/105020

Cappello, L., Galloway, K. C., Sanan, S., Wagner, D. A., Granberry, R., Engelhardt, S., Haufe, F. L., Peisner, J. D., & Walsh, C. J. (2018). Exploiting Textile Mechanical Anisotropy for Fabric-Based Pneumatic Actuators. *Soft Robotics*, *5*(5), 662–674. https://doi.org/10.1089/soro.2017.0076

Carvalho, A. D. D. R., Karanth P, N., & Desai, V. (2022). Characterization of pneumatic muscle actuators and their implementation on an elbow exoskeleton with a novel hinge design. *Sensors and Actuators Reports*, *4*(June), 100109. https://doi.org/10.1016/j.snr.2022.100109

Castilho Junior, O. T., Dezotti, N. R. A., Dalio, M. B., Joviliano, E. E., & Piccinato, C. E. (2018). Effect of graduated compression stockings on venous lower limb hemodynamics in healthy amateur runners. *Journal of Vascular Surgery: Venous and Lymphatic Disorders*, *6*(1), 83–89. https://doi.org/10.1016/j.jvsv.2017.08.011

Chassagne, F. (2018). *Biomechanical study of the action of compression bandages on the lower leg To cite this version : HAL Id : tel-01848712 Fanette CHASSAGNE É tude biomécanique de l ' action des bandes de compression sur le membre inférieur Biomechanical study of the action*.

Chi, Y.-W. (2017). A new compression pressure measuring device. *Veins and Lymphatics*, *6*(1). https://doi.org/10.4081/vl.2017.6636

Chou, L. B., Niu, E. L., Williams, A. A., Duester, R., Anderson, S. E., Harris, A. H. S., & Hunt, K. J. (2018). Postoperative Pain After Surgical Treatment of Ankle Fractures: A Prospective Study. *Journal of the American Academy of Orthopaedic Surgeons Global Research and Reviews*, *2*(9). https://doi.org/10.5435/JAAOSGlobal-D-18-00021

Christianson, C., Goldberg, N. N., Deheyn, D. D., Cai, S., & Tolley, M. T. (2018). Translucent soft robots driven by frameless fluid electrode dielectric elastomer actuators. *Science Robotics*, *3*(17), 1–9. https://doi.org/10.1126/SCIROBOTICS.AAT1893

Chua, M. C. H., Lim, J. H., & Yeow, R. C. H. (2019). Design and Characterization of a Soft Robotic Therapeutic Glove for Rheumatoid Arthritis. *Assistive Technology*, *31*(1), 44–52. https://doi.org/10.1080/10400435.2017.1346000

Cimmino, M. A., Ferrone, C., & Cutolo, M. (2011). Epidemiology of chronic musculoskeletal pain. *Best Practice and Research: Clinical Rheumatology*, *25*(2), 173–183. https://doi.org/10.1016/j.berh.2010.01.012

Conde Montero, E., Serra Perrucho, N., & de la Cueva Dobao, P. (2020). Theory and Practice of Compression Therapy for Treating and Preventing Venous Ulcers. *Actas Dermo-Sifiliográficas (English Edition)*, *111*(10), 829–834. https://doi.org/10.1016/j.adengl.2020.10.022

Coyle, S., Majidi, C., Leduc, P., & Hsia, K. J. (2018). *Bio-inspired Soft Robotics : Material Selection , Actuation , and Design*. 1–22.

Craddock, M., Augustine, E., Konerman, S., & Shin, M. (2022). Biorobotics: An Overview of Recent Innovations in Artificial Muscles. *Actuators*, *11*(6). https://doi.org/10.3390/act11060168

Craighead, D. H., Shank, S. W., Gottschall, J. S., Passe, D. H., Murray, B., Alexander, L. M., & Kenney, W. L. (2017). *Lengthening our Perspective: Morphological, Cellular and Molecular Responses to Eccentric Exercise*. *56*(3), 379–385. https://www.ncbi.nlm.nih.gov/pmc/articles/PMC5554746/pdf/nihms847268.pdf

Davidson, M. J., Bryant, A. L., Bower, W. F., & Frawley, H. C. (2017). Myotonometry reliably measures muscle stiffness in the thenar and perineal muscles. *Physiotherapy Canada*, *69*(2), 104–112. https://doi.org/10.3138/ptc.2015-85

Deimel, R., & Brock, O. (2013). A compliant hand based on a novel pneumatic actuator. *Proceedings - IEEE International Conference on Robotics and Automation*, 2047–2053. https://doi.org/10.1109/ICRA.2013.6630851

Di Lecce, M., Onaizah, O., Lloyd, P., Chandler, J. H., & Valdastri, P. (2022). Evolutionary Inverse Material Identification: Bespoke Characterization of Soft Materials Using a Metaheuristic Algorithm. *Frontiers in Robotics and AI*, *8*(January), 1–16. https://doi.org/10.3389/frobt.2021.790571

Do, J. H., Choi, K. H., Ahn, J. S., & Jeon, J. Y. (2017). Effects of a complex rehabilitation program on edema status, physical function, and quality of life in lower-limb lymphedema after gynecological cancer surgery. *Gynecologic Oncology*, *147*(2), 450–455. https://doi.org/10.1016/j.ygyno.2017.09.003

Dolibog, P. T., Dolibog, P., & Chmielewska, D. (2022). Analysis of predicted full recovery time for venous leg ulcers treated with intermittent pneumatic compression. *Postepy Dermatologii i Alergologii*, *39*(1), 52–58. https://doi.org/10.5114/ADA.2020.99369

Dong, M., Fan, W., Li, J., & Zhang, P. (2022). Patient-Specific Exercises with the Development of an End-Effector Type Upper Limb Rehabilitation Robot. *Journal of Healthcare Engineering*, *2022*. https://doi.org/10.1155/2022/4125606

Doss, A. S. A., & Sharma, H. (2021). Analysis of Fiber-reinforced Soft Bending Actuators on Various Parameters for Hand Rehabilitation. *ACM International Conference Proceeding Series*, 0–5. https://doi.org/10.1145/3478586.3478587

Draper, S. N., Kullman, E. L., Sparks, K. E., Little, K., & Thoman, J. (2020). Effects of intermittent pneumatic compression on delayed onset muscle soreness (DOMS) in long distance runners. *International Journal of Exercise Science*, *13*(2), 75–86.

Dunn, N., Williams, E. M., Fishbourne, M., Dolan, G., & Davies, J. H. (2019). Home management of lower limb lymphoedema with an intermittent pneumatic compression device: A feasibility study. *Pilot and Feasibility Studies*, *5*(1), 1–9. https://doi.org/10.1186/s40814-019-0496-4

Ehrström, S., Gruet, M., Giandolini, M., Chapuis, S., Morin, J. B., & Vercruyssen, F. (2018). Acute and Delayed Neuromuscular Alterations Induced by Downhill Running in Trained Trail Runners: Beneficial Effects of High-Pressure Compression Garments. *Frontiers in Physiology*, *9*(November), 1–18. https://doi.org/10.3389/fphys.2018.01627

Eiammanussakul, T., & Sangveraphunsiri, V. (2018). A lower limb rehabilitation robot in sitting position with a review of training activities. *Journal of Healthcare Engineering*, *2018*. https://doi.org/10.1155/2018/1927807

El-Tallawy, S. N., Nalamasu, R., Salem, G. I., LeQuang, J. A. K., Pergolizzi, J. V., & Christo, P. J. (2021). Management of Musculoskeletal Pain: An Update with Emphasis on Chronic Musculoskeletal Pain. *Pain and Therapy*, *10*(1), 181–209. https://doi.org/10.1007/s40122-021-00235-2

El Tumi, H., Johnson, M. I., Dantas, P. B. F., Maynard, M. J., & Tashani, O. A. (2017).

Age-related changes in pain sensitivity in healthy humans: A systematic review with meta-analysis. *European Journal of Pain (United Kingdom)*, *21*(6), 955–964. https://doi.org/10.1002/ejp.1011

Elastosil, M. A. B., Temperature, R., & Silicone, C. (2021). *Creating Tomorrow ' S Solutions*. 2–5.

Electronics, I. (n.d.). *FSR Integration Guide*.

Esquenazi, A. (2019). *Robotic for Lower Limb Rehabilitation*. https://doi.org/10.1016/j.pmr.2018.12.012

Fang, J., Yuan, J., Wang, M., Xiao, L., Yang, J., Lin, Z., Xu, P., & Hou, L. (2020). Novel Accordion-Inspired Foldable Pneumatic Actuators for Knee Assistive Devices. *Soft Robotics*, *7*(1), 95–108. https://doi.org/10.1089/soro.2018.0155

Fernandes, T. L., Pedrinelli, A., & Hernandez, A. J. (2011). Muscle Injury – Physiopathology, Diagnosis, Treatment and Clinical Presentation. *Revista Brasileira de Ortopedia (English Edition)*, *46*(3), 247–255. https://doi.org/10.1016/s2255-4971(15)30190-7

Fernández-González, P., Koutsou, A., Cuesta-Gómez, A., Carratalá-Tejada, M., Miangolarra-Page, J. C., & Molina-Rueda, F. (2020). Reliability of kinovea® software and agreement with a three-dimensional motion system for gait analysis in healthy subjects. *Sensors (Switzerland)*, *20*(11). https://doi.org/10.3390/s20113154

Filippini, R., Sen, S., & Bicchi, A. (2008). Toward soft robots you can depend on. *IEEE Robotics and Automation Magazine*, *15*(3), 31–41. https://doi.org/10.1109/MRA.2008.927696

Fino, P. C., Becker, L. N., Fino, N. F., Griesemer, B., Goforth, M., & Brolinson, P. G. (2019). Effects of Recent Concussion and Injury History on Instantaneous Relative Risk of Lower Extremity Injury in Division i Collegiate Athletes. *Clinical Journal of Sport Medicine*, *29*(3), 218–223. https://doi.org/10.1097/JSM.0000000000000502

Franke, T. P. C., Backx, F. J. G., & Huisstede, B. M. A. (2021). Lower extremity compression garments use by athletes: why, how often, and perceived benefit. *BMC Sports Science, Medicine and Rehabilitation*, *13*(1), 1–14. https://doi.org/10.1186/s13102-020-00230-8

Fu, Q., Han, M., Mu, Y., Hao, L., Lu, L., Huang, X., Li, J., & Kang, F. (2023). Does the pain sensitivity questionnaire correlate with tourniquet pain in patients undergoing ankle surgery? *Frontiers in Surgery*, *10*(February), 1–5. https://doi.org/10.3389/fsurg.2023.1102319

Fukushima, T., Tsuji, T., Sano, Y., & Miyata, C. (2017). *Immediate effects of active exercise with compression therapy on lower-limb lymphedema*. 2603–2610. https://doi.org/10.1007/s00520-017-3671-2

Garcia, L., Kerns, G., O'reilley, K., Okesanjo, O., Lozano, J., Narendran, J., Broeking, C., Ma, X., Thompson, H., Njeuha, P. N., Sikligar, D., Brockstein, R., & Golecki,

H. M. (2022). The role of soft robotic micromachines in the future of medical devices and personalized medicine. *Micromachines*, *13*(1). https://doi.org/10.3390/mi13010028

Gerke, O. (2020). Reporting standards for a bland-altman agreement analysis: A review of methodological reviews. *Diagnostics*, *10*(5), 1–17. https://doi.org/10.3390/diagnostics10050334

Gianesini, S., Raffetto, J. D., Mosti, G., Maietti, E., Sibilla, M. G., Zamboni, P., & Menegatti, E. (2020). Volume control of the lower limb with graduated compression during different muscle pump activation conditions and the relation to limb circumference variation. *Journal of Vascular Surgery: Venous and Lymphatic Disorders*, *8*(5), 814–820. https://doi.org/10.1016/j.jvsv.2019.12.073

Gibbons, T. D., Zuj, K. A., Prince, C. N., Kingston, D. C., Peterson, S. D., & Hughson, R. L. (2019). Haemodynamic and cerebrovascular effects of intermittent lower-leg compression as countermeasure to orthostatic stress. *Experimental Physiology*, *104*(12), 1790–1800. https://doi.org/10.1113/EP088077

Gil-Castillo, J., Barria, P., Aguilar Cárdenas, R., Baleta Abarza, K., Andrade Gallardo, A., Biskupovic Mancilla, A., Azorín, J. M., & Moreno, J. C. (2022). A Robot-Assisted Therapy to Increase Muscle Strength in Hemiplegic Gait Rehabilitation. *Frontiers in Neurorobotics*, *16*(April), 1–13. https://doi.org/10.3389/fnbot.2022.837494

Gorissen, B., Reynaerts, D., Konishi, S., Yoshida, K., Kim, J. W., & De Volder, M. (2017). Elastic Inflatable Actuators for Soft Robotic Applications. *Advanced Materials*, *29*(43). https://doi.org/10.1002/adma.201604977

Guan, D., Liu, R., Fei, C., Zhao, S., & Jing, L. (2020). Fluid-Structure Coupling Model and Experimental Validation of Interaction between Pneumatic Soft Actuator and Lower Limb. *Soft Robotics*, *7*(5), 627–638. https://doi.org/10.1089/soro.2019.0035

Hadžić, V., Širok, B., Malneršič, A., & Čoh, M. (2019). Can infrared thermography be used to monitor fatigue during exercise? A case study. *Journal of Sport and Health Science*, *8*(1), 89–92. https://doi.org/10.1016/j.jshs.2015.08.002

Harris, A. M., Althausen, P. L., Kellam, J., Bosse, M. J., & Castillo, R. (2009). Complications following limb-threatening lower extremity trauma. *Journal of Orthopaedic Trauma*, *23*(1), 1–6. https://doi.org/10.1097/BOT.0b013e31818e43dd

Haun, C. T., Roberts, M. D., Romero, M. A., Osburn, S. C., Mobley, C. B., Anderson, R. G., Goodlett, M. D., Pascoe, D. D., & Martin, J. S. (2017). Does external pneumatic compression treatment between bouts of overreaching resistance training sessions exert differential effects on molecular signaling and performance-related variables compared to passive recovery? An exploratory study. *PLoS ONE*, *12*(6), 1–24. https://doi.org/10.1371/journal.pone.0180429

Hawker, G. A., Mian, S., Kendzerska, T., & French, M. (2011). Measures of adult pain: Visual Analog Scale for Pain (VAS Pain), Numeric Rating Scale for Pain (NRS Pain), McGill Pain Questionnaire (MPQ), Short-Form McGill Pain Questionnaire (SF-MPQ), Chronic Pain Grade Scale (CPGS), Short Form-36 Bodily Pain Scale

(SF-36 BPS), and Measure of Intermittent and Constant Osteoarthritis Pain (ICOAP). *Arthritis Care and Research*, *63*(SUPPL. 11), 240–252. https://doi.org/10.1002/acr.20543

Heiss, R., Kellermann, M., Swoboda, B., Grim, C., Lutter, C., May, M. S., Wuest, W., Uder, M., Nagel, A. M., & Hotfiel, T. (2018). Effect of compression garments on the development of delayed-onset muscle soreness: A multimodal approach using contrast-enhanced ultrasound and acoustic radiation force impulse elastography. *Journal of Orthopaedic and Sports Physical Therapy*, *48*(11), 887–894. https://doi.org/10.2519/jospt.2018.8038

Heung, K. H. L., Tong, R. K. Y., Lau, A. T. H., & Li, Z. (2019). Robotic Glove with Soft-Elastic Composite Actuators for Assisting Activities of Daily Living. *Soft Robotics*, *6*(2), 289–304. https://doi.org/10.1089/soro.2017.0125

Huri, D., & Mankovits, T. (2018). Comparison of the material models in rubber finite element analysis. *IOP Conference Series: Materials Science and Engineering*, *393*(1). https://doi.org/10.1088/1757-899X/393/1/012018

Hurtgen, B. J., Ward, C. L., Garg, K., Pollot, B. E., Goldma, S. M., McKinley, T. O., Wenke, J. C., & Corona, B. T. (2016). Severe muscle trauma triggers heightened and prolonged local musculoskeletal inflammation and impairs adjacent tibia fracture healing. *Journal of Musculoskeletal Neuronal Interactions*, *16*(2), 122–134.

Ibancos-Losada, M. D. R., Osuna-Pérez, M. C., Cortés-Pérez, I., Montoro-Cárdenas, D., & Díaz-Fernández, Á. (2022). Validation and cross-cultural adaptation of the spanish version of the pain sensitivity questionnaire (Psq-s). *Journal of Clinical Medicine*, *11*(1). https://doi.org/10.3390/jcm11010151

Igolnikov, I., Gallagher, R. M., & Hainline, B. (2018). Sport-related injury and pain classification. In *Handbook of Clinical Neurology* (1st ed., Vol. 158). Elsevier B.V. https://doi.org/10.1016/B978-0-444-63954-7.00039-2

Irshaidat, M., Soufian, M., Al-Ibadi, A., & Nefti-Meziani, S. (2019). A novel elbow pneumatic muscle actuator for exoskeleton arm in post-stroke rehabilitation. *RoboSoft 2019 - 2019 IEEE International Conference on Soft Robotics*, 630–635. https://doi.org/10.1109/ROBOSOFT.2019.8722813

Jaimo Ahn, MD, PhD, F., Arvind D Nana, M., Gudrun Mirick, M., & Anna N Miller, MD, F. (2015). *The Burden of Muscoluskeletal Disease in United State*. https://www.boneandjointburden.org/fourth-edition/va2/locationactivity-time-injury

James Walker, Thomas Zidek , Cory Harbel , Sanghyun Yoon, F. Sterling Strickland, S. K. and M. S. (2020). Soft Robotics: A Review of Recent Developments of Pneumatic Soft Actuators. *Actuators*, *9*. https://doi.org/doi:10.3390/act9010003

K.A. Zuj, Prince, R.L. Hughson, and S. D. P. (2019). *Enhanced muscle blood flow with intermittent pneumatic compression of the lower leg during plantar flexion exercise and recovery*. *1*, 1–14.

Kato, E., & Mariko Nakamura, and H. T. (2018). EFFECT OF COMPRESSION

GARMENTS ON CONTROLLED FORCE OUTPUT AFTER HEEL-RISE EXERCISE. *Journal of Strength and Conditioning Research*, 1174–1179.

Kisilewicz, A., Madeleine, P., Ignasiak, Z., Ciszek, B., Kawczynski, A., & Larsen, R. G. (2020). Eccentric Exercise Reduces Upper Trapezius Muscle Stiffness Assessed by Shear Wave Elastography and Myotonometry. *Frontiers in Bioengineering and Biotechnology*, *8*(August), 1–9. https://doi.org/10.3389/fbioe.2020.00928

Kojima, A., Okui, M., & Nakamura, T. (2021). *Development of Soft Pneumatic Actuators Using High-Strain Elastic Materials with Stress Anisotropy of Short Fibers*. 41. https://doi.org/10.3390/iecat2020-08526

Konishi, S., & Hirata, A. (2019). Flexible Temperature Sensor Integrated with Soft Pneumatic Microactuators for Functional Microfingers. *Scientific Reports*, *9*(1), 1–10. https://doi.org/10.1038/s41598-019-52022-x

Kristensen, N. S., Hertel, E., Skadhauge, C. H., Kronborg, S. H., Petersen, K. K., & McPhee, M. E. (2021). Psychophysical predictors of experimental muscle pain intensity following fatiguing calf exercise. *PLoS ONE*, *16*(7 July), 1–17. https://doi.org/10.1371/journal.pone.0253945

Kumar, N., Parveen, S., Srivastava, T., Patra, A., Sharma, N., & Kumar, N. (2019). To compare the efficacy of pneumatic compression therapy (PCT), lymphatic drainage exercises (LDE) and control group in patient with lower limb lymph edema. *International Journal of Surgery Science*, *3*(1), 262–272. https://doi.org/10.33545/surgery.2019.v3.i1e.45

Kurth, J. D., & Klenosky, D. B. (2021). Validity Evidence for a Daily, Online-delivered, Adapted Version of the International Physical Activity Questionnaire Short Form (IPAQ-SF). *Measurement in Physical Education and Exercise Science*, *25*(2), 127–136. https://doi.org/10.1080/1091367X.2020.1847721

Lateef, S., & Earp, J. E. (2023). *Contrast With Compression Therapy Enhances Muscle Function Recovery and Attenuates Glycogen Disruption After Exercise*. https://doi.org/10.1177/19417381221080172

Lau, E. (2020). *Accuracy of bromocresol green (BCG) method for plasma albumin* [Norwegian University of Science and Technology,Norway]. https://ntnuopen.ntnu.no/ntnu-xmlui/bitstream/handle/11250/2661296/no.ntnu%3Ainspera%3A58241340%3A58300792.pdf?sequence=1&isAllowed=y

Leabeater, A. J., James, L. P., & Driller, M. W. (2022). *Tight Margins : Compression Garment Use during Exercise and Recovery — A Systematic Review*. 395–421.

Lee, C., Kim, M., Kim, Y. J., Hong, N., Ryu, S., Kim, H. J., & Kim, S. (2017). Soft robot review. *International Journal of Control, Automation and Systems*, *15*(1), 3–15. https://doi.org/10.1007/S12555-016-0462-3/METRICS

Leitner, J., Chiang, P. H., & Dey, S. (2022). Personalized Blood Pressure Estimation Using Photoplethysmography: A Transfer Learning Approach. *IEEE Journal of Biomedical and Health Informatics*, *26*(1), 218–228.

https://doi.org/10.1109/JBHI.2021.3085526

Li, Q., Sun, G., Chen, Y., Chen, X., Shen, Y., Xie, H., & Li, Y. (2022). Fabricated leg mannequin for the pressure measurement of compression stockings. *Textile Research Journal*, *92*(19–20), 3500–3510. https://doi.org/10.1177/00405175221083216

Lin, H. T., Leisk, G. G., & Trimmer, B. (2011). GoQBot: A caterpillar-inspired soft-bodied rolling robot. *Bioinspiration and Biomimetics*, *6*(2). https://doi.org/10.1088/1748-3182/6/2/026007

Lin, N., Zheng, H., Li, Y., Wang, R., Chen, X., & Zhang, X. (2020). Self-Sensing Pneumatic Compressing Actuator. *Frontiers in Neurorobotics*, *14*(December), 1–18. https://doi.org/10.3389/fnbot.2020.572856

Liu, J., Liu, Y., Wang, J., Zuo, X., Wang, X., Zhang, Y., & He, H. (2021). Dental measurements based on a three-dimensional digital technique: A comparative study on reliability and validity. *Archives of Oral Biology*, *124*, 105059. https://doi.org/10.1016/j.archoralbio.2021.105059

Lovejoy, T. I., Turk, D. C., & Morasco, B. J. (2012). Evaluation of the psychometric properties of the revised short-form McGill pain questionnaire. *Journal of Pain*, *13*(12), 1250–1257. https://doi.org/10.1016/j.jpain.2012.09.011

Low, F. Z., Lim, J. H., Kapur, J., & Yeow, R. C. H. (2019). Effect of a Soft Robotic Sock Device on Lower Extremity Rehabilitation Following Stroke: A Preliminary Clinical Study with Focus on Deep Vein Thrombosis Prevention. *IEEE Journal of Translational Engineering in Health and Medicine*, *7*(March 2018), 1–6. https://doi.org/10.1109/JTEHM.2019.2894753

Majidi, C. (2014). Soft Robotics: A Perspective - Current Trends and Prospects for the Future. *Soft Robotics*, *1*(1), 5–11. https://doi.org/10.1089/SORO.2013.0001

Manti, M., Pratesi, A., Falotico, E., Cianchetti, M., & Laschi, C. (2016). Soft assistive robot for personal care of elderly people. *Proceedings of the IEEE RAS and EMBS International Conference on Biomedical Robotics and Biomechatronics*, *2016-July*, 833–838. https://doi.org/10.1109/BIOROB.2016.7523731

Manuello Bertetto, A., Cadeddu, A., Besalduch, L. A., Ricciu, R., & Ferraresi, C. (2016). Energy balance and mechanical behaviour of a flexible pneumatic actuator for fish-like propulsion. *International Journal of Mechanics and Control*, *17*(1), 23–30.

Marathamuthu, S., Selvanayagam, V. S., & Yusof, A. (2022). Contralateral Effects of Eccentric Exercise and DOMS of the Plantar Flexors: Evidence of Central Involvement. *Research Quarterly for Exercise and Sport*, *93*(2), 240–249. https://doi.org/10.1080/02701367.2020.1819526

Maruthavanan, D., Seibel, A., & Schlattmann, J. (2021). Fluid-structure interaction modelling of a soft pneumatic actuator. *Actuators*, *10*(7). https://doi.org/10.3390/act10070163

Maugeri, G., Castrogiovanni, P., Battaglia, G., Pippi, R., D'Agata, V., Palma, A., Di

Rosa, M., & Musumeci, G. (2020). The impact of physical activity on psychological health during Covid-19 pandemic in Italy. *Heliyon*, *6*(6), e04315. https://doi.org/10.1016/j.heliyon.2020.e04315

Maurer, A., Deckert, S., Levenig, C., Schörkmaier, T., Stangier, C., Attenberger, U., Hasenbring, M., & Boecker, H. (2020). Body image relates to exercise-induced antinociception and mood changes in young adults: A randomized longitudinal exercise intervention. *International Journal of Environmental Research and Public Health*, *17*(18), 1–14. https://doi.org/10.3390/ijerph17186801

Mazzolai, B., & Mattoli, V. (2016). Generation soft. *Nature*, *536*(7617), 400–401. https://doi.org/10.1038/536400a

Melzack, R. (1975). The McGill Pain Questionnaire: Major properties and scoring methods. *Pain*, *1*(3), 277–299. https://doi.org/10.1016/0304-3959(75)90044-5

Miriyev, A., Stack, K., & Lipson, H. (2017). Soft material for soft actuators. *Nature Communications*, *8*(1), 1–8. https://doi.org/10.1038/s41467-017-00685-3

Mohammadi, A., Lavranos, J., Zhou, H., Mutlu, R., Alici, G., Tan, Y., Choong, P., & Oetomo, D. (2020). A practical 3D-printed soft robotic prosthetic hand with multi-articulating capabilities. *PLoS ONE*, *15*(5). https://doi.org/10.1371/JOURNAL.PONE.0232766

Morris, L., Diteesawat, R. S., Rahman, N., Turton, A., Cramp, M., & Rossiter, J. (2023). The-state-of-the-art of soft robotics to assist mobility: a review of physiotherapist and patient identified limitations of current lower-limb exoskeletons and the potential soft-robotic solutions. *Journal of NeuroEngineering and Rehabilitation*, *20*(1), 1–15. https://doi.org/10.1186/S12984-022-01122-3/METRICS

Mosadegh, B., Polygerinos, P., Keplinger, C., Wennstedt, S., Shepherd, R. F., Gupta, U., Shim, J., Bertoldi, K., Walsh, C. J., & Whitesides, G. M. (2014). Pneumatic networks for soft robotics that actuate rapidly. *Advanced Functional Materials*, *24*(15), 2163–2170. https://doi.org/10.1002/adfm.201303288

Moscicka, P., Szewczyk, M. T., Cwajda-Bialasik, J., & Jawien, A. (2019). The role of compression therapy in the treatment of venous leg ulcers. *Advances in Clinical and Experimental Medicine*, *28*(6), 847–852. https://doi.org/10.17219/acem/78768

Mosti, G., Cavezzi, A., Bastiani, L., & Partsch, H. (2020). Compression Therapy Is Not Contraindicated in Diabetic Patients with Venous or Mixed Leg Ulcer. *Journal of Clinical Medicine 2020, Vol. 9, Page 3709*, *9*(11), 3709. https://doi.org/10.3390/JCM9113709

Mosti, G., & Partsch, H. (2010). Inelastic bandages maintain their hemodynamic effectiveness over time despite significant pressure loss. *Journal of Vascular Surgery*, *52*(4), 925–931. https://doi.org/10.1016/J.JVS.2010.04.081

Mourtzis, D. (2020). Simulation in the design and operation of manufacturing systems: state of the art and new trends. *International Journal of Production Research*, *58*(7), 1927–1949. https://doi.org/10.1080/00207543.2019.1636321

Murphy, E. C., Dumont, J. H., Park, C. H., Kestell, G., Lee, K. S., & Labouriau, A. (2020). Tailoring properties and processing of Sylgard 184: Curing time, adhesion, and water affinity. *Journal of Applied Polymer Science*, *137*(14), 1–10. https://doi.org/10.1002/app.48530

Nesler, C. R., Swift, T. A., & Rouse, E. J. (2018). Initial Design and Experimental Evaluation of a Pneumatic Interference Actuator. *Soft Robotics*, *5*(2), 138–148. https://doi.org/10.1089/soro.2017.0004

O'Neill, C. T., McCann, C. M., Hohimer, C. J., Bertoldi, K., & Walsh, C. J. (2022). Unfolding Textile-Based Pneumatic Actuators for Wearable Applications. *Soft Robotics*, *9*(1), 163–172. https://doi.org/10.1089/soro.2020.0064

Ossipov, M. H., Dussor, G. O., & Porreca, F. (2010). Review series Central modulation of pain. *The Journal of Clinical Investigation*, *120*(11), 3779–3787. https://doi.org/10.1172/JCI43766.reduced

Ostrovsky-Snider, N. (2017). *Modeling, Design and Fabrication of Biocompatible Silk-Based Electronics and Actuators*. 76. http://files/1811/Ostrovsky-Snider - Modeling, Design and Fabrication of Biocompatible .pdf

Pagoli, A., Chapelle, F., Antonio, J., Ramon, C., Lapusta, Y., Pagoli, A., Chapelle, F., Antonio, J., Ramon, C., Mezouar, Y., & Re-, Y. L. (2021). *Review of soft fluidic actuators : classification and materials modeling analysis To cite this version : HAL Id : hal-03474847 Review of soft fluidic actuators : classification and materials modeling analysis*.

Pagoli, A., Chapelle, F., Corrales-Ramon, J. A., Mezouar, Y., & Lapusta, Y. (2022). Review of soft fluidic actuators: Classification and materials modeling analysis. *Smart Materials and Structures*, *31*(1). https://doi.org/10.1088/1361-665X/ac383a

Pan, M., Yuan, C., Liang, X., Dong, T., Liu, T., Zhang, J., Zou, J., Yang, H., & Bowen, C. (2022). Soft Actuators and Robotic Devices for Rehabilitation and Assistance. *Advanced Intelligent Systems*, *4*(4), 2100140. https://doi.org/10.1002/aisy.202100140

Park, S., Mondal, K., Treadway, R. M., Kumar, V., Ma, S., Holbery, J. D., & Dickey, M. D. (2018). Silicones for Stretchable and Durable Soft Devices: Beyond Sylgard-184. *ACS Applied Materials and Interfaces*, *10*(13), 11261–11268. https://doi.org/10.1021/acsami.7b18394

Partsch, H., & Mortimer, P. (2015). Compression for leg wounds. *The British Journal of Dermatology*, *173*(2), 359–369. https://doi.org/10.1111/BJD.13851

Partsch, H., Partsch, B., & Braun, W. (2006). Interface pressure and stiffness of ready made compression stockings: comparison of in vivo and in vitro measurements. *Journal of Vascular Surgery*, *44*(4), 809–814. https://doi.org/10.1016/J.JVS.2006.06.024

Partsch, H., Schuren, J., Mosti, G., & Benigni, J. P. (2016). The Static Stiffness Index: an important parameter to characterise compression therapy in vivo. *Journal of Wound Care*, *25 Suppl 9*(9), S4–S10. https://doi.org/10.12968/JOWC.2016.25.SUP9.S4

Peake, J. M., Neubauer, O., Gatta, P. A. D., & Nosaka, K. (2017). Muscle damage and inflammation during recovery from exercise. *Journal of Applied Physiology*, *122*(3), 559–570. https://doi.org/10.1152/japplphysiol.00971.2016

Peng, Z., & Huang, J. (2019). Soft Rehabilitation and Nursing-Care Robots: A Review and Future Outlook. *Applied Sciences 2019, Vol. 9, Page 3102*, *9*(15), 3102. https://doi.org/10.3390/APP9153102

Pini, L. (2020). *Geometry optimization for biaxial testing of polydimethylsiloxane SYLGARD 184 and finite element modelling* [Politecnico di Milano,Public university in Milan, Italy]. http://hdl.handle.net/10589/154541

Polygerinos, P., Correll, N., Morin, S. A., Mosadegh, B., Onal, C. D., Petersen, K., Cianchetti, M., Tolley, M. T., & Shepherd, R. F. (2017). Soft Robotics: Review of Fluid-Driven Intrinsically Soft Devices; Manufacturing, Sensing, Control, and Applications in Human-Robot Interaction. *Advanced Engineering Materials*, *19*(12). https://doi.org/10.1002/ADEM.201700016

Prieto-González, P., Martínez-Castillo, J. L., Fernández-Galván, L. M., Casado, A., Soporki, S., & Sánchez-Infante, J. (2021). Epidemiology of sports-related injuries and associated risk factors in adolescent athletes: An injury surveillance. *International Journal of Environmental Research and Public Health*, *18*(9). https://doi.org/10.3390/ijerph18094857

Product, A. (2022). *Axel Products Physical Testing Services*. Axel Product. http://www.axelproducts.com/

Rabe, E., Partsch, H., Hafner, J., Lattimer, C., Mosti, G., Neumann, M., Urbanek, T., Huebner, M., Gaillard, S., & Carpentier, P. (2018). Indications for medical compression stockings in venous and lymphatic disorders: An evidence-based consensus statement. *Phlebology*, *33*(3), 163–184. https://doi.org/10.1177/0268355516689631

Rackl, M. (2017). Article + Errata Curve Fitting for Ogden, Yeoh and Polynomial Models. *Ostbayerishce Technische Hochschule Regensburg*, *September*.

Ramamoorthy, D. (2018). *Muscle fatigue detection using Infrared Thermography : Image segmentation to extract the region of interest from thermograms*.

Ren, W., Duan, Y., Jan, Y. K., Li, J., Liu, W., Pu, F., & Fan, Y. (2022). Effect of intermittent pneumatic compression with different inflation pressures on the distal microvascular responses of the foot in people with type 2 diabetes mellitus. *International Wound Journal*, *19*(5), 968–977. https://doi.org/10.1111/iwj.13693

Rosalia, L., Lamberti, K. K., Landry, M. K., Leclerc, C. M., Shuler, F. D., Hanumara, N. C., & Roche, E. T. (2021). A Soft Robotic Sleeve for Compression Therapy of the Lower Limb. *Proceedings of the Annual International Conference of the IEEE Engineering in Medicine and Biology Society, EMBS*. https://doi.org/10.1109/EMBC46164.2021.9630924

Rossiter, J., & Hauser, H. (2016). Soft robotics - The next industrial revolution? [Industrial Activities]. *IEEE Robotics and Automation Magazine*, *23*(3), 17–20.

https://doi.org/10.1109/MRA.2016.2588018

Rotsch, C., Oschatz, H., Schwabe, D., Weiser, M., & Möhring, U. (2011). Medical bandages and stockings with enhanced patient acceptance. In *Handbook of Medical Textiles*. Woodhead Publishing Limited. https://doi.org/10.1533/9780857093691.4.481

Rus, D., & Tolley, M. T. (2015). Design, fabrication and control of soft robots. *Nature 2015 521:7553*, *521*(7553), 467–475. https://doi.org/10.1038/nature14543

Ruscheweyh, R., Marziniak, M., Stumpenhorst, F., Reinholz, J., & Knecht, S. (2009). Pain sensitivity can be assessed by self-rating: Development and validation of the Pain Sensitivity Questionnaire. *Pain*, *146*(1–2), 65–74. https://doi.org/10.1016/j.pain.2009.06.020

Sakai, K., Takahira, N., Tsuda, K., & Akamine, A. (2021). Effects of intermittent pneumatic compression on femoral vein peak venous velocity during active ankle exercise. *Journal of Orthopaedic Surgery*, *29*(1), 1–8. https://doi.org/10.1177/2309499021998105

Schuren, J., & Mohr, K. (2010). Pascal's law and the dynamics of compression therapy: A study on healthy volunteers. *International Angiology*, *29*(5), 431–435.

Schwellnus, M. P., Swanevelder, S., Jordaan, E., Derman, W., & Van Rensburg, D. C. J. (2018). Underlying Chronic Disease, Medication Use, History of Running Injuries and Being a More Experienced Runner Are Independent Factors Associated with Exercise-Associated Muscle Cramping: A Cross-Sectional Study in 15778 Distance Runners. *Clinical Journal of Sport Medicine*, *28*(3), 289–298. https://doi.org/10.1097/JSM.0000000000000456

Shallwani, S. M., & Towers, A. (2018). Self-management strategies for malignant lymphedema: A case report with 1-year and 4-year follow-up data. *Physiotherapy Canada*, *70*(3), 204–211. https://doi.org/10.3138/ptc.2016-94

Shepherd, R. F., Ilievski, F., Choi, W., Morin, S. A., Stokes, A. A., Mazzeo, A. D., Chen, X., Wang, M., & Whitesides, G. M. (2011). Multigait soft robot. *Proceedings of the National Academy of Sciences of the United States of America*, *108*(51), 20400–20403. https://doi.org/10.1073/PNAS.1116564108/-/DCSUPPLEMENTAL

Shi, Q., Liu, H., Tang, D., Li, Y., Li, X. J., & Xu, F. (2019). Bioactuators based on stimulus-responsive hydrogels and their emerging biomedical applications. *NPG Asia Materials*, *11*(1). https://doi.org/10.1038/s41427-019-0165-3

Simon, J. E., & Docherty, C. L. (2018). Health-related quality of life is decreased in middle-aged adults with chronic ankle instability. *Journal of Science and Medicine in Sport*, *21*(12), 1206–1209. https://doi.org/10.1016/j.jsams.2018.05.008

Smooth-On. (n.d.). *Durometer Shore Hardness Scale*. Retrieved November 20, 2022, from https://www.smooth-on.com/page/durometer-shore-hardness-scale/

Smooth-On. (2015). *Dragon Skin ® Series - Technical Data Sheet*. http://www.smooth-on.com/tb/files/DRAGON_SKIN_SERIES_TB.pdf

Soft Robotics Toolkit. (2017). *Soft Robotics Toolkit*. https://softroboticstoolkit.com/

Solowiej, K., Mason, V., & Upton, D. (2010). Psychological stress and pain in wound care, part 2: a review of pain and stress assessment tools. *JOURNAL OF WOUND CARE*.

Song, Y., Cen, X., Zhang, Y., Bíró, I., Ji, Y., & Gu, Y. (2022). Development and Validation of a Subject-Specific Coupled Model for Foot and Sports Shoe Complex: A Pilot Computational Study. *Bioengineering*, *9*(10). https://doi.org/10.3390/bioengineering9100553

Sonkodi, B., Berkes, I., & Koltai, E. (2020). Have we looked in the wrong direction for more than 100 years? Delayed onset muscle soreness is, in fact, neural microdamage rather than muscle damage. *Antioxidants*, *9*(3). https://doi.org/10.3390/antiox9030212

Sparrman, B., Thomsen, C., Darbari, S., Rustom, R., Laucks, J., Shea, K., & Tibbits, S. (2021). Printed silicone pneumatic actuators for soft robotics. *Additive Manufacturing*, *40*(September 2020), 101860. https://doi.org/10.1016/j.addma.2021.101860

Srivastava, A., Sood, A., Joy, P. S., Mandal, S., Panwar, R., Ravichandran, S., Sarangi, S., & Woodcock, J. (2010). Principles of physics in surgery: the laws of mechanics and vectors physics for surgeons-part 2. *The Indian Journal of Surgery*, *72*(5), 355–361. https://doi.org/10.1007/S12262-010-0155-8

Stable, A. (2014). *The Design and Analysis of Clinical Experiments . by J . L . Fleiss Review*. *43*(4), 43–44.

States, U. (2016). National Health Statistics Reports, Number 99, November 18, 2016. *Centers for Disease Control and Prevention*, *99*, 2011–2014.

Steck, D., Qu, J., Kordmahale, S. B., Tscharnuter, D., Muliana, A., & Kameoka, J. (2019). Mechanical responses of Ecoflex silicone rubber: Compressible and incompressible behaviors. *Journal of Applied Polymer Science*, *136*(5), 1–11. https://doi.org/10.1002/app.47025

Stedge, H. L., & Armstrong, K. (2021). The effects of intermittent pneumatic compression on the reduction of exercise-induced muscle damage in endurance athletes: A critically appraised topic. *Journal of Sport Rehabilitation*, *30*(4), 668–671. https://doi.org/10.1123/JSR.2020-0364

Stožer, A., Vodopivc, P., & Bombek, L. K. (2020). Pathophysiology of exercise-induced muscle damage and its structural, functional, metabolic, and clinical consequences. *Physiological Research*, *69*(4), 565–598. https://doi.org/10.33549/physiolres.934371

Struhár, I., Kumstát, M., & Králová, D. M. (2018). Effect of Compression Garments on Physiological Responses after Uphill Running. *Journal of Human Kinetics*, *61*(1), 119–129. https://doi.org/10.1515/hukin-2017-0136

Su, H., Hou, X., Zhang, X., Qi, W., Cai, S., Xiong, X., & Guo, J. (2022). Pneumatic Soft

Robots: Challenges and Benefits. *Actuators 2022, Vol. 11, Page 92*, *11*(3), 92. https://doi.org/10.3390/ACT11030092

Suarez, E., Huaroto, J. J., Reymundo, A. A., Holland, D., Walsh, C., & Vela, E. (2018). A Soft Pneumatic Fabric-Polymer Actuator for Wearable Biomedical Devices: Proof of Concept for Lymphedema Treatment. *Proceedings - IEEE International Conference on Robotics and Automation*, 5452–5458. https://doi.org/10.1109/ICRA.2018.8460790

Sugahara, I., Doi, M., Nakayama, R., & Sasaki, K. (2018). Acute effect of wearing compression stockings on lower leg swelling and muscle stiffness in healthy young women. *Clinical Physiology and Functional Imaging*, *38*(6), 1046–1053. https://doi.org/10.1111/cpf.12527

Sun, Y. (2017). *Stiffness Customization and Patterning*. *4*(3). https://doi.org/10.1089/soro.2016.0047

Tawk, C., & Alici, G. (2020). Finite element modeling in the design process of 3D printed pneumatic soft actuators and sensors. *Robotics*, *9*(9). https://doi.org/10.3390/ROBOTICS9030052

Thalman, C., & Artemiadis, P. (2020). A review of soft wearable robots that provide active assistance: Trends, common actuation methods, fabrication, and applications. *Wearable Technologies*, *1*, 1–27. https://doi.org/10.1017/wtc.2020.4

Thalman, C. M., & Lee, H. (2020). Design and Validation of a Soft Robotic Ankle-Foot Orthosis (SR-AFO) Exosuit for Inversion and Eversion Ankle Support. *Proceedings - IEEE International Conference on Robotics and Automation*, 1735–1741. https://doi.org/10.1109/ICRA40945.2020.9197531

Velez, J. C., Friedman, L. E., Barbosa, C., Castillo, J., Juvinao-Quintero, D. L., Williams, M. A., & Gelaye, B. (2022). Evaluating the performance of the Pain Interference Index and the Short Form McGill Pain Questionnaire among Chilean injured working adults. *PLoS ONE*, *17*(5 May), 6–16. https://doi.org/10.1371/journal.pone.0268672

Volpe, E. F. T., Resqueti, V. R., Da Silva, A. A. M., Gualdi, L. P., & Fregonezi, G. A. F. (2020). Supervised exercise protocol for lower limbs in subjects with chronic venous disease: An evaluator-blinded, randomized clinical trial. *Trials*, *21*(1), 1–9. https://doi.org/10.1186/s13063-020-04314-1

Wan, J. J., Qin, Z., Wang, P. Y., Sun, Y., & Liu, X. (2017). Muscle fatigue: General understanding and treatment. *Experimental and Molecular Medicine*, *49*(10), e384-11. https://doi.org/10.1038/emm.2017.194

Warutkar, V., Dadgal, R., & Mangulkar, U. R. (2022). Use of Robotics in Gait Rehabilitation Following Stroke: A Review. *Cureus*, *14*(11). https://doi.org/10.7759/cureus.31075

Wassertheil, S., & Cohen, J. (1970). Statistical Power Analysis for the Behavioral Sciences. In *Biometrics* (Vol. 26, Issue 3, p. 588). https://doi.org/10.2307/2529115

Whitaker, J. C. (2012). Self-management in combating chronic skin disorders. *Journal of Lymphoedema*, *7*(1), 46–50.

Williams, A. (2016). A review of the evidence for adjustable compression wrap devices. *Journal of Wound Care*, *25*(5), 242–247. https://doi.org/10.12968/jowc.2016.25.5.242

Wong, I. K. Y., Man, M. B. L., Chan, O. S. H., Siu, F. C., Abel, M., & Andriessen, A. (2012). Comparison of the interface pressure and stiffness of four types of compression systems. *Journal of Wound Care*, *21*(4), 161–167. https://doi.org/10.12968/jowc.2012.21.4.161

Xavier, M. S., Fleming, A. J., & Yong, Y. K. (2021). Finite Element Modeling of Soft Fluidic Actuators: Overview and Recent Developments. *Advanced Intelligent Systems*, *3*(2), 2000187. https://doi.org/10.1002/aisy.202000187

Yanaoka, T., Numata, U., Nagano, K., Kurosaka, S., & Kawashima, H. (2022). Effects of different intermittent pneumatic compression stimuli on ankle dorsiflexion range of motion. *Frontiers in Physiology*, *13*(November), 1–11. https://doi.org/10.3389/fphys.2022.1054806

Yap, H. K., Khin, P. M., Koh, T. H., Sun, Y., Liang, X., Lim, J. H., & Yeow, C. H. (2017). A Fully Fabric-Based Bidirectional Soft Robotic Glove for Assistance and Rehabilitation of Hand Impaired Patients. *IEEE Robotics and Automation Letters*, *2*(3), 1383–1390. https://doi.org/10.1109/LRA.2017.2669366

Yap, H. K., Lim, J. H., Nasrallah, F., Cho Hong Goh, J., & Yeow, C. H. (2016). Characterisation and evaluation of soft elastomeric actuators for hand assistive and rehabilitation applications. *Journal of Medical Engineering & Technology*, *40*(4), 199–209. https://doi.org/10.3109/03091902.2016.1161853

Yap, H. K., Technologies, R., & Yeow, R. C. (2016). *High-Force Soft Printable Pneumatics for Soft*. *September*. https://doi.org/10.1089/soro.2016.0030

Youn, Y. J., & Lee, J. (2019). Chronic venous insufficiency and varicose veins of the lower extremities. *Korean Journal of Internal Medicine*, *34*(2), 269–283. https://doi.org/10.3904/kjim.2018.230

Yu, H., Randhawa, K., Côté, P., Carroll, L. J., Sutton, D., Wong, J. J., Varatharajan, S., Southerst, D., Stern, P. J., Bohay, R., Shearer, H. M., Mior, S., Lindsay, G. M., Goldgrub, R., Chung, C. L., Ameis, A., Nordin, M., Stupar, M., & Taylor-Vaisey, A. (2016). The effectiveness of physical agents for lower-limb soft tissue injuries: A systematic review. *Journal of Orthopaedic and Sports Physical Therapy*, *46*(7), 523–554. https://doi.org/10.2519/jospt.2016.6521

Yun, S., Kang, Y. J., Kim, J. H., Do, H. H., Shin, S. Y., Lee, S. Bin, & Kwon, J. W. (2023). Effect of Elastic Compression Stocking and Kinesio Taping during Heel-raise Exercise on Muscle Activity, Mechanical Properties, and Muscle Fatigue in Healthy Women. *The Journal of Korean Physical Therapy*, *35*(1), 24–30. https://doi.org/10.18857/jkpt.2023.35.1.24

Zhang, K., Chen, X., Liu, F., Tang, H., Wang, J., & Wen, W. (2018). System framework

of robotics in upper limb rehabilitation on poststroke motor recovery. *Behavioural Neurology*, *2018*(December 2017). https://doi.org/10.1155/2018/6737056

Zhao, S., Liu, R., Fei, C., & Guan, D. (2019). Dynamic Interface Pressure Monitoring System for. *Sensors*, *19*(13).

Zhu, Z., & Ma, Y. (2021). Sports injury and rehabilitation of lower limb soft tissue. *Revista Brasileira de Medicina Do Esporte*, *27*(8), 804–806. https://doi.org/10.1590/1517-8692202127082021_0365

Zuj, K. A., Prince, C. N., Hughson, R. L., & Peterson, S. D. (2019). Superficial femoral artery blood flow with intermittent pneumatic compression of the lower leg applied during walking exercise and recovery. *Journal of Applied Physiology*, *127*(2), 559–567. https://doi.org/10.1152/japplphysiol.00656.2018